INVESTIGATION OF BAGASSE ASH AS A PARTIAL SUPPLEMENTARY CEMENTITIOUS MATERIAL

MOHAMMAD MAHMUDUL HASAN

MASTER OF SCIENCE IN CIVIL ENGINEERING
(STRUCTURAL)

DEPARTMENT OF CIVIL ENGINEEIRG
BANGLADESH UNIVERSITY OF ENGINEERING & TECHNOLOGY
DHAKA

OCTOBER, 2018

INVESTIGATION OF BAGASSE ASH AS A PARTIAL SUPPLEMENTARY CEMENTITIOUS MATERIAL

by

MOHAMMAD MAHMUDUL HASAN

Student ID: 1015042351

A thesis submitted to Department of Civil Engineering, Bangladesh University of Engineering and Technology, Dhaka in partial fulfilment of the requirement for the degree of Master of Science in Civil Engineering (Structural)

DEPARTMENT OF CIVIL ENGINEEIRG

BANGLADESH UNIVERSITY OF ENGINEERING & TECHNOLOGY

DHAKA

OCTOBER, 2018

The thesis titled "Investigation of Bagasse Ash as a Partial Supplementary Cementitious Material" Submitted by Mohammad Mahmudul Hasan, Roll: 1015042351 Session: October, 2015, has been accepted as satisfactory in partial fulfilment of the requirement for the degree of Master of Science in Civil Engineering (Structural) on October 6, 2018.

Board of Examiners

(1)	Dr. Tanvir Manzur Professor Department of Civil Engineering BUET, Dhaka-1000	Chairman (Supervisor)
(2)	Dr. Ahsanul Kabir 6.10.18 Professor and Head Department of Civil Engineering BUET, Dhaka-1000	Member (Ex-officio)
(3)	Dr. Tahsin Reza Hossain Professor Department of Civil Engineering BUET, Dhaka-1000	Member
(4)	Dr. Muhammad Hasanuzzaman Assistant Professor Department of Glass and Ceramic Engineering BUET, Dhaka-1000	Member (External)

DECLARATION

It is hereby declared that the studies embodied in this thesis are the results of experiments carried out by the authors under the supervision of Dr. Tanvir Manzur, Professor, Department of Civil Engineering, BUET except where specified by reference to other works. Neither the thesis nor any part of it has been submitted elsewhere for any other purposes.

6.10.18

Mohammad Mahmudul Hasan
Student ID: 1015042351
Date: 06.10.2018

Acknowledgements

The author expresses his utmost gratitude to the Almighty Allah for the successful completion of the research work as planned.

I would like to express my sincere gratitude and profound respect to my thesis supervisor Dr. Tanvir Manzur, Professor, Department of Civil Engineering, BUET for giving me the opportunity to work under his cordial supervision. His invaluable suggestions, motivation in difficult times and affectionate encouragement were extremely helpful in accomplishing this study. His comments, guidance and ideas benefited me a lot in preparing my thesis. I am indebted to him for acquainting me with the world of advanced research.

The author also takes the opportunity to pay his heartfelt thanks to Dr. Md. Shakhawat Hossain Firoz for his contributions in conducting some part of the experimental work.

The author would also like to express his gratefulness towards all the staffs of the Concrete Laboratory, Department of Civil Engineering, BUET for their relentless support during the experimental works. The author also expresses his gratitude to the Department of Glass and Ceramic Engineering, BUET for their assistance in analysis of samples.

Abstract

Bagasse is a fibrous waste product of the sugarcane industry that remains after sugarcane or sorghum stalks are crushed to extract their juice. In Bangladesh, Sugarcane is produced in 2.05% land of the country and it contributes almost 5.52% to agricultural GDP. Bagasse is most often used as a biofuel for the generation of steam and power required to operate boiler in the sugar factory and in the manufacture of pulp in paper industry. As a result, these industries produce huge amounts of a solid waste material known as sugarcane bagasse ash (SCBA) in Bangladesh. The waste of bagasse ash is generally disposed in landfills or dumped nearby the industrial sites. Consequently, it is creating waste management problem, especially in the sugar milling sites. These wastes have an adverse effect on the environment, creating air pollution due to smell, dust and also affecting the fertility of soil.

The utilization of such waste materials as a supplement in cement manufacture provides two folds benefit; a) it makes cement production cleaner and b) it solves problems associated with waste management. From limited previous studies available, it is found that sugarcane bagasse ash could have pozzolanic properties and thereby, could be used as supplementary cementing materials. However, pozzolanic behavior of SCBA depends on burning process and temperature. The high carbon content is an obstacle to its use in cement/mortars. Therefore, it would be valuable if the unburnt carbon in SCBA could be removed through proper calcination.

This research work aims at exhibiting the idea of utilizing bagasse ash as supplementary cementitious material by elaborating upon their morphological, physical and chemical properties. Locally available bagasse and industrially leached bagasse were collected and burnt at various temperature ranges to obtain the most suitable burning process. The corresponding chemical composition of SCBA was investigated through XRF to investigate the suitability of bagasse ash to be used as supplementary cementitious material. The morphology and chemistry of bagasse ash was also studied by performing EDS analysis coupled with Scanning Electron Microscopy (SEM) technique. It was found that industrially leached bagasse burnt at 600-650 ^{o} C temperature shows satisfactory result to be used as pozzolan which have similar composition of class F fly ash. The burning of relatively fresh locally available bagasse did not yield suitable

amount silica due to high alkali content like K_2O, Na_2O, CaO etc. Ash produced from industrially leached bagasse was then mixed with Portland cement at partial replacement level of 10%, 15% and 20% by weight to make mortar samples. Control samples with no bagasse ash were also made for comparison. It was observed that addition of bagasse ash increased the water demand and reduced drying shrinkage of cement mortar. Moreover, up to 10% replacement level, the compressive strength of mortar was found to be increased and then the strength showed a decreasing trend with 15% replacement level exhibited almost equal strength of the OPC mortar. It is therefore, evident that sugarcane bagasse ash has the potential to be used in cement production and thereby could resolve the waste management issues related to it.

Table of Contents

List of Figure

List of Tables

Acronyms and Abbreviations

SCBA	Sugar Cane Bagasse Ash
GDP	Gross Domestic Product
XRF	X-Ray Fluorescence
SEM	Scanning Electron Microscopy
FESEM	Field Emission Scanning Electron Microscope
FAO	Food and Agriculture Organization of the United Nations
BSFIC	Bangladesh Sugar and Food Industries Corporation
ASTM	American Society for Testing and Materials
OPC	Ordinary Portland Cement
PPC	Portland Pozzolan Cement
GBA	Ground Bagasse Ash
RHA	Rice Husk Ash
C3A	Tricalcium Aluminate
C3S	Tricalcium Silicate
LOI	Loss on Ignition
XRD	X-Ray Diffraction
ITZ	Interfacial Transition Zone
TGA	Thermogravimetric Analysis
FA	Fly Ash
DTA	Differential Thermal Analysis

SA	Slag Ash
ASR	Alkali–Silica Reaction
EDS	Energy Dispersive Spectroscopy

Chapter 1

Introduction

1.1 General

Concrete is the most widely used construction material all over the world and more so in the developing countries. As such there are global concerns of the environmentalists for depletion of non-renewable mineral deposits (limestone, silica, aluminates, ferric minerals etc.) used for manufacturing of cement. Besides amount emission of the greenhouse gas associated with burning of those minerals for cement production is ranked third as producer of anthropogenic (man-made) CO_2 in the world after transport and energy generation. Therefore, the need for low-cost and more environmental-friendly cementitous materials is gaining interest of the researchers. Different types of supplementary cementing materials (SCMs) are being used in many researches of late that can be used as partial or total replacements of the Portland cement. Such efforts of increasing or promoting the use of supplementary cementitious materials in cement production are of immense importance since cement production consumes high energy and is responsible for 5% of global carbon dioxide (CO_2) emission. Fairbairn et al. [1] reported that one ton of CO_2 is released for every ton of cement produced. It has now become a global concern to limit CO_2 release in the environment due to cement production. Moreover, many of the SCMs are by product of different industries that eventually cause waste management problems. Therefore, utilization of such waste materials as a supplement in cement manufacture makes cement production cleaner as well as solves problems associated with waste management. It is, therefore, evident that research on any potential supplementary cementitious material is of great importance both in terms of global and local context.

1.2 Background of the Study

One of the most effective ways to reduce the environmental impact of cement industry is to use mineral admixtures or SCMs as a partial replacement of cement in producing concrete. It has the potential to reduce costs, conserve energy and minimize emission of greenhouse gases. Mineral admixtures are found in various forms in nature, include fly ash (FA), silica fume (SF),

ground granulated blast furnace slag (GGBS), metakaolin (MK) which possess certain characteristics through which they influence the properties of cement. Agro based products like coconut shale, rice-husk ash, wheat straw ash have almost same potential of mineral admixtures. Amorphous silicon dioxide (SiO_2) present in such pozzolanic materials leads to the formation of additional calcium silicate hydrate(C-S-H). When it reacts with calcium hydroxide (free lime formed during cement hydration) and water, this is called secondary gel. This additional C-S-H, thus formed, increases the density of the matrix and improves the pore structure. It also leads to better durability of concrete and most of the time results in increase in strength [2]. The use of such mineral admixtures improves the strength, pore structure, and permeability of cement composites due to reduced total porosity as a result of late hydration [3]. The use of sugar cane bagasse ash (SCBA) as SCM is relatively new concept and is still to gain popularity. However, SCBA has potential to be used as SCM particularly in countries that grow sugar cane abundantly. Rauf et al. [4] reported that SCBA blended mortar has a good chemical composition and physical properties in terms of fineness, expansion, setting time and compressive strength. Shafiq et al. [5] reported that up to 20% SCBA content showed a remarkably high compressive strength compared to reference cement concrete and also remarkable improvement in tensile strength and bond strength with reinforcing bars. Amin [3] mentioned in his study that up to 20% of Portland cement can be optimally replaced with well-burnt bagasse ash without any adverse effect on the desirable properties. Some authors [6, 7, 8] also reported that blending of bagasse ash with cement increases pozzolanic activity and reduces interfacial transition zone porosity. However, the burning process and temperature required to produce suitable SCBA has not been elaborated in most of the available studies. Also, bagasse is found in two forms in Bangladesh; a) fresh bagasse from local juice producers and b) leached industrial bagasse. There has been no detailed study on production process of ash from these two sources of bagasse and their relative advantages and/or disadvantages with respect to cement industry. Hence, an in-depth research program has been designed and conducted in this study to address critical issues related to production of ash from local bagasse sources and utilization of produced ash within cement composites.

In Bangladesh, sugar cane is grown almost all over the country. The major sugarcane growing districts are Rajshahi, kustia, jessore, Dinajpur, Rangpur, Faridpur, Mymensingh, Tangail, jamalpur, and Dhaka. In Figure 1.1, the sugarcane production in Bangladesh from the year 1978 to 2017 has been shown. The sugar cane harvesting area in Bangladesh has fluctuated

substantially in recent years and showed a decreasing trend from 1978 to 2016 period. However, in 2017, a considerable increase in sugar cane production is observed which is equal to 124 MT.

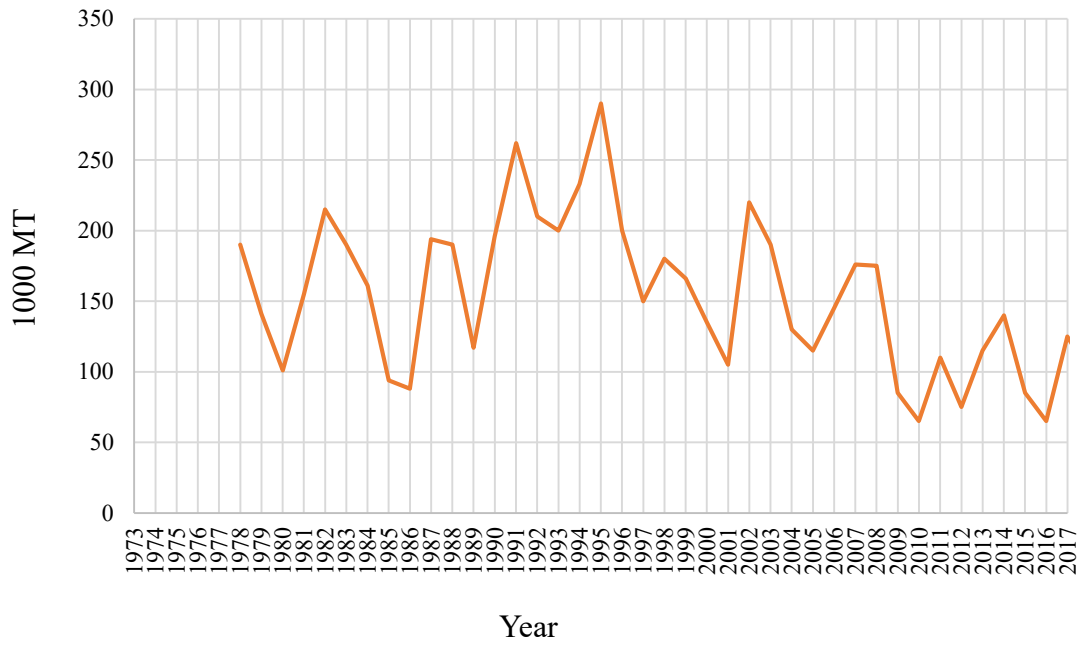

Figure 1.1 - Sugarcane Production in Bangladesh by Year [9]

The amount of sugarcane production in sugar mill area and local production outside the mill area is shown in Table 1.1. Sugarcane is cultivated on an area of about 0.16 million hectare of land. About 50% sugar cane cultivation area is located within the sugar mills zone. The remaining 50% cultivation area is outside the purview of the mill zone, where sugarcane is mostly diverted for jaggary and juice production. At present, 15 sugar mills are in operation under Bangladesh Sugar and Food Industries Corporation (BSFIC) with a capacity of 0.21 million tons of sugar production per year [10].

Table 1.1 - Sugarcane Production in Bangladesh [11]

Producti-on Year	Sugarcane Production Area (Thousand Hectare)			Sugarcane Production (Thousand Ton)			Production (Ton/Hectare)		
	Mill Area	Excluding mill Area	Total	Sugar mill Area	Excluding mill Area	Total	Mill Area	Excluding mill Area	Total
2012-13	65	43	108	3063	2056	5119	47.12	47.81	47.40
2013-14	70	48	118	3262	2249	5511	46.60	46.85	46.70
2014-15	63	42	105	2656	2300	4956	42.16	54.76	47.20
2015-16	52.42	32.1	84.52	2101	1548	3649	40.08	48.22	43.17
2016-17	47.71	66	113.7	2031	3182	5213	42.57	48.21	45.84

Sugarcane bagasse, shown in Figure 1.2, is the fibrous matter that remains after sugarcane or sorghum stalks are crushed to extract their juice. It is dry pulpy residue left after the extraction of juice from sugar cane. Bagasse is mostly used as a biofuel in the sugar mill for having high calorific value and in the manufacture of pulp and building materials (brick, lightweight partition panels etc.). In Figure 1.3, amount of bagasse that is generated each year in Bangladesh is shown.

Figure 1.2 - Sugarcane Bagasse

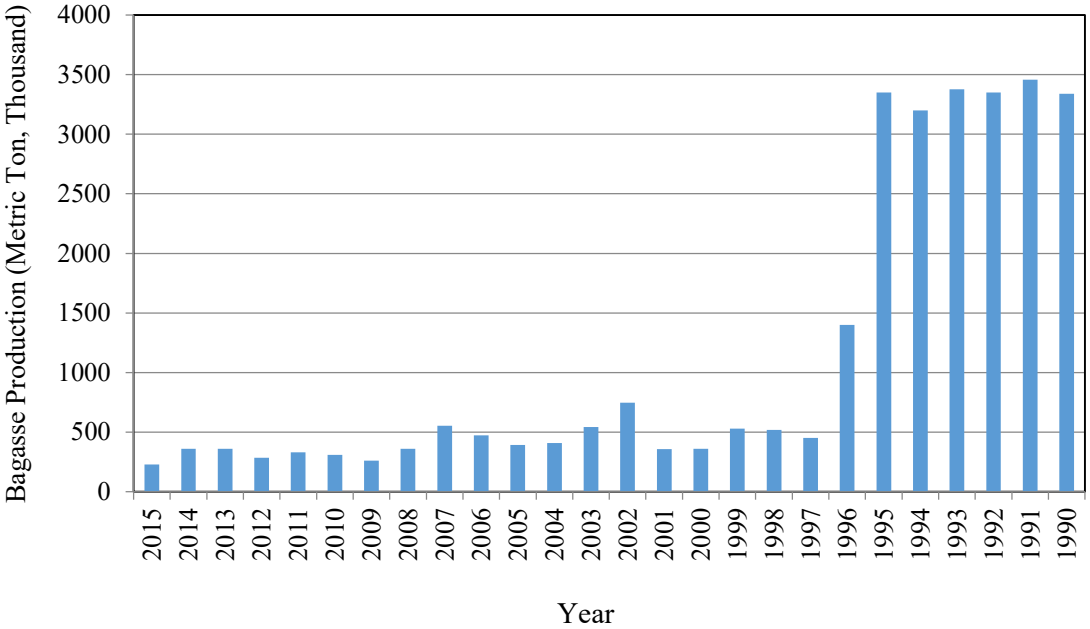

Figure 1.3 - Bagasse Production in Bangladesh [9]

A typical chemical analysis of washed and dried bagasse has the following constituents [12]:

- Cellulose 45–55 percent
- Hemicellulose 20–25 percent
- Lignin 18–24 percent
- Ash 1–4 percent
- Waxes <1 percent

So it is clear from dried bagasse composition that it has not significant nutrition value to increase the fertility of soil. Ganesan et al. [13] stated that 1 ton of sugarcane generates as much as 280 kg of bagasse. Based on economics as well as environmental issues, enormous efforts have been directed worldwide towards bagasse waste management like utilization, storage, transportation and disposal. In the industries, airborne ash from bagasse-fired boilers could also pose a respiratory health hazard although the exact nature of the hazard has not been yet determined Another related emission source is that SCBA which is often spread on sugarcane fields as a fertilizer or piled in waste dumps and is, therefore, prone to re-suspension by the wind. In Bangladesh, locally produced bagasse is used mostly as bio-fuel and the waste is left in open environment. This may cause serious health hazard. Besides, industrially dumped bagasse gets leached over the years due to rain water. The leached water, being alkaline in nature, affects the optimum pH level of soil. Besides The potential of power generation from bagasse by is around 100MWe in Bangladesh over the year [14]. If power generation is started using bagasse, country will face additional bagasse ash waste management problem. Considering the critical issues, blending bagasse ash with cement seems to be the most eco-friendly and cost-effective solution. With this end in view, this research initiative has focus on the potential of bagasse ash as supplementary cementitious material to produce composite cement in the country. The details of calcination of bagasse to obtain ash collected from different sources, their chemical composition, effect of calcination temperature on alkali and silica content, microstructural and morphological study of bagasse ash, effect of bagasse ash addition on cement properties like compressive strength, consistency, flow, drying shrinkage have been investigated and presented in this study.

1.3 Objectives

Since SCBA has pozzolanic properties and can be used to reduce the amount of cement clinker required to produce cementitious composite, influence of SCBA on cement composite properties need to be studied. Hence, the focus of this work is to investigate the effect of SCBA content on properties of cement composite. However, burning of bagasse to produce ash having desirable pozzalonic properties is another important aspect of this research. The study involves both the production issues of bagasse ash and experimental investigations on behavior of bagasse ash blended cement composite. The primary objectives of the study are as follows:

- To study the effect of temperature range on the chemical composition of bagasse ash (XRF test on specimens).
- To study the morphology and chemistry of bagasse ash by Scanning Electron Microscopy (SEM).
- To study the effect of use of sugarcane bagasse ash on compressive strength of cement mortar cube by partial replacement of cement at the ratio of 0%, 10%, 15% and 20% by weight.
- To study the effect of sugarcane bagasse ash on flow, shrinkage, and consistency of cement composite.

1.4: Methodology

Fresh bagasse ash was collected from local juice seller and industrial bagasse was collected from Faridpur Sugar mill. The bagasse was then burnt under various temperature ranges to find the optimum temperature to get maximum pozzolanic compounds. XRF analysis was conducted on each sample to get the percentages of chemical compounds. Bagasse ash after burning at suitable temperature found from analysis was then partially replaced in the ratio of 0%, 5%, 10%, 15% and 20% by weight of cement to produce cement mortar. ASTM Type I Ordinary Portland Cement (OPC) was used in all mixes. Mortar cubes were made varying the bagasse ash composition to test the compressive strength at 3, 7, 28 and 56 days as per ASTM C 109/C 109M [15]. Particle size and fineness of the bagasse ash is expected to influence the flow and consistency of cement paste. So the effects of bagasse ash addition within cement on flow,

consistency and shrinkage were studied as per ASTMC 596-01 [16], ASTM C 1437 – 07 [17], ASTM C 187 – 98 [18] standards, respectively.

1.5: Organization of the Thesis

For clear and through understanding of the work done, the entire thesis has been divided into five chapters. A brief description of each chapter is given below:

Chapter 1: This introductory chapter contains the background and objectives of the research. The methodology followed in the study has also been outlined briefly in this chapter.

Chapter 2: This chapter contains a concise and selective review of the relevant literature which provides brief discussion on physical properties and chemical composition at various temperature, particle size distribution, thermo-gravimetric analysis, microstructure and morphological analysis of bagasse ash and fresh and hardened properties of bagasse ash blended cement composite.

Chapter 3: This chapter describes the experimental investigations carried out in the present study. It includes production of ash from bagasse collected from different source and effect of different burning condition and temperature. The chapter also describes XRF analysis of bagasse ash for determination of chemical composition and SEM analysis for microstructure and morphological characteristics of ash. This chapter also incorporates compressive strength, consistency, drying shrinkage, and flowability test results of bagasse ash blended cement mortar.

Chapter 4: This chapter presents the various test results conducted in the study along with relevant discussion on obtained test results. It also discusses micro-structural studies to understand the mechanical properties of the bagasse ash blended cement mortar.

Chapter 5: Conclusions drawn from the present investigations are provided in this chapter. In addition, some relevant future research opportunities are also discussed. Finally, Appendix A and Appendix B are provided to include other relevant information from the study.

1.6: Scope of the Study

The study was performed to investigate the effect of bagasse ash on the behavior of cement mortar properties like compressive strength, workability, consistency and drying shrinkage. Variation of water/cement ratio in those experiments was not incorporated. All of the extracted siliceous ash was chemically analyzed by performing X-ray fluorescence (XRF) analysis. Apart from silica, other chemical compounds consisting calcined bagasse ash (Alkalis, Cl, C, P, Al etc.) have marked effect on the characteristics of cement. The percentage and allowable limits of those compounds as per codes have been discussed. However, no additional experiment was conducted in this research. The particle size of ash was approximated using SEM images. The energy-dispersive X-ray microanalysis (EDS) was performed for morphological and qualitative chemical characterization of the calcined bagasse ash in the study.

Chapter 2

Literature Review

2.1 Introduction

Studies have been performed to investigate the chemical composition and microstructure of sugarcane bagasse. Those studies clearly show that bagasse ash is very rich in silica content and it conforms the conditions to be used as a pozzolan in cement. Many researchers have used bagasse ash as a partially substituted material with cement and found its effect on the behavior of cement in terms of compressive strength, splitting and tensile strength, absorptivity, flow, shrinkage, permeability etc. The review of these studies along with the highlights has been discussed in the following sections. Thus this chapter presents the summary of research efforts on use of bagasse ash as SCM in cement.

Ganesan et al. [13] studied the effects of SCBA content as partial replacement of cement (0-30%) on physical and mechanical properties of hardened concrete. The properties of hardened concrete were investigated include compressive strength, splitting tensile strength, water absorption, permeability, chloride diffusion and resistance to chloride penetration. All tests were carried out in accordance with Indian Standards. The test results indicated that SCBA is an effective mineral admixture when it is blended up to 20%. The increase in strength may be partially due to the pozzolanic reaction.

Kawade et al. [19] studied the effect of using SCBA on strength of concrete by partial replacement of cement at the ratio of 0%, 10%, 15%, 20%, 25% and 30% by weight for compressive strength. If some of raw material having similar composition can be replaced by weight of cement in concrete then cost could be reduced without affecting its desirable properties. It was found that the cement could be effectively replaced with SCBA up to maximum limit of 15%. Blending cement by SCBA increases workability of fresh concrete; therefore use of super plasticizer is not essential. All tests were done in accordance with American Standards.

Chusilp et al. [20], examined the effect of bagasse ash as pozzolanic materials in concrete. The physical properties of concrete containing ground bagasse ash including compressive

strength, water permeability, and heat evolution were investigated. All tests were done in accordance with American Standards. When bagasse ash is ground up into fine particles, the compressive strength of concrete containing this ground bagasse ash improves significantly. The low water permeability values of concretes containing ground bagasse ash at 90 days were mostly caused by the pozzolanic reaction of ash. The higher the replacement fraction of Portland cement by ground bagasse ash, the longer the delay time to obtain the highest temperature rise. Concrete containing up to 30% ground bagasse ash had a higher compressive strength and a lower water permeability than the control concrete, both at ages of 28 and 90 days.

Dhengare et al. [21] Studied on Investigation into Utilization of Sugarcane Bagasse Ash as Supplementary Cementations Material in Concrete. This paper presents the use of sugarcane bagasse ash (SCBA) as a pozzolanic material for producing high-strength concrete. The utilization of industrial and agricultural waste produced by industrial processes has been the focus on waste reduction. Ordinary Portland cement (OPC) is partially replaced with finely sugarcane bagasse ash. The concrete mixtures, in part, are replaced with 0%, 10%, 15%, 20%, 25% and 30% of SCBA respectively. In addition, the compressive strength, the flexural strength, the split tensile tests were determined. The bagasse ash was sieved through No. 600 sieve. The mix design used for making the concrete specimens was based on previous research work from literature. The water – cement ratios varied from 0.44 to 0.63. The tests were performed at 7, 28, 56 and 90 days of age in order to evaluate the effects of the addition SCBA on the concrete. The test result indicate that the strength of concrete increase up to 15% SCBA replacement with cement.

Srinivasan et al. [22] studied chemical and physical characterization of SCBA, and partially replaced in the ratio of 0%, 5%, 15% and 25% by weight of cement in concrete. Compressive strength, split tensile strength, flexural strength and modulus of elasticity at the age of 7 and 28 days was obtained as per Indian Standards. It was found that the cement could be advantageously replaced with SCBA up to a maximum limit of 10%. Therefore it is possible to use sugarcane bagasse ash (SCBA) as cement replacement material to improve quality and reduce the cost of construction materials such as concrete.

Chaysuwan et al. [23] studied the use of bagasse ash as a replacement for silica in ordinary Portland cement. With a cement to bagasse ash ratio of 70:30 by weight, the sample gave excellent results for both mechanical and physical properties as compared to the control sample. It was also shown from the microstructure that the presence of bagasse ash definitely reduced the porosity of samples. Consequently, the bending strengths were improved for samples replaced with 30% bagasse ash.

Hailu et al. [24] studied the application of sugarcane bagasse ash as a partial cement replacement material. OPC and PPC was replaced by sugarcane bagasse at different % ratio for M-35concrete at w/c ratio 0.55. The test results indicated that up to 10% replacement of OPC cement by bagasse ash results in better or similar concrete properties and further environmental and economic advantages can also be exploited by using bagasse ash as a partial cement replacement material.

Somna et al. [25] studied the utilization of a pozzolanic material to improve the mechanical properties and durability of recycled aggregate concrete. Ground bagasse ash (GBA) was used to replace Portland cement at the percentages of 20, 35, and 50 by weight of binder. SCBA used to replace natural coarse aggregate not more than 25% by weight. When GBA was used to partially replace cement in recycled aggregate concrete, the chloride penetration decreased and was lower than those of control concrete at the same immersed time. Compressive strength, modulus of elasticity, water permeability, and chloride penetration depth of the concretes were determined as per American Standards. Recycled aggregate concrete by incorporating SCBA has the modulus of elasticity, lower than that of the conventional concrete by approximately 25–26%.

Otuoze et al. [26] concluded that SCBA was a good pozzolan for concrete cementation and partial blends of it with OPC could give good strength development and other engineering properties in concrete. An optimum of 10% SCBA with OPC could be used for reinforced concrete with dense aggregate. The replacement of cement by SCBA was 0-30% and in accordance with American and Brazilian Standards all tests were carried out.

Lavanya et al. [27] examined the partial replacement for cement in conventional concrete. The tests were conducted as per Bureau of Indian Standards (BIS), IS 516-1959 codes to evaluate the suitability of SCBA for partial replacements up to 30% of cement with varying water cement (w/c) ratio .The physical properties of SCBA were studied. Compressive strengths (7, 14 and 28 days) were determined in accordance with Indian Standards. The results showed that the addition of sugarcane bagasse ash improves the strengths in all cases. The maximum strength increase happens at 15% with 0.35 w/c ratio.

2.2 Physical properties of Bagasse Ash

The basic characteristics such as specific gravity and mean grain size of sugarcane bagasse ash are usually lower than those of the ordinary Portland cement (OPC) while specific surface area may be higher that of OPC. These physical properties also influence the mix proportions and different properties of SCBA blended concrete are discussed below.

2.2.1 Density

The density basically defines as the mass per unit volume. The density of RHA and SCBA depends on the constituents (iron, silica, aluminium and calcium) and higher carbon content tents to lower the density. Aigbodion et al. [28] mentioned that the sugarcane bagasse ash is very light weight material and its density normally about 1.95g/cm^3. The obtained density value fall within the category of carbon and silica which is 1.8 and 2.2 g/cm3 respectively [29, 30].

2.2.2 Specific Gravity

Specific gravity is the ratio of the density of a substance to the density of a reference substance; equivalently, it is the ratio of the mass of a substance to the mass of a reference substance for the same given volume. Specific gravity of SCBA is reported to be lower

than that of OPC as shown in Table 2.1. It is found to vary from 1.8 to 2.35 with mineral composition (source of SCBA) and temperature SCBA was exposed to.

Table 2.1 - Specific gravity in various studies

Authors	Specific gravity	Temperature exposed to SCBA
Ganesan et al. [13]	1.81	600 ° C
Montakarntiwong et al. [31]	1.91	-
Rukzon, S. et al. [32]	2.25	750 ° C
Aprianti et al. [33]	1.90	400 ° C
Sua-iam, G. et al. [34]	2.35	850 ° C

The specific gravity is important in determining concrete mix design and gives an indication of the volume of material used, which in turn will influence the consistency of concrete [35].

2.2.3 Blaine's Specific Surface Area

From the literature in Table 2.2, it is seen that the Blaine's air permeability of bagasse ash is higher than that of cement, and all the blended powders show a higher fineness than cement which may be due to the lower density of the bagasse ash and its small particle size. Ajay Goyal et al. [36] has reported that large specific surface area favors pozzolanic reactivity of amorphous silica and other minerals, and also nucleation reaction. From the table it can be seen that the blain air of the bagasse ash is higher than that of cement, and all the blended powders show a higher fineness than cement which is due to the lower density of the bagasse ash.

Table 2.2: Blaine's specific surface area of SCBA in various studies

Authors	Blaine's specific surface (m^2/kg) area(m^2
Ganesan et al. [13]	943
Montakarntiwong et al. [31]	940
Rukzon, S. et al. [32]	1240
Aprianti et al. [33]	140 (Raw SCBA)
Sua-iam, G. et al. [34]	274 (Raw SCBA)

2.3 Chemical Composition of Bagasse Ash

SCBA is termed an aluminosilicate because of the presence of silica (SiO_2) and alumina (Al_2O_3), however silica is the major constituent. Silica in SCBA, may present in two different phases, either a crystalline phase usually in a form of quartz or cristobalite an amorphous phase, and is highly dependent on combustion conditions and processing methods [1]. Hence, in some cases the major phase of silica present is crystalline [37, 38] and in other cases the silica is in substantially amorphous phase [13, 20]. The distinction between amorphous and crystalline silica is important for determination of its potential reactivity; amorphous phase silica is reactive for pozzolanic applications [1] whereas crystalline silica will be suitable for zeolitic applications [39] or as a filler replacement in concretes [40].

Table 2.3: Chemical composition of the bagasse ash

Researcher	SiO_2	Al_2O_3	Fe_2O_3	CaO	MgO	SO_3	Na_2O	K_2O	LOI
Sua-iam et al. [34]	65.2	6.9	3.7	4	1.1	0.2	0.3	2	15.3
Montakarntiwong et al. [31]	76.8	4.4	8	5.4	0.9	0.1	N.R.	N.R.	3.3
	67.1	5.7	2.5	2.9	0.5	0	N.R.	N.R.	20.4
Castaldelli et al. [37]	31.4	7.6	6	16.1	1.1	0.8	0.1	1.6	32.2
Cordeiro [1]	78.3	8.6	3.6	2.2	1.7	N.R.	0.1	3.5	0.4
Frias et al. [38]	66.6	9.5	10.1	1.4	0.9	0.1	0.2	3.2	4.3
Martirena Hernández et al. [41]	72.7	5.3	3.9	8	2.8	0.1	0.8	3.5	0.8
Ganesan et al. [13]	64.2	9.1	5.5	8.1	2.9	N.R.	0.9	1.4	4.9
Sumrerng Rukzon & Chindaprasirt [32]	65	4.8	0.9	3.9	N.R.	0.9	N.R.	2	N.R.
Sales & Lima [40]	88.2	2.3	5.1	0.6	0.4	<0.1	0.1	1.3	0.35
Affandi et al. [42]	50.3	N.R.	18.8	8.8	N.R.	N.R.	N.R.	19.3	N.R.
Akram et al. [43]	62.4	6.8	5.8	6.2	3	0.7	3.2	6.9	2.6

Researcher	SiO_2	Al_2O_3	Fe_2O_3	CaO	MgO	SO_3	Na_2O	K_2O	LOI
Janjaturaphan & Wansom [44]	76	5.3	2.2	3.9	1.2	0.2	0	3.1	6.6
	77.2	4.7	2.1	3.3	1	0.2	0	2.6	7.5
	75.3	5.4	2.5	3.7	1.2	0.1	0	2.8	7.2
	74.7	4.9	2.1	3.8	1	0.3	0	3	8.6
Lima et al. [45]	96.2	<1.9	<1.9	0.1	<0.1	0.1	<0.3	<0.3	1.04
Payá et al. [46]	59.9	20.7	5.8	3.4	1.9	1.1	1.1	1.4	0.6
Purnomo et al. [47]	50	2.2	1.2	2.8	1.7	N.R.	N.R.	4	37.5
Rehab & El Anany [48]	76.8	N.R.	0.4	9	7.5	N.R.	3.2	N.R.	N.R.
Salim et al. [49]	73	6.7	6.3	2.8	3.2	N.R.	1.1	2.4	0.9
Singh, N.B et al. [50]	63.2	9.7	5.4	8.4	2.9	2.9	N.R.	N.R.	6.9
Tantawy et al. [51]	61.7	11.6	9.8	5.6	3.2	0	1.1	0.5	1.4
Teixeira et al. [52]	85.6	5.3	1.3	2.1	1.1	N.R.	N.R.	3.5	N.R.
Tonnayopas [53]	38.3	2.8	3.4	10.8	0.9	0.5	N.R.	1.8	40.2

* N.R. = Not Reported

The chemical composition of bagasse ash, as reported by some of the authors is reported in Table 2.3. It is seen that silica constitutes major component of bagasse ash in all the

investigations. High specific surface area and chemical composition (SiO_2+Al_2O_3+Fe_2O_3>70%) and CaO >10% suggest that it is a Pozzolanic and cementitious material respectively according to ASTM C-618 specifications. The loss on ignition (LOI) value for the bagasse ash as reported varied from 0.4% to 37.5 %.depending upon the temperature SCBA was exposed to and its source. Bagasse ash in Bahuruddin et al. [35] was found to have high alkali content (K_2O) implying high potential for alkali-silica reaction when used in concrete with silica rich aggregates.

2.4 Heat of Hydration

Cement hydration is mainly understood by the rate of heat evolution and the hydration products. Higher CSH and its density produce greater strength. High rate of heat evolution causes thermal cracking due to the temperature gradient and thermal stresses. Heat evolution of concrete, considering the water cement ratio to be constant is primarily due to:

- Chemical characteristics of cement
- Physical characteristics of cement
- Mineralogical characteristics of cement.

The key factors on which the hydration process of bagasse ash blended cement matrix depends are specific surface area of the bagasse ash in the matrix and amount of bagasse ash relative to that of cement. The total heat liberated in control specimen was found to be higher (285 kJ/kg) than that liberated in blended concrete specimens at 10% replacement level (215 kJ/kg) at 5 days. Further reduction was observed for 20% replacement. The reason for this is attributed to the significant reduction in the content of C_3A and C_3S due to the replacement of cement with bagasse ash [35]. Heat of hydration of concrete with 20%, 30% and 40% SCBA when measured by inserting a thermocouple at the center of the concrete specimen (creating adiabatic condition) had a temperature rise of 7.5 ^{o}C, 6.1 ^{o}C and 5.5 ^{o}C. The temperature of concrete can be reduced by 4 ^{o}C - 11 ^{o}C when cement was replaced with bagasse ash. Also, the time in obtaining the peak temperature was delayed up to 3 hours [20].

2.5 Compressive Strength

The variation in strength may be attributed to various factors such as water-binder ratio, replacement level, curing conditions, etc. Compressive strength test are generally conducted on 7, 14, 28 and 90 days. The compressive strength of SCBA blended concrete specimens showed an increase up to the replacement level of 20% in most cases and decreased for higher replacements at all curing periods [1, 13, 20]. The increase in compressive strength up to 20% may be due to the fineness, high specific surface area, degree of reactivity of bagasse ash and also the pozzolanic reaction of the bagasse ash. The later age strength is attributed to the hydration process of cement to form additional C-S-H and improves the interfacial bond between aggregates and paste. These characteristics tend to improve the compressive strength [31].

2.6 Thermo-gravimetric Analysis

The distributions of TGA and the derivative thermogravimetric (DTG) analyses of raw bagasse at at three different heating rates are displayed in Figure 2.1. It was observed that mass loss of 8.4, 8.7 and 7.4 mass% at 5, 7.5 and 10 C min-1, respectively occured. This mass loss is associated with water evaporation, and then, a slight mass loss took place which could be due to the loss of volatiles. Thermal decomposition and degradation for biomass samples in air and nitrogen atmosphere initiated at corresponding anticipated temperatures of 236, 210 ^{o}C , and these variations in initial degradation temperatures of biomass have been related to the differences in the elemental and chemical compositions of the samples and degradation or decomposition processes. Total mass loss due to total degradation was higher in those samples which have higher volatile matter and lower ash content [54]. It was reported (Yang et al.[55]; Chen et al. [56]) that the decomposition temperatures of hemicellulose, cellulose, and lignin were in the ranges of 200–315, 315–400, and 160–900 ^{o} C, respectively, stemming from their inherent difference in lignocellulosic structure. When the temperature is higher than 400 ^{o}C, the continuous and slow decomposition of the biomass can be explained by lignin decomposition in a high temperature environment. The TGA curve indicates that over 78 wt. % of bagasse is

thermally degradated when the reaction temperature is beyond 400 ° C. It follows that the bagasse pyrolysis should be performed at temperatures higher than 400 ° C. For this reason, bagasse pyrolysis at three reaction temperatures of 400, 480,700 and 850 ° C are taken into account in the present study. Langan et al. [57], Pane and Hansen [58] reported that differential thermal analysis (DTA) combined with thermo-gravimetric analysis (TGA) is more suitable for studying the hydration or pozzolanic reaction that takes place at later stages of hydration.

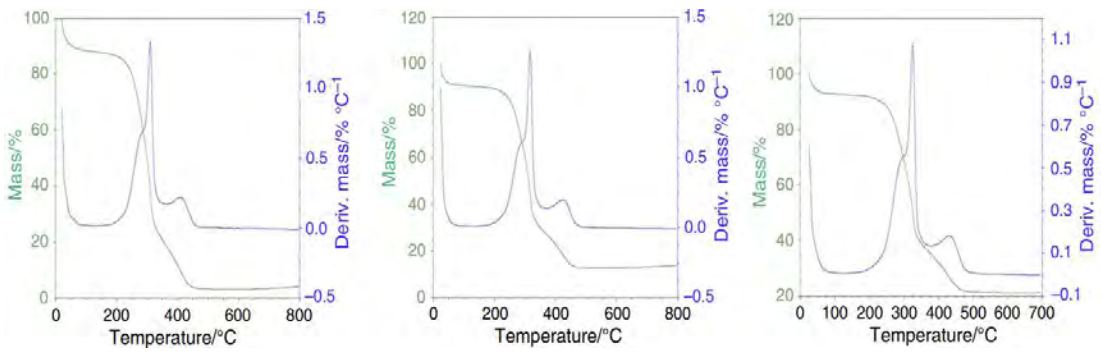

(a) 5 ° C min-1 (b) 7.5 ° C min-1 (c) 10 ° C min-1

Figure 2.1: TG and DTG curves of SCB at three different heating rates and oxidative atmosphere [54]

2.7 Pozzolanic Activity of Bagasse Ash

Pozzolanic properties of bagasse ash generally get affected by the temperature at which ash was formed or exposed to and size of particles also. Sometimes, different methods are employed to improve the pozzolanic property. The most common ones are described the following sections.

2.7.1 Effect of Burning

Manusanthanam et al. [59] reported that raw bagasse ash has a strength activity index of 71% and 72% at 7 days and 28 days respectively and so SCBA is not acceptable as pozzolanic material as the index is less than 75%. This might be due to the presence of unburnt coarse fibrous particles and hence, burning under controlled conditions up to a temperature 700°C is suggested to get desired pozzolanic properties. White particles (formed by the burning of the ash at higher temperatures) are found to be more reactive due to the presence of prismatic particles as observed in microstructure of thermally treated bagasse ash.

Bagasse ash waste powder contains a significant amount of silica and this amount increase with increasing temperature. Table 2.4 shows chemical composition of the bagasse ash with increasing calcination temperature. The carbon and volatile compounds present in the SCBA are expected to be considerably removed at higher calcinations temperature. Thus at higher calcination temperature the chemical compositions of the calcined SCBA is seen to resemble that of Class F coal fly ash especially in terms of the total of alumina, silica and ferric oxide content. Therefore, it may behave like class F Fly ash in its properties.

Table 2.4: Chemical composition of bagasse ash with increasing calcination temperature [60]

Oxides (%)	Raw SCBA	400°C	600°C	800°C	1000°C
SiO_2	60.75	62.55	61.93	62.57	62.40
Al_2O_3	4.14	4.31	4.44	4.70	5.02
Na_2O	0.77	0.66	0.74	0.86	0.83
MgO	2.39	2.20	2.43	2.34	2.27
P_2O_5	3.39	3.37	3.42	3.40	3.46
SO_3	1.81	1.70	1.73	1.71	1.79
K_2O	14.63	14.37	14.25	13.86	13.40
CaO	4.48	3.56	3.71	3.49	3.69
Fe_2O_3	5.27	4.88	5.01	4.87	5.71

The burning of organic materials containing higher amounts of silica in their cuticle parts produced crystallization of amorphous silica which gradually converted to different phases of silica with the increase in temperature [61]. The XRD patterns showed a remarkable difference between calcined and raw SCBA, which suggests that phase silica (quartz) is the primary component with small amounts of calcium compound at the temperature of 400 and 600 ^{o}C. At 800 ^{o}C, some sharp and intense peaks started (quartz and sillimanite) to show up, which implies that the crystallinity increases as temperature rises. Ribeiro and Morell [62] also reported similar observation on SCBA.

2.7.2 Effect of Grinding

Fineness also influences the reactivity of pozzolanic material. Bahuruddin et al. [35] studied the effect of grinding of raw bagasse ash when it was ground to different particle sizes ranging from 210 µm to 45µm. Results showed that the most grounded material had the lesser pozzolanic activity index than the raw bagasse ash which contradicts with other pozzolanic materials such as rice husk ash and fly ash. He observed that the samples grounded to 45µm size had higher pozzolanic activity at 28 days. Thus, he concluded by saying that the minimum requirement to achieve pozzolanic activity index of 75% should be 53µm.

2.8 Particle Size Distribution

Sugar-cane bagasse ash typically presents as a grey to black porous ash with a combination of both fine and coarse particles. The fine fraction is the completely burnt, high in silica, particles whereas the coarse fraction is the unburnt, and partially burnt, high in black carbon particles [35]. SCBA is a fine aggregate with similar particle size distributions to a fine sand (Aigbodion et al., [28]; Sales & Lima [40]). The particle size typically falls in the 1 - 100 µm range with an average particle size between 20 µm and 70, which is larger than the average ordinary Portland cement (OPC) particle size of around 16 µm [1,37].

Additional strength gain and a significant reduction in permeability was reported by Bahurudeen et al. [35]for blended cement concrete compared to control concrete because of pore refinement, enhancement in the interfacial transition zone as well as additional Calcium Silicate Hydrate (C-S-H) formation. The particle size distribution of sieved and ground bagasse ash is presented in Figure 2.2 and compared with the ordinary portland cement used in that study.

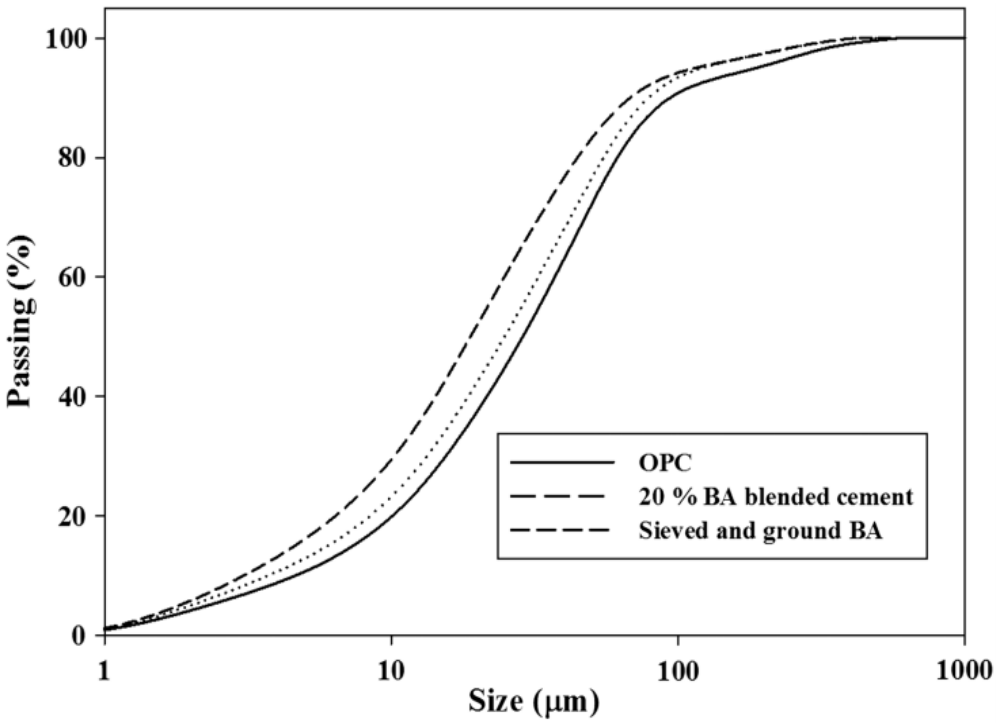

Figure 2.2 - Particle size distributions of OPC and 20% SCBA blended cement [35]

Recognizing the need to investigate how particle size influences the pozzolanic potential of SCBA, Cordeiro et al. [1] studied the effect of grinding on the pozzolanic activity index (PAI) of SCBA.

Reduced particle size and increased surface area resulted in increased pozzolanic activity classifying SCBA as a pozzolan. Cordeiro et al. [1] pointed out that the increased

pozzolanic activity was not from a phase change from crystalline to amorphous silica, rather the pozzolanic activity is dependent on the particle size of the SCBA.

2.9 Morphology

Morphology of SCBA is highly dependent on the burning temperatures in the combustion chamber. High temperatures (>700 ˚C) will tend to produce greater amounts of molten spherical particles and lower temperatures lead to an increase in fibrous irregular and prismatic shaped particles [37]. Incomplete combustion of bagasse yields irregular particles with a similar morphology to the bagasse fibers. Complete combustion produces a fine powder because the fibrous structure collapses [46]. Furthermore, when combustion temperatures are high, particles may present as molten with porous air bubbles. Prismatic particles are indicative of silica, spherical particles are indicative of silica in the presence of a metal usually aluminium, iron or calcium and fibrous particles are indicative of carbon [28]. SCBA particles are often porous with uneven surfaces [1, 46]. Bottom boiler ash is high in coarse and irregular particles and fly ash particles collected from filtration systems are finer [38].

The variations in SCBA particle morphologies are evident in the scanning electron microscopy (SEM) images from various researchers, which show spherical, prismatic, fibrous and irregular particles as shown in Figure 2.3. In the context of SCBA in concrete spherical smooth particles with low porosity will reduce friction leading to increased workability in concrete whereas porous and irregular particles increase friction and water demand leading to reduced workability in concrete [63].

Hence SCBA is an aluminosilicate material with varying amounts of silica and carbon content. The phase of silica is sometimes substantially crystalline and sometimes amorphous. SCBA has both coarse and fine particles, is lightweight and often porous. These properties are highly dependent on combustion and processing methods [1].

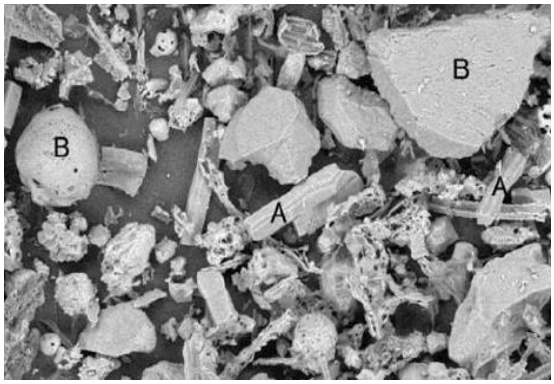

Figure 2.3(a) - SEM images of SCBA from varied sources showing prismatic particles (A); spherical particles (B); fibrous particles (C); irregular particles and non-spherical particles [64]

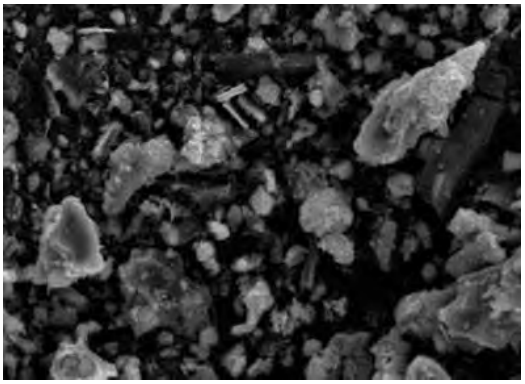

Figure 2.3(b) - irregular, tubular and porous particles [47]

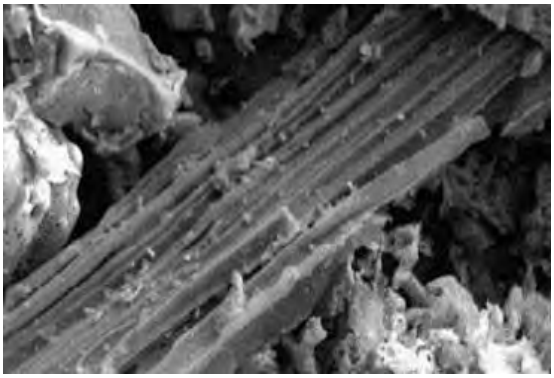

Figure 2.3 (c) - prismatic, porous irregular [20]

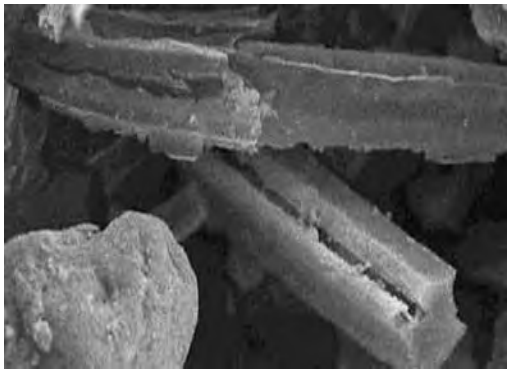

Figure 2.3 (d) partly spherical particles [34]

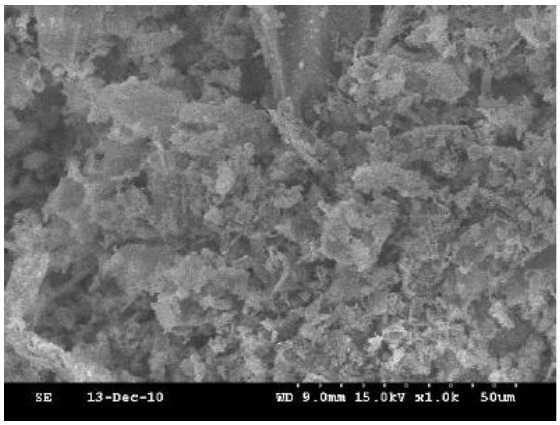

Figure 2.4(a) - Bagasse Ash (x1000) [7]

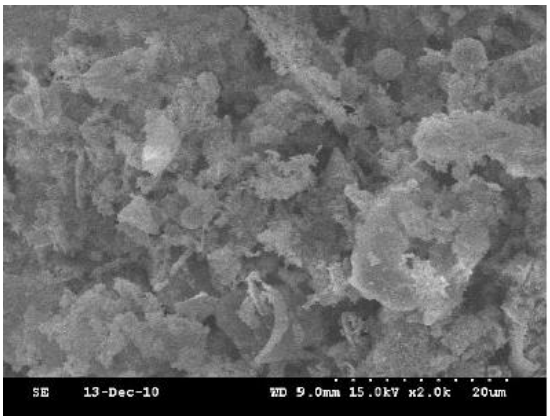

Figure 2.4(b) - Bagasse Ash(x2000) [7]

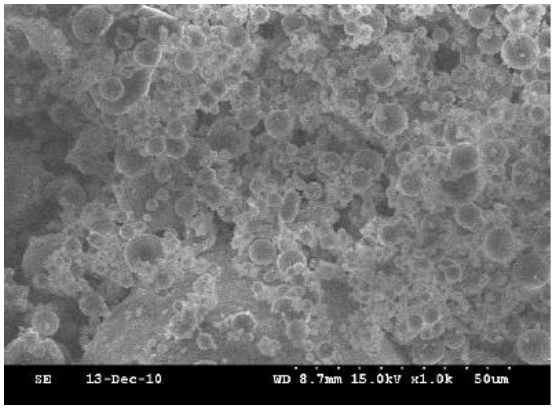

Figure 2.4(c) - Fly Ash (x1000) [7]

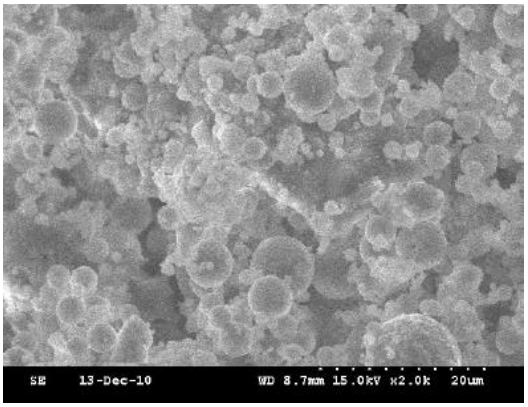

Figure 2.4(d) - Fly Ash (x2000) [7]

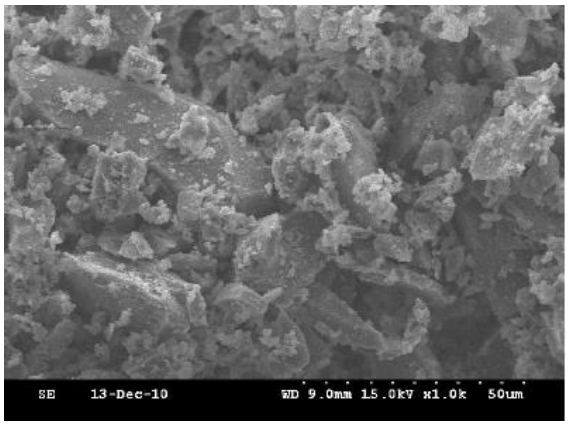

Figure 2.4(e) - Slag Ash (x1000) [7]

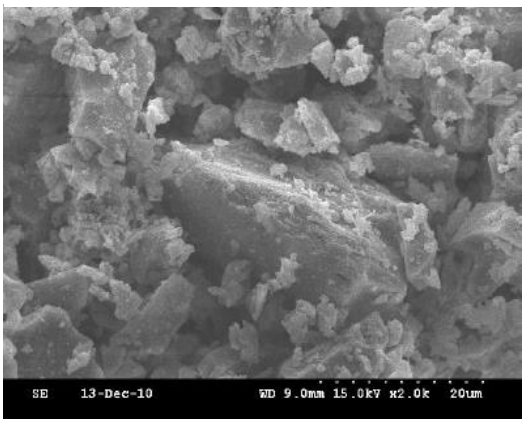

Figure 2.4(f) - Slag Ash (x2000) [7]

The SEM images of the SCBA, FA, and SA morphology is shown in Figure 2.4(a,b,c,d,e,f). The SCBA morphology was irregular with few spherical particles attached to it. The FA morphology revealed complete spherical particles, whereas the SA

morphology revealed broken particles. The morphology of the three types of powder differed substantially; thus, the hydration effect on the powders differed [7].

Shafiq et al. [8] have studied microstructure of Sugar Cane Bagasse Ash Concrete. The study is regarding the effectiveness of replacement of sugar cane bagasse ash along with cement. Bagasse ash was replaced with ordinary Portland cement at 0, 5, 10, 15, 20, 25 and 30% respectively. Effect of ash on workability, compressive strength and microstructure of Interfacial Transition Zone (ITZ) of concrete was examined as shown in Figures 2.5-2.12. The results showed that inclusion of Sugar cane Bagasse Ash in concrete up to 20% level significantly enhanced the compressive strength of concrete at all ages; the highest compressive strength was obtained at 5% SCBA replacement level. It was observed that at 15% bagasse ash replacement level, the interfacial transition zone was homogeneous and there was almost no gap between the coarse aggregate and the paste matrix. Optimum replacement is considered as level up to 20% SCBA in concrete. In the new cement mix of 25% and 30%, SCBA improved the compressive strength after 28 days.

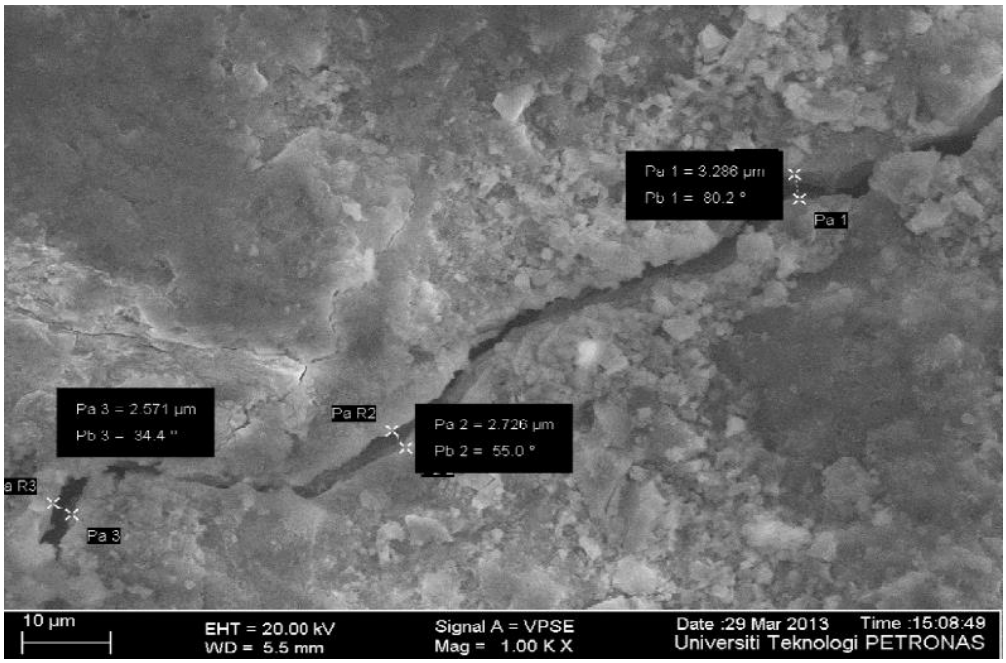

Figure 2.5: - ITZ thickness measurements [8]

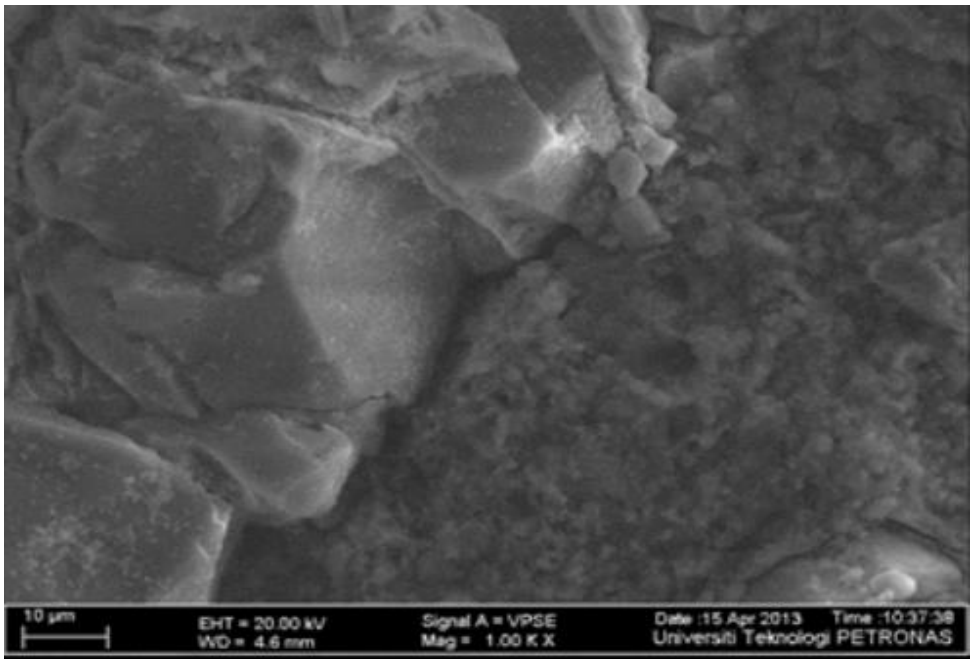

Figure 2.6 - FESEM image of 5% SCBA [8]

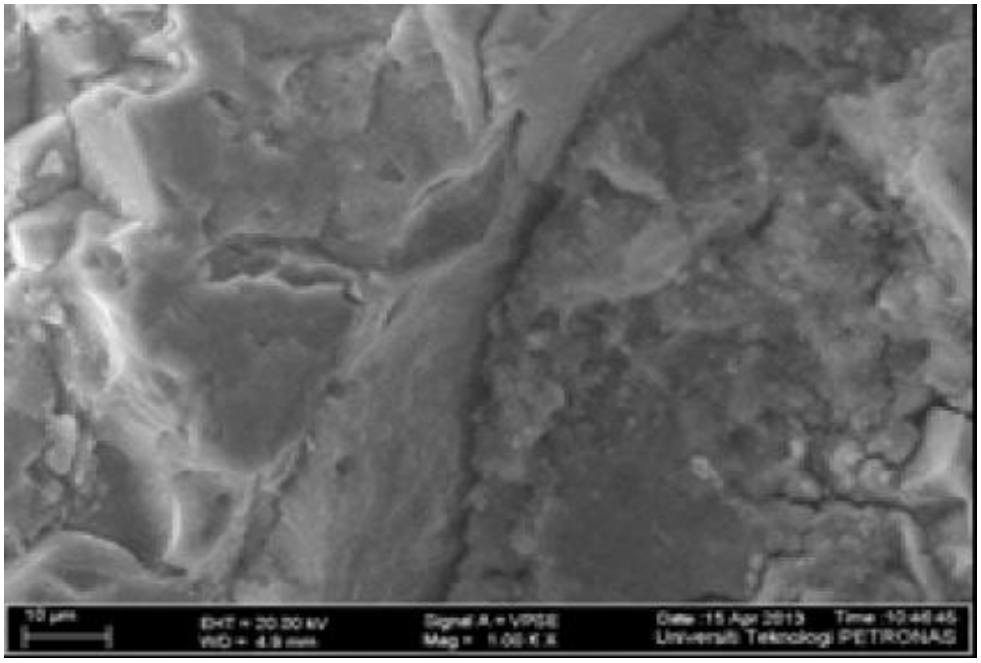

Figure 2.7 - FESEM image of 10% SCBA [8]

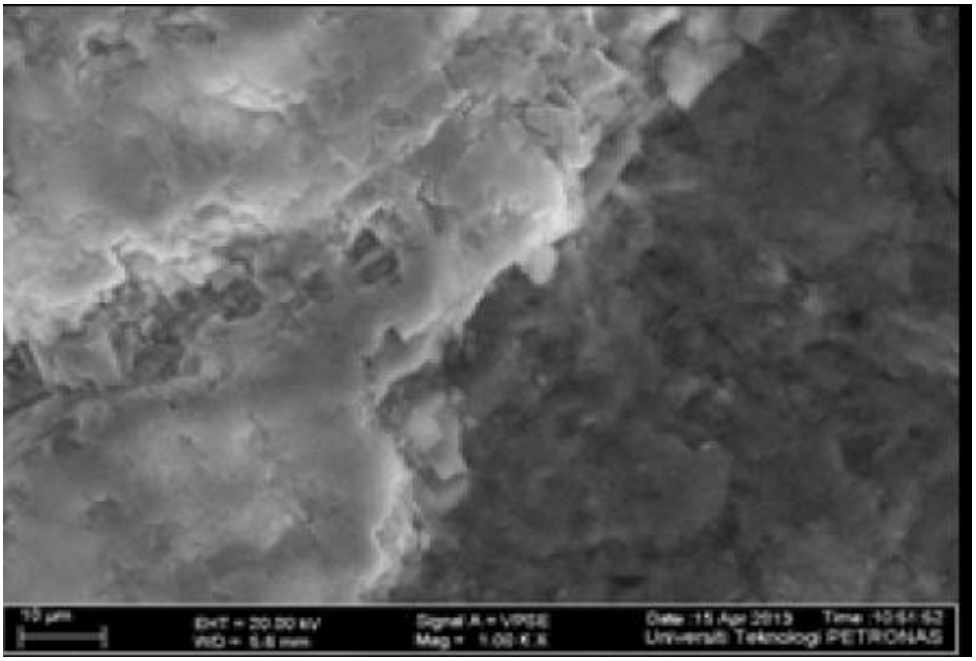

Fig. 2.8: FESEM image of 15% SCBA [8]

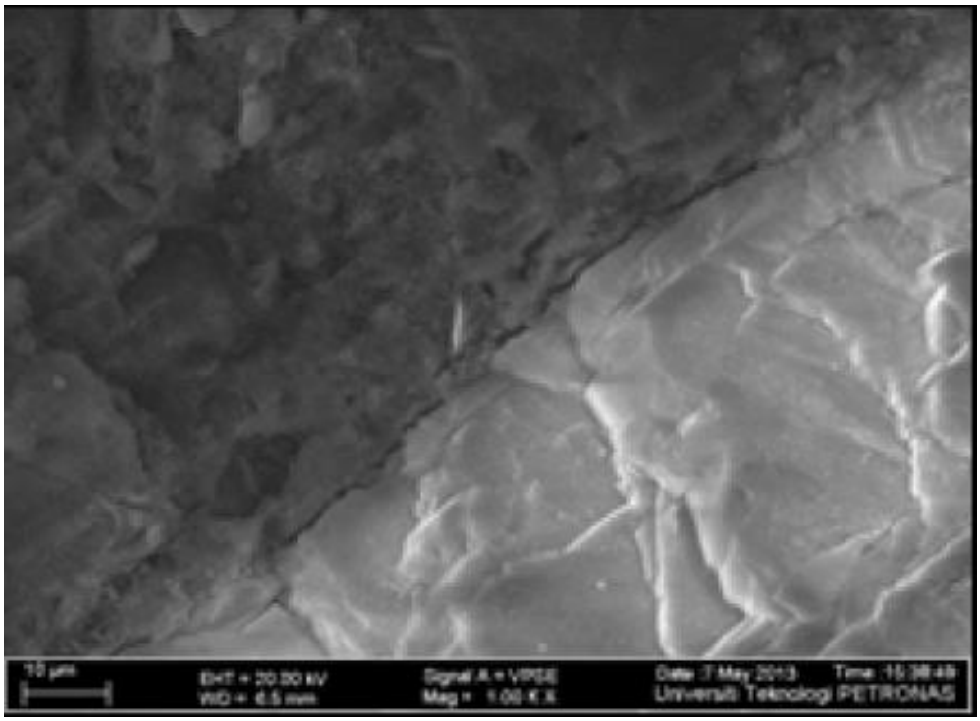

Fig. 2.9: FESEM image of 20% SCBA [8]

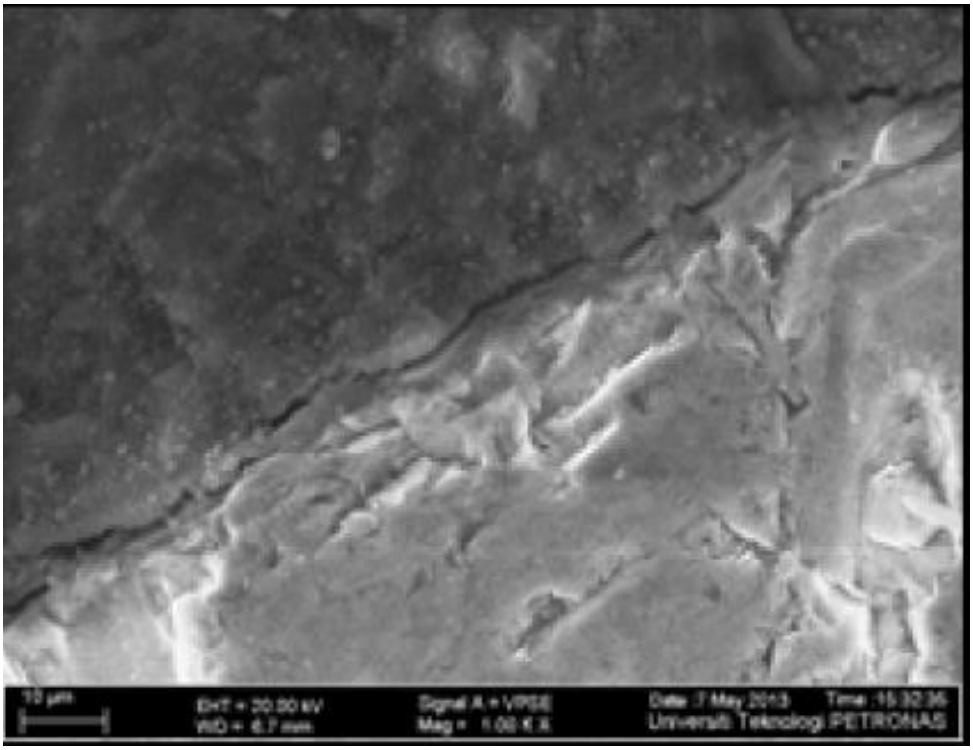

Fig. 2.10: FESEM image of 25% SCBA [8]

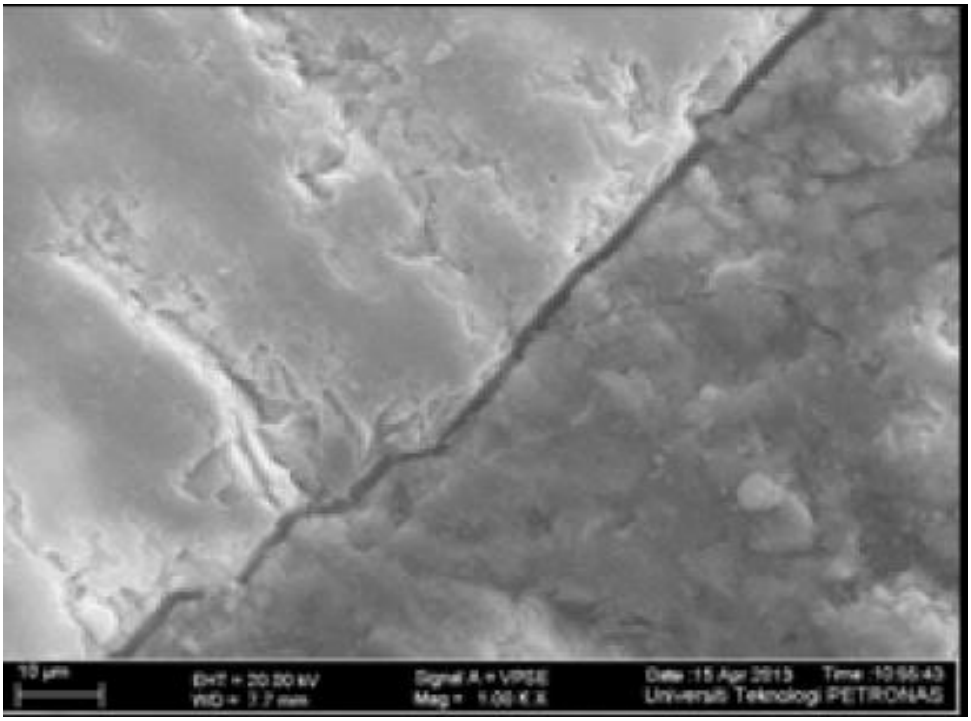

Figure 2.11: FESEM image of 30% SCBA [8]

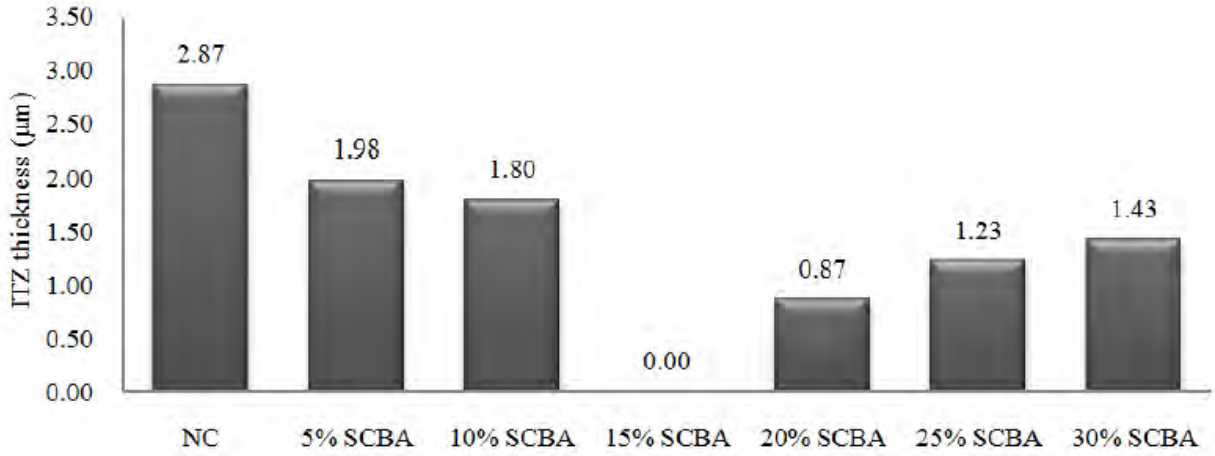

Figure 2.12: Effect of SCBA on ITZ thickness [8]

This interfacial transition zone is known to generally measure 15–20 µm in width in PC-based materials, surrounding each aggregate particle [65]. A key feature of the ITZ is that it often contains a deficit of large cement grains that cannot physically pack close to the aggregate, i.e., the "wall effect" [66], leading to a higher effective water/binder ratio than in the bulk paste.

Chapter 3

Experimental Investigations

3.1 Introduction

Experimental investigations were carried out to study the behavior of bagasse ash blended cement. Before that vigorous studies were performed to extract bagasse ash with maximum silica content and to find suitable burning temperature range. Since accumulation of mineral nutrients in sugarcane depends largely on climatic condition, applied doses of fertilizers, geography and temperature of the region, chemical composition of bagasse ash should vary based on the previously stated parameters. The K_2O doses in raw cane may be of the order of 0.81.0 kg/t of harvested cane K_2O, resulting in the relation N/K_2O of 1.0-1.3/1.0 [67]. Such high reactive N, K and volatile compounds get depleted when bagasse is left in open atmosphere as bagasse has quick exothermic fermentation tendency. So bagasse ash was chemically analyzed collecting from different sources and different fermentation periods. Based on literature, the proportions of bagasse ash with respect to weight fractions were taken as 0%, 5%, 10%, 15% and 20% to get optimum replacement level. This chapter includes plan of experiments, material properties, mortar mix proportioning, and details of testing.

3.2 Characterizations of Bagasse Ash

For this study, locally produced fresh and industrial fermented bagasse were collected. Local method of juice extraction from sugarcane is basically pressing method which is very easy and less costly. This Pressed cane stalks, or "farm bagasse" is obtained from on-farm or small factory cane fractionation that uses only 2 or 3 crushers. Due to the reduced efficiency of the extraction process (50% vs. 70% extraction rate), it contains higher amounts of sugar-rich juice. Upon drying in open air reduces the moisture content of bagasse but contains surplus amount of alkali matters from sugarcane juice like calcium and potassium unless no leaching has occurred. On the contrary, in most sugar factories, prepared cane is initially crushed using a conventional six-roll milling unit, consisting of six circumferentially grooved rolls, ranging 1-1.4 meters in diameter and 1.8-2.7 meters in length. Roll milling unit of Faridpur Sugar Mill have been shown in Figure 3.1.Cane stalks are feed in the conveyor belt and the roll milling

units apply high level of compressive stress to extract maximum level of sucrose. After that bagasse is rewetted (or macerated) with a hot water solution between further successive milling units to dissolve the soluble sugar and minerals. Alternatively in some industries, the moist bagasse is placed in a diffuser, where it is saturated with high temperature solution for the purpose of diffusing the soluble sugars from cane fiber. The principle of the diffuser is the application of imbibition water in the cane for the extraction of the juice through a lixiviation process. The water and the juice, re-circulated in the equipment, are heated with low pressure steam (2 bar or lower). There are also dewatering mills at the piece of equipment exit that are used as pre-dryers, reducing the moisture of the bagasse to approximately 50% and extracting the remaining juice for re-circulation [68]. Regardless of the intermediate extraction procedure employed, all bagasse is finally dewatered with six-roll milling unit in order to minimize the moisture content of final bagasse. Reducing the moisture content of final bagasse increases its calorific value and hence the efficiency of the boilers and co-generation plants which utilize bagasse as a fuel. Hence, chemical composition of ashes collected from different bagasse sources varies.

(a) Roll mill

(b) Extraction unit

Figure 3.1: Roll milling unit at Faridpur sugar mill.

For this study, fresh bagasse was collected from local juice seller. Bagasse was dried immediately after collection in open air and burnt. A black colored with heavy carbon content ash was obtained as shown in Figure 3.2.

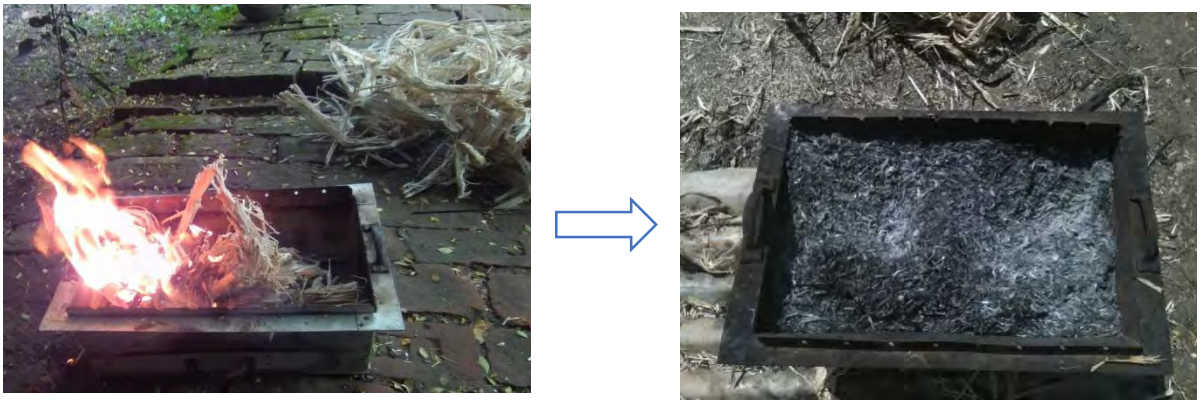

(a) Self burning of bagasse (b) After burning

Figure 3.2: Fresh bagasse after burning

Industrial bagasse which has not been undergone ignition, was collected from Faridpur Sugar Mill, Madhukhali, Faridpur. Those bagasse was kept in stack at the industrial site for about three years. The color of bagasse was reddish brown.

Figure 3.3: Stack Bagasse at Faridpur sugar mill

Several thousand ton bagasse was left there to be used as fuel during the season of sugar production. Local people also buy bagasse to use as fertilizer. It sells at a price of BDT 400tk/ton which is very cheap. However, due to high cost of transportation, it cannot be used at large

scale. As such surplus amount of bagasse remain unused each year. Those are used for landfill nearby.

3.2.1 Calcination of Fresh Bagasse Ash

Calcination is the heating of solids at a high temperature for the purpose of removing volatile substances, oxidizing a portion of mass, or rendering them friable. Calcination, therefore, is sometimes considered a process of purification. For present study, dry ashing method was employed for calcination but subsequent treatment using wet ashing or fusion techniques was not incorporated as complete removal of all volatile matters was not necessary. This procedure involves heating a sample in an open dish or crucible in air, usually in a muffle furnace to control the temperature and flow of air.

Black colored bagasse ash was placed in muffle furnace. A muffle or retort furnace is used for the heat treating process when a controlled atmosphere is needed. Sample was placed in covered porcelain crucible as shown in Figure 3.4.

(a) Before sample placement

(b) Placing of sample

Figure 3.4: Bagasse ash sample in Muffle furnace

To investigate the effect of calcination temperature on amorphous silica content, sample was heated at 400, 480, 700 and 850 ^{o}C for six hours. From the literature review presented earlier, the suggested calcination temperature should higher than 400 ^{o}C since major loss of mass occurs above this temperature. Samples was dried before dry ashing and placed in an unheated furnace; then, the furnace temperature was gradually increased. The sample was spread as thinly and evenly as possible on the bottom of the container to allow for its equal heating. To ensure even heating of the sample and to minimize the chance of ignition, the temperature of the furnace was raised slowly. This rate is slow enough that small amounts of organic material or water can be removed from the sample without violent reactions. In each case, temperature reached up to desired degree within 30 minutes and in the last 30 minutes; temperature was increased 50 degree Celsius above the desired temperature to get amorphous silica. Muffle furnace allows to maintain desired temperature profile. After that, sample was cooled in the furnace for 12 hours at room temperature and sample was removed from cold furnace. This procedure helps prevent sudden changes in temperature that could cause air currents that may potentially disturb the ash.

When black bagasse ash, shown in Figure 3.5, was calcined at 400 ^{o}C, it turned into grey color with significant reduction in volume as shown in Figure 3.6. At 480 ^{o}C, no significant change in volume was observed but from Figure 3.7, it is clear from color of ash that some reduction in carbon content has occurred. At 700 ^{o}C, the ash turned lightly sintered but distinguished color change was not observed.

Figure 3.5: Raw bagasse ash

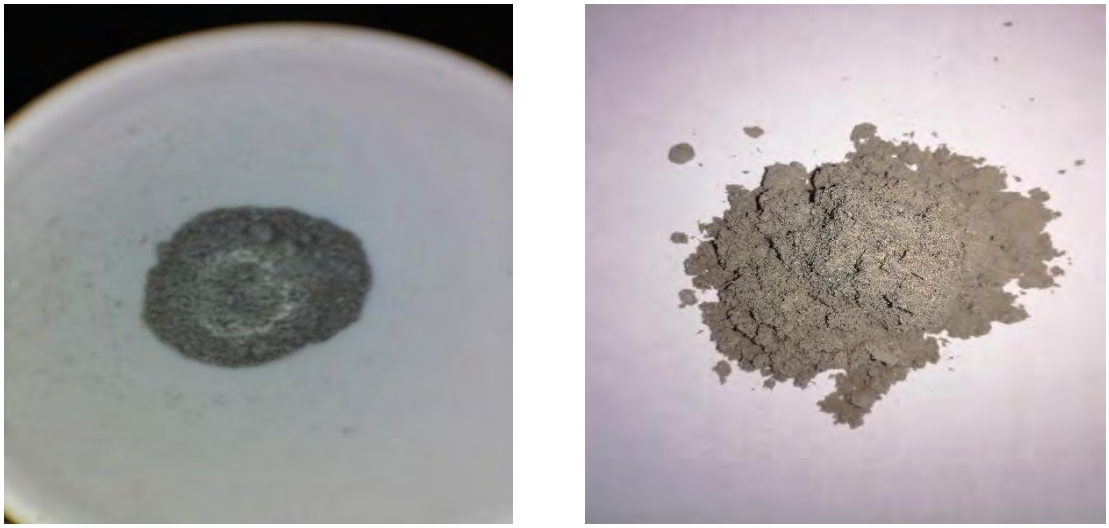

Figure 3.6: Bagasse ash calcined at 400 ^{o}C

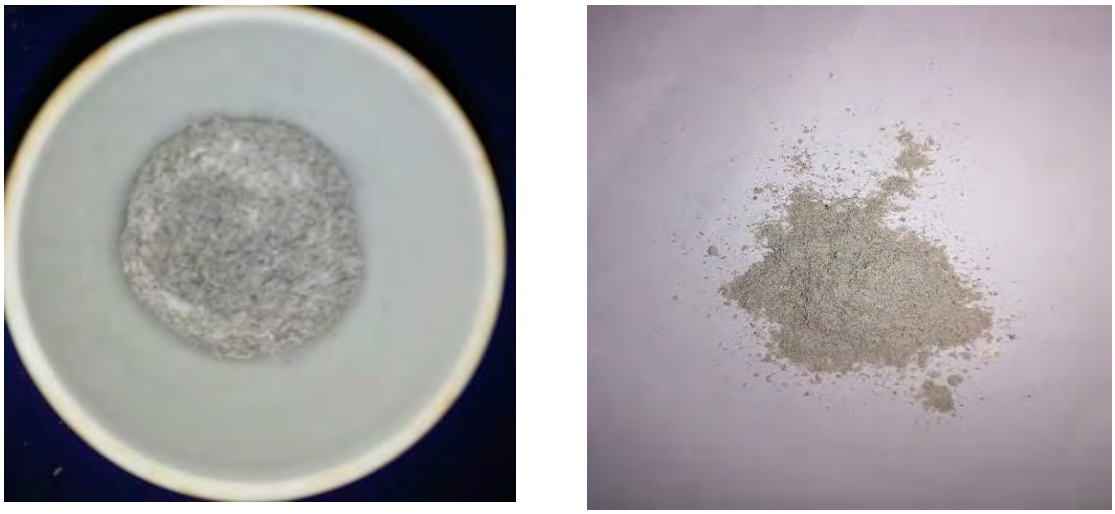

Figure 3.7: Bagasse ash calcined at 480 ^{o}C

Figure 3.8: Bagasse ash calcined at 700 ^{o}C

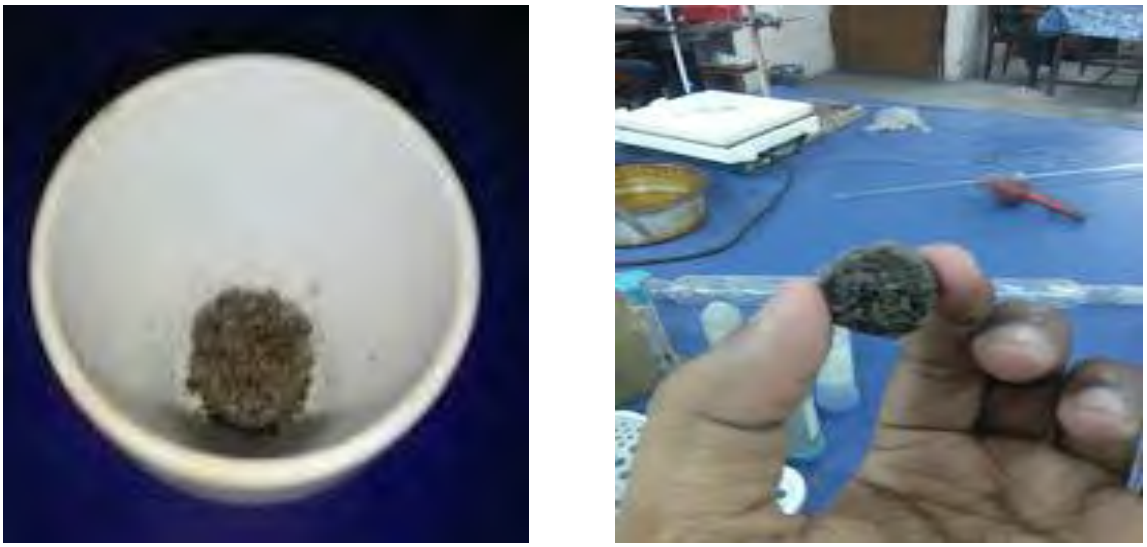

Figure 3.9: Bagasse ash calcined at 850 ^{o}C

In case of calcination temperature 850 ^{o}C, the ash turned into hard sintered object. This has been shown in Figure 3.9.

3.2.2 Calcination of Industrial Bagasse Ash

To avoid contamination of bagasse ash from other types of biofuels, ash was not directly collected from industries. For calcination of industrial bagasse ash, a brick furnace (5'x3'x2.5') as shown in Figure 3.10, was constructed. Heat was generated by burning of firewood and anthracite coal, almost the same methodology that is used for fixed bed coal fired furnace in industrial boilers. Anthracite coal is a high-ranking coal with more fixed carbon and less volatile matter than bituminous, subbituminous, or lignite varieties. Anthracite also has higher ignition and ash fusion temperatures. Coal was pulverized before feeding in the furnace. Generally, fuels with finer size distributions, higher volatile matter contents, and lower moisture contents result in a greater percentage of combustion and corresponding heat release rates in suspension above the bed [69].

(a) Brick furnace after construction

(b) Brick furnace during calcination

Figure 3.10: Brick furnace

Emissions from anthracite coal firing primarily include particulate matter (PM), sulfur oxides (SOx), nitrogen oxides (NOx), and carbon monoxide (CO); and trace amounts of organic compounds and trace elements. So bagasse was placed in the furnace with a covered metal tray which was perforated at the top as shown in Figure 3.11. The movable slab of the furnace allows insertion of tray at the upper portion of the furnace.

(a) Bagasse ash

(b) Supplement of fuel

(c) After firing (d) Placing of raw bagasse ash

Figure 3.11: Bagasse being burnt in brick furnace

Feed coal is pushed through the opening and upward towards the tuyere. Air was supplied through the tuyere blocks on sides of the walls and through openings below the slab, continuous supply of fuel helped to maintain uniform temperature throughout the total burning period of 6 hours. The temperature inside the furnace was within 600-650 ^{o} C.

Figure 3.12: Infrared laser thermometer

The temperature was measured with an infrared laser thermometer which is shown in Figure 3.12. An infrared thermometer is a thermometer which infers temperature from a portion of the thermal radiation sometimes called blackbody radiation emitted by the object being measured. It emits laser which acts as pointer that was directly pointed to sample through the small opening of the slab. The infrared thermometer that was used in this study can read temperature up to 1350 ^{o} C.

After combustion period of 6 hours, the slab of the furnace was opened and water was sprayed over fuel .The sample was then allowed to cool down at normal temperature. Figure 3.13 shows industrial bagasse ash after calcination.

(a) Industrial Bagasse ash (b) After calcination

Figure 3.13: Industrial bagasse ash after calcination.

After cooling for about 6 hours, ash was extracted from furnace. Paula et al [70] noted that: for a calcination temperature of 600°C for a period of 6 hours, it is possible to obtain ash with SiO_2 content 84 wt. %. They suggest that the optimal temperature for the production of pozzolanic sugar cane bagasse ash is 600°C because at this temperature it is possible to generate predominantly amorphous silica with a good pozzolanic activity index.

3.3 Microscopic Study of the Ash

The x-rays fluorescence (XRF) technique was used to determine the chemical composition of produced bagasse ash. Pressed powder method was used for sample preparation of x-rays fluorescence analysis. Pressed pellets were prepared by pressing sample by press machine. Powders which particles are spherically shaped such as SiO_2 or burnt ash are difficult to pelletize [71]. Since bagasse has surplus of silica, binders was used to pelletize the sample. Without binder, fine powder particles may fall off or scatter from the pellet surface and can cause contamination of the spectrometers' sample chamber in vacuum mood. Binder was mixed with bagasse with a mortar grinder as shown in Figure 3.14.

Figure 3.14: Binder mixing with bagasse ash

After mixing with binder, sample was placed into cylindrical type dies. Load was applied by an automatic press machine and pressed pellet sample was obtained after application of load of 39 kN. This has been shown in Figure 3.15 below.

(a) Sample preparation

(b) Prepared sample

Figure 3.15: Sample pressed in automatic load machine to obtain pellet.

The sample was then dried in oven for around 24 hours and XRF test was performed. Surface structure of the sample, shape and particle size were taken on scanning electron microscopy (SEM) for three-dimensional appearance. Since bagasse ash is not conductive, it does not have inherent ability to conduct electricity. So the powder sample was sprinkled on a carbon sticky tab of aluminum specimen mount and coated with a nanometer-thick layer of gold (Au) using a sputter coater before being examined. Both XRF and SEM were performed at the laboratory of Department of Glass and Ceramic Engineering, BUET.

3.4 Study of Bagasse Ash in Cement

3.4.1 Material Properties

The cement used in this study was locally manufacture Ordinary Portland Cement (OPC). The properties of bagasse ash supplemented cement in terms of compressive strength, consistency, shrinkage, flow were evaluated. In each of the test bagasse ash was partially replaced in the ratio of 0%, 5%, 10%, 15%, and 20% by weight of cement in mortar. Locally available free of debris and riverbed sand was used as fine aggregate. Potable water free from deleterious

materials viz. oil and other impurities such as chloride was used for casting of concrete specimens.

3.4.2 Consistency Test

The initial parameter which needs to be determined for cement is consistency test. It is to estimate that the quantity of water required to produce a cement paste of standard consistency. The apparatus required for the determination of consistency of standard cement paste is Vicat apparatus, 10 mm diameter plunger, stopwatch and non-porous plate as shown in Figure 3.16. The standard consistency of cement paste is defined as that consistency which will permit Vicat plunger to penetrate to a point 10 ± 1.0 mm below the original surface in 30 s after being released from the bottom of the mold.

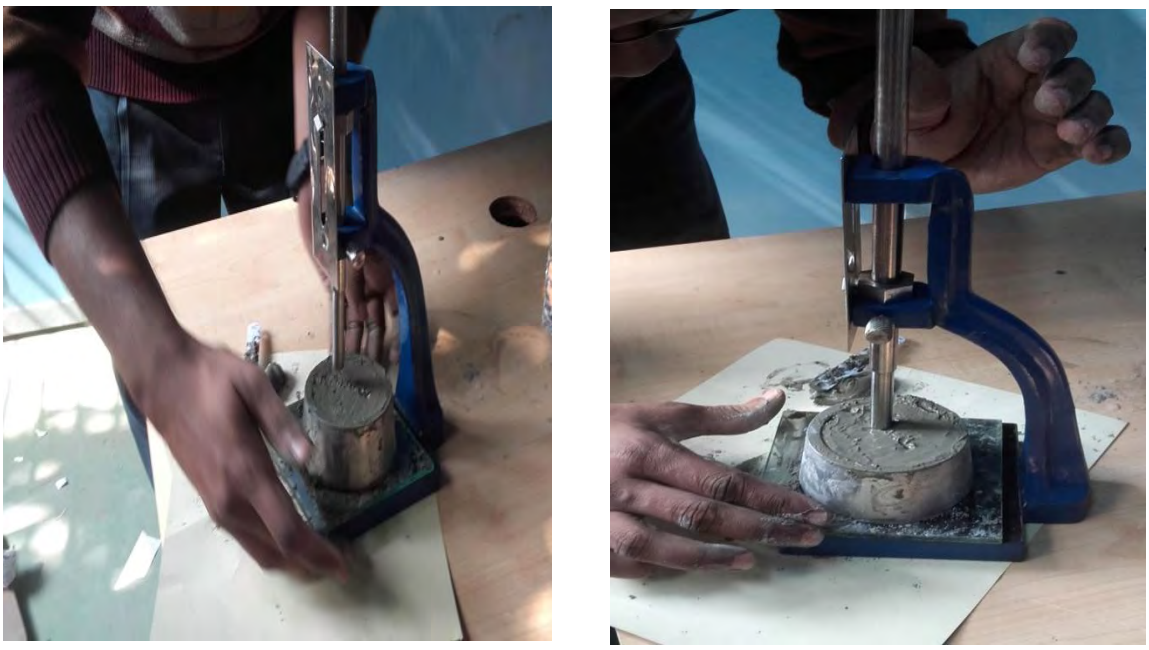

Figure 3.16: Consistency test of SCBA blended mortar

To study the effect of bagasse ash replacement on consistency of cement mortar, consistency test was performed, cement was replaced in the ratio of 0%, 5%, 10%, 15% and 20%. 650 gm of cement was mixed with a measured quantity of water following the procedure prescribed in the Procedure for Mixing Pastes of Practice ASTM C 305-14[72]. In the Vicat Apparatus, the

large-sized plunger was released to penetrate the sample. When the penetration of the plunger was 10 ± 1.0 mm below the original surface in 30 s after being released, then the consistency was reported as the normal consistency. In each trial, the amount of water required for normal consistency was calculated to the nearest 0.1% and reported it to the nearest 0.5% of the weight of the dry cement. The amount of mixing water used was plotted as abscissa and penetration was observed as ordinate in a plain graph paper. Then using this plot, the amount of water required for 10 mm penetration was determined.

3.4.3 Flow test

Flow test shows that the water demand for a required workability of cement mortar. Bagasse ash was partially replaced in the ratio of 0%, 5%, 10%, 15% and 20% by weight of cement to compare the effect of bagasse ash on flow of blended cement.

The mortar flow test utilizes a specially designed table conforming ASTM C 230/C 230M – 08[73], repeatedly raises and drops a known quantity of mortar 25 times. The flow table apparatus consists of an integrally cast rigid iron frame and a circular rigid table top 10 ± 0.1 in. [255 ± 2.5 mm] in diameter, with a shaft attached perpendicular to the table top by means of a screw thread as shown in Figure 3.17.

Figure 3.17: Flow test Apparatus

The flow mold is placed at the center. A layer of mortar about 25 mm (1 in.) in thickness was placed in the mold and tamped 20 times with the tamper as shown in Figure 3.18. The tamping pressure shall be just sufficient to ensure uniform filling of the mold. Then the mold was filled with mortar and tamped as specified for the first layer.

Figure 3.18: Tamping for flow test of SCBA blended mortar

The flow is the resulting increase in average base diameter of the mortar mass, expressed as a percentage of the original base diameter. The diameter of the mortar along the four lines scribed in the table top was measured.

Figure 3.19: Flow test of SCBA blended mortar

Total four diameter reading scribed on the table top (marked by arrow in Figure 3.19(b)) was taken and averaged. The flow was computed in percent by dividing "A" by the original inside base diameter in millimeters and multiplying by 100 where: A = average of four readings in millimeters, minus the original inside base diameter in millimeters. The flow was reported to the nearest 1 %.

3.4.4 Compressive Strength Test

This is probably the most relevant test to evaluate the performance of bagasse ash-cement composites since cement is valued mainly for its high compressive strength. Flow test was performed and repeated, using a fresh batch of mortar each time, until the desired flow is achieved. The quantity of water needed to achieve flow was recorded, and this mortar was then tested for compressive strength. A total of 60 mortar cubes (2 in) was made varying the bagasse ash composition to determine the compressive strength at 3, 7, 28 and 56 days as per ASTM C 109/C 109M [15]. The mortar used consists of 1 part bagasse ash supplemented cement and 2.75 parts of sand proportioned by mass. The mix was then placed to automatic mortar mixture machine as shown in Figure 3.20.

Figure 3.20: Automatic mortar mixer for proper mixing of ingredients

A thin coating of release agent (for lubrication) was applied to the interior faces of the mold. Once the proper flow is achieved, the mortar is placed and compacted into bronze cube-shaped molds. The tamping pressure was just sufficient to ensure uniform filling of the molds. The 4 rounds of tamping (32 strokes) of the mortar was completed in one cube before going to

the next. When the tamping of the first layer in all of the cube compartments was completed, the compartments was filled with the remaining mortar and then tamped as specified for the first layer. The mortar was cut off to a plane surface flush with the top of the mold by drawing the straight edge of the trowel (held nearly perpendicular to the mold) with a sawing motion over the length of the mold. Figure 3.21 shows the molded test specimens.

Figure 3.21: Molding of test specimens

Immediately upon completion of molding, the test specimens were placed in such condition that their upper surfaces exposed to the moist air but protected from dripping water. After 24 hour, the specimens were marked for identification and immersed in saturated lime water as shown in Figure 3.22.

Figure 3.22: Curing of test specimens

During transportation, the cube samples were protected from jarring, freezing, and moisture loss.After the required period of curing, specimens were brought to testing machine for determining cube compressive strength corresponding to 3, 7, 28 and 56 days. Specimens upon removal from water storage, was immediately wiped out to a surface-dry condition.

Figure 3.23: Cube compressive strength testing

It is placed on the machine such that the load is applied centrally as shown in Figure 3.23. The smooth surfaces of the specimen are placed on the bearing surfaces. Load was applied at a

relative rate of movement between the upper and lower platens corresponding to a loading on the specimen with the range of 200 to 400 lbs/s [900 to 1800 N/s]. The maximum load indicated by the testing machine before failure was divided by area of cube to get corresponding compressive strength. Average compressive strength of all specimens from the same sample was reported to the nearest 10 psi [0.1 MPa].

3.4.5 Shrinkage Test

This test method has established a selected set of conditions of temperature, relative humidity of the environment to which a mortar specimen of stated composition shall be subjected for a specified period of time during which its change in length is determined and designated as "drying shrinkage" [16]. It determines the change in length on drying of mortar bars containing hydraulic cement and sand.

A batch of mortar was consisted of 750 g of cement, 1500 g of graded standard sand, and an amount of mixing water sufficient to produce a flow of 110± 5 %. Bagasse ash was partially replaced in the ratio of 0%, 5%, 10%, 15% and 20% by weight of cement to compare the effect of bagasse ash on drying shrinkage of blended cement. Mixing of the ingredients was done in an automatic mortar mixer and molded in the shrinkage apparatus with proper hand tamping as shown in Figure 3.24.

Figure 3.24: Molding of specimens for shrinkage test.

Molds for test specimens were provided for 25 by 25 by 285-mm or 1 by 1 by 11-1⁄4-in. prisms having an effective gage length of 250 mm or 10 in, respectively and conformed to the requirements of Practice C596-01[16]. The specimens were moist cured in the mold for 48 h and then cured in lime-saturated water for 24h as shown in Figure 3.25.

Figure 3.25: Curing of specimens for shrinkage test.

At the age of 72 h, the specimens were removed from water, wiped with damp cloth and immediately a length comparator reading was obtained for each specimen as shown in Figure 3.26. Then the specimens were placed in air storage for 25 days. A length comparator reading for each specimen was obtained after 4, 11, 18, and 25 days of air storage.

Figure 3.26: Comparator readings of test specimens

The length change was calculated of each specimen at each age of air drying by subtracting the initial comparator reading, taken after removal from water storage, from the comparator reading taken at each age of air drying and expressed as millionths and as the percent of the effective gage length.

Chapter *4*

Results and Discussion

4.1 Introduction

In this present study, the behavior of bagasse ash blended cement was investigated. Though it is evident from previous studies that bagasse ash substitution might have positive impact on properties of cement composites, the percentage of amorphous silica is very crucial in determining the optimum replacement level. Nevertheless, only few studies that have discussed in detail on the percentage variation of silica content for different extraction method. Based on research scopes and methods, most of the literatures present similar objectives, i.e. identifying the effect of SCBA as pozzolanic materials in cement without any consideration of alkali content present in SCBA. Alkali-silica reaction (ASR) can cause serious expansion and cracking in concrete, resulting in major structural problems and eventually, necessitates demolition.

In this study, chemical compositions found from XRF analysis of bagasse ash collected from different sources and burnt at various temperature ranges is presented. The compressive strength, drying linear shrinkage, consistency, flow test results of bagasse ash blended cement and the microstructure test results of bagasse ash have been incorporated as well.

4.2 X-ray Fluorescence (XRF) Analysis Result

4.2.1 Local Fresh Bagasse Ash

Air dry bagasse ash was heated at different temperature ranges in a muffle furnace until melting of the ash sample was observed and in each case XRF analysis was performed to determine the chemical composition. The fuel characteristics of biomass like sugarcane bagasse is very different from those common fossil fuels, including moisture content, ash content, calorific value, and alkali/alkaline earth metal content, etc. [74, 75, 76]. The particulate matter emission and weight loss is different from coal mass. Due to having varied chemical composition especially alkali matter, ASTM fusion test of ash could not be performed. Hjuler [77] claims that the primary reason for unsuitability of the standard ash fusion test for biomass ashes is that

biomass typically contains relatively high amounts of low melting components. Many authors have reported melting at temperatures below the standard measured ash fusion temperatures due to the presence of alkalis [78, 79, 80]. For instance, Skrifvars et al. [79] found that the ASTM standard ash fusion test generally gave temperatures 50−500°C higher than combustion tests.

Bagasse ash sample was initially burnt at temperature around 280 ^{o}C, in which the initial weight loss is mainly associated with degradation of thermally unstable organic constituents, which mostly include hemicellulose and lignin [55, 81]. These compounds have simple structures and get decomposed by biological oxidation, and these compounds easily get broken down at higher temperature.

The XRF result obtained from burning bagasse ash at 280° C for 6 hours in open air has been shown in Table 4.1.The oxides in biomass ashes can be divided into acidic oxides (SiO_2, Al_2O_3, SO_3, and P_2O_5, *etc*.) and basic oxides (K_2O, CaO, MgO, Na_2O and Fe_2O_3, *etc*.) according to the acidic and basic capacity. These results show that the content of inorganic matter in various biomass ashes at different ashing temperatures is much different; the primary content of the inorganic matter included Si, K, Na, Ca, Mg, Fe, Al, *etc*. It shows very high potassium content as much as 50.766% and silica content only 15.50%. As per Specifications for fly ash in PCC, AASHTO M 295 (ASTM C 618), to classify fly ash as class C, the minimum total percentage of SiO_2 , Al_2O_3 and Fe_2O_3 must be above 50% [82].From Table 4.1, the total percentage of SiO_2, $Al2O_3$ and Fe_2O_3 is only (15.50 + 0.1995 + 4.8344)=20.5339%. Besides, if the total alkali of fly ash is high (> 5% Na_2O equivalent), the fly ash has not been found to be effective in controlling ASR. These high-alkali fly ashes, when tested with reactive aggregate, will exceed the ASTM C1567 expansion limits [83].

Table 4.1: Chemical composition of bagasse ash at 280 ° C

Analyte	Result	Remarks
K_2O	50.766 %	Sample: Fresh bagasse ash Burning: In Gas burner Temperature :around 280°C Duration: 6 Hours
SiO_2	15.5028 %	
P_2O_5	13.0846 %	
CaO	5.5224 %	
Fe_2O_3	4.8344 %	
MgO	4.3682 %	
SO_3	4.1460 %	Sample Initial Weight 6.884 gm After Burning sample weight 4.773 gm % loss = 30.66%
Na_2O	0.8194 %	
MnO	0.6525 %	
Al_2O_3	0.1995 %	
TiO_2	0.1257 %	

At 400 ° C, burnt at muffle furnace, the silica content increased up to 28.55% and potassium oxide decreased to 39.82%. More than 8% weight loss occurred at this temperature. This is due to the emission of volatile gases from bagasse ash due to high temperature. The weight loss at these stages is still attributed to rapid devolatilization as a consequence of cellulose and lignin decomposition at temperatures above 360 ° C for cellulose and up to 870 ° C for lignin. These are the maximum decomposition temperatures for these components when the material undergoes complete combustion; beyond these temperature ranges, complete decomposition of the material may have occurred [84, 85]. Thermo-gravimetric analysis of the SCBA sample also shows a significant weight loss in the 400-750 ° C and from derivative thermo-gravimetric analysis, maximum weight degradation is at 400 ° C [86].

Table 4.2: Chemical composition of bagasse ash at 400 ° C

Analyte	Result	Remarks
K_2O	39.8204 %	Sample: Fresh bagasse ash Burning: In Muffle Furnace Temperature: 400 ° C Duration: 6 Hours
SiO_2	28.5549 %	
P_2O_5	13.8707 %	
CaO	6.3490 %	
MgO	4.6336 %	
SO_3	3.3799 %	Sample Initial Weight 6.825 gm After Burning sample weight 4.173 gm % loss = 38.86%
Fe_2O_3	1.4466 %	
Al_2O_3	1.0751 %	
Na_2O	0.6533 %	
TiO_2	0.2164 %	

The temperature was further increased to 480 ° C and no significant change was observed in chemical composition but additional 2% weight loss occurred as shown in Table 4.3. Yao et al. [87] reported that biomass combustion weight loss between 140 ° C and 420 ° C is mainly attributed to evolution of the volatiles from biomass pyrolysis. The weight loss within 140 ° C and 420 ° C contributes to most of the weight loss (around 80 to 90 %). At temperatures above 420 ° C, an insignificant weight loss was found at a very slow degradation rate. Chemical composition of bagasse ash at 480 ° C also shows negligible changes in comparison with 400 ° C.

Table 4.3: Chemical composition of bagasse ash at 480 ° C

Analyte	Result	Remarks
K_2O	39.5601 %	Sample: Fresh bagasse ash Burning: In Muffle Furnace Temperature: 480 ° C Duration: 6 Hours
SiO_2	27.7812 %	
P_2O_5	14.2166 %	
CaO	6.7756 %	
Fe_2O_3	4.8612 %	
MgO	3.2695 %	Sample Initial Weight 5.307 gm After Burning sample weight 3.184 gm % loss = 40 %
SO_3	1.3593 %	
Na_2O	0.9780 %	
MnO	0.8312 %	
Al_2O_3	0.1949 %	
TiO_2	0.1725 %	

At 700 ° C burning temperature, significant reduction in alkali content and as such, increase in silica content as shown in Table 4.4, conforms the study previously mentioned. At this temperature, the sample was in a lightly sintered stage. The sintered particle could be broken apart manually. At temperatures of 600-700 ° C, the binary K_2O-SiO_2 system can be expected to start melting [88,89]. Due to melting of alkali silicates, sintered particle was observed.

Table 4.4: Chemical composition of bagasse ash at 700 ° C

Analyte	Result	Remarks
K_2O	34.6481 %	Sample: Fresh bagasse ash Burning: In Muffle Furnace Temperature: 700 ° C for 5.5 hours ,750 °C for last 30 min
SiO_2	32.1219 %	
P_2O_5	14.6765 %	
CaO	6.5524 %	
MgO	4.8295 %	
SO_3	3.3822 %	Sample Initial Weight 8.195 gm After Burning sample weight 4.78 gm % loss = 41.67 %
Fe_2O_3	1.6015 %	
Al_2O_3	1.3712 %	
Na_2O	0.6034 %	
TiO_2	0.2132 %	

When sample is burnt at 800–900 ° C temperature range, it leads to sintered stage of the sample (porous ash block which is difficult to break apart manually). The fusion temperature of bagasse ash is expected to have reached at this temperature. The chemical composition of this temperature has been shown in Table 4.5. Ashes that are rich in alkaline metals (potassium, phosphorus, chlorine and sodium) which form complex eutectic salts that effectively lower the melting point of the ashes during combustion [86].Though the melting point of pure silica is 1710 ° C, the whole sample turned into a solid rock at this temperature (700 ° C-750 ° C) due to melting of other compounds. Besides, silica in combination with alkali and alkaline earth metals, especially with the readily volatilized forms of potassium present in biomas, can lead to the formation of low melting point compounds which readily slag and foul at this temperatures (800–900 °C) [90, 91].To avoid contamination of the sample with the slag material, bagasse ash sample was placed in covered condition having opening at the sides. It allows the evaporation of the volatile materials but obstruct the slag material to contaminate the sample.

Table 4.5: Chemical composition of bagasse ash at 850 ° C

Analyte	Result	Remarks
SiO_2	36.8618 %	Sample: Fresh bagasse ash Burning: In Muffle Furnace Temperature: 850 ° C for 5.5 hours , 900°C for last 30 min
K_2O	36.1044 %	
P_2O_5	11.5570 %	
CaO	5.6366 %	
MgO	3.3005 %	
SO_3	2.2207 %	Sample Initial Weight 9.838 gm After Burning sample weight 5.699 gm % loss = 42.07 %
Fe_2O_3	1.5929 %	
Al_2O_3	1.2975 %	
Na_2O	1.0084 %	
TiO_2	0.2515 %	
MnO	0.1687 %	

No significant change was observed in silica/alkali content when the ash was calcined at brick furnace. The temperature at the furnace was 650°C. The chemical composition has been shown in Table 4.6. It shows comparatively higher Cl content (1.8083%). Whether this Cl source is due to different sample source or inadequate gasification in brick furnace is beyond the scope of this study.

Table 4.6: Chemical composition of bagasse ash at 650 ° C in brick furnace

Analyte	Result	Remarks
SiO_2	30.6394 %	Sample: Fresh bagasse ash Burning: In Brick furnace Temperature: Around 650 ° C for 6 hours
K_2O	28.8038 %	
P_2O_5	10.8690 %	
SO_3	9.5685 %	
CaO	8.0332 %	
MgO	4.5651 %	
Fe_2O_3	2.3369 %	
Al_2O_3	1.9466 %	
Cl	1.8083 %	
Na_2O	0.6381 %	
TiO_2	0.3134 %	
ZnO	0.2963 %	
RbO_2	0.0856 %	
Cr_2O_3	0.0656 %	
SrO	0.0254 %	
ZrO_2	0.0074 %	

The carbon and volatile compounds present in the SCBA are expected to be considerably removed at higher duration of calcination temperature. Sample was calcined for 12 hours at 650 ° C. Almost 4% potassium was reduced with 2% increase in silica content.

Table 4.7: Chemical composition of bagasse ash at 650 ° C

Analyte	Result	Remarks
SiO_2	32.8895 %	Sample: Fresh bagasse ash Burning: In Brick furnace Temperature: Around 650 ° C for 12 hours
K_2O	26.6076 %	
SO_3	11.1611 %	
P_2O_5	9.9742 %	
CaO	6.7185 %	
MgO	4.7332 %	
Fe_2O_3	2.5271 %	
Al_2O_3	2.3410 %	
Cl	1.4251 %	
Na_2O	0.5845 %	
TiO_2	0.5437 %	
ZnO	0.3815 %	
RbO_2	0.0821 %	
SrO	0.0241 %	
ZrO_2	0.0069 %	

From above test results, it is certain that other than acid-treatment, this ash is not suitable for use as partial replacement of cement due to high alkali content. However, the chemical composition of bagasse ash is not independent of its source.

From the chemical composition of sugarcane juice shown in Table 4.8, in 1 oz. of juice, the potassium content is as high as 162.86 mg. If juice is extracted by tradition method, without further washing or acid treatment, surplus amount of potassium is expected in ash.

Table 4.8: Nutritional value & calories in Cane Juice [92]

Nutrients	Amount
Basic Components	
Proteins	0.20 g
Water	0.19 g
Ash	0.66 g
Fat	0.09 g
Calories	
Total Calories	111. 43
Calories From Carbohydrates	
Calories From Fats	0.03
Calories From Proteins	
Carbohydrates	
Total Carbohydrates	
Sugar	27.40 g
Vitamins	
Riboflavin	0.16 mg
Niacin	0.20 mg
Pantothenic Acid	0.09 mg
Minerals	
Calcium	32.57 mg
Iron	0.57 mg
Magnesium	2.49 mg
Phosphorus	0.01 mg
Potassium	162.86 mg
Copper	0.09 mg
Manganese	0.09 mg

Local juice extraction method cannot remove sugarcane juice adequately from stalk fiber and thus surplus potassium is found when chemically analyzed.

4.2.2 Industrial Leached Bagasse Ash

In case of industrial bagasse, proper extraction of juice and subsequent washing leads to almost complete removal of potassium. Besides, in industry, stack bagasse is left on open air for years. Since potassium is highly soluble, when rain drops percolates through stack bagasse, its amount decreases due to leaching effect. It shows that 1 hour of water leaching reduces almost 90% potassium which is even better than washing with a 5M HCl acid solution [93]. Silica content with acid treating and oxygen feeding in the furnace can be achieved up to 89.037% with burning period of only 3 hours [94]. Though acid treatment of bagasse ash can remove this excess potassium but this may not be economical for industrial use of bagasse ash as supplementary cementitious material.

To explore the properties of ash obtained from industrial leached bagasse ash, XRF test was carried out on stack bagasse sample, almost three years left on open air. The results found are shown in Table 4.9.

Table 4.9: Chemical composition of bagasse ash at 650 ^{o}C

Analyte	Result	Remarks
SiO_2	61.6530 %	Sample left in stack around 3 years. Burning: In Brick furnace Temperature: Around 600-650 ^{o}C for 6 hours
SO_3	10.9614 %	
Al_2O_3	6.9240 %	
CaO	5.1400 %	
Fe_2O_3	4.9130 %	
K_2O	4.1911 %	
MgO	2.3954 %	

P_2O_5	1.8630 %	
TiO_2	0.7953 %	
Na_2O	0.6622 %	
ZnO	0.3697 %	
Cr_2O_3	0.0553 %	
ZrO_2	0.0358 %	
SrO	0.0209 %	
RbO_2	0.0200 %	

Test result shows surplus of silica percentage and drastically reduced potassium content. Water leaching resulted in a high removal of alkali metal ions like potassium, sodium and chloride. When these alkali matters are removed, the consequent ash melting behavior changes, increasing the characteristic temperatures during the ash fusion test in 300 ^{o}C to 400 ^{o}C for the herbaceous biomass. [95]

From Table 4.9, the total percentage of SiO_2 ,Al_2O_3 and Fe_2O_3 is (61.6530 + 6.9240 + 4.9130) 73.49%. The chemical composition of the bagasse ash has nearly similar composition of Class F fly ash. As such, all the tests performed in the study, belong to this ash.

4.3 Microstructural Investigation

The main composition of bagasse ash is unburnt carbon and siliceous oxide. Siliceous oxide reacts with free lime from cement hydration and made a consistent composition. But only un-crystal silica oxide has such reactive properties. Heat and burning duration, are the main factors on crystal structure and composition of ash [96]. Therefore for obtain maximum percentage of silica, the specimens were burnt at 600-650 ^{o}C temperature for long 6 hours. Since industrial leached bagasse ash was found having maximum silica content, microstructural investigation was carried out using that ash. Scanning electron microscopy (SEM) was coupled with Energy

Dispersive X-ray Spectroscopy (EDS or EDX) operated with at 0-20 KeV energy range. It was used to analyze the morphology of ash samples.

Energy Dispersive X-ray Spectroscopy (EDS or EDX) is a micro-chemical analysis that is used in conjunction with SEM. Based on the relative counts of the electron ejected from each element, EDX shows the probable chemical compounds that may be present in the sample. EDX performed along with SEM image shows that bagasse ash has higher percentage of oxygen and silica in it. Reading was taken on five spots [001, 002, 00, 004, and 005] for determining elemental composition and the results have been shown in Figures 4.1-4.5.

In our study, standardless quantitative analysis of elements was followed by using commercial "standardless" analysis software. The standardless analysis protocol only requires the list of elements to be analyzed, which is typically and often automatically supplied by the peak identification software. ZAF(Z- atomic number effects, A-absorption effects and F-fluorescence effects) corrections was applied to EDX measurements in the SEM to convert apparent concentrations (raw peak intensity) into (semi-quantitative) concentrations corrected for inter-element matrix effects. All the analysis results have been tabulated below the SEM image of sample in each figure. In quantitative EDS microanalysis in SEM, the mass fractions or weight percent of the elements present in the sample are calculated.

Each element within the sample will have its own critical ionization energy and its own excitation depth. The most of the elements observed in SCBA are observed well below 3 keV and some others up to 7 keV as shown in Figures 4.1-4.5. The energies of the characteristic X-rays allow to detect the elements making up the sample to be identified, while the intensities of the characteristic X-ray peaks allow the concentrations of the elements to be quantified. The presence of Si with oxygen elements shows broadest and tallest peak in comparison to all other chemical compounds. The presence of low energy range minerals like Al, K, Mn, P, and Fe having low atomic numbers in the SCBA was also observed with EDX. From Figure 4.1, Si and O was detected at ionization energy of 1.739 KeV and 0.525 KeV respectively. Corresponding concentration was found 17.44 % and 32.10 % respectively which higher than other minerals observed. Since excitation energy (KeV) is a unique characteristic of an element, no variation is observed in excitation energy for any element throughout the sample. But variation in percent mass was observed in different spots. For example, the percent mass of Mg was found 2.06, 2.11, 1.99, 2.05, and 1.93 in the spots 001, 002, 003, 004, 005 respectively as

shown in the Figures 4.1-4.5 below. However this variation in concentration seems to be very minor to consider. The most of minerals are observed within 3keV ranges which indicate that the minerals present are lower energy range. For lower energy range, the peaks correspond to the k-shell X- rays. Since the compounds are having lower excitation energy, they have high reactive tendency. However they have no cementitius value. It acts as a pozzolanic material when added to cement because of its silica (SiO2) content which reacts with free lime released during the hydration of the cement and forms additional calcium silicate hydrate (CSH) as a new hydration product [97]. This additional CSH improves the mechanical strength of the cement mortar.

Chemical analysis on SCBA showed that silica makes up more than 60% of the oxide components in the ash. The total value of alkalis (K_2O+Na_2O) was more than 6%, which immediately raises a concern about the potential for an alkaline-silica reaction. However, Zerbino et al. [98] reported that although alkali content may exceed the allowable limits stipulated in ASTM C618 (2012), the potential for alkali-silica reactivity is strongly dependent upon the particle size of the ash. In their study on, Zerbino et al. also reported that so long as the entire ash passed through the no. 200 sieve (75 microns), there was no alkali-silica reactivity even with more than 5% alkali (K_2O+Na_2O). As noted in Figures 4.1-4.5, the SCBA used in this study was in its entirety finer than 100 microns. Details of particle size and shape of ash particles have been discussed in detail below. Therefore, based on the above, the expectation is that although the alkali content was 7.5%, for the relatively small particle size precludes any potential alkali-silica reaction.

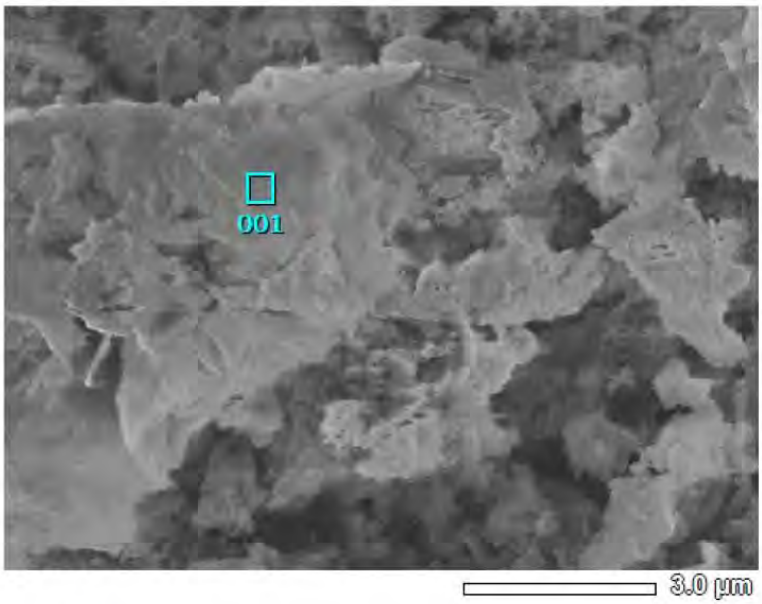

Title : IMG1

Instrument : 7600F
Volt : 15.00 kV
Mag. : x 10,000
Date : 2017/07/18
Pixel : 512 x 384

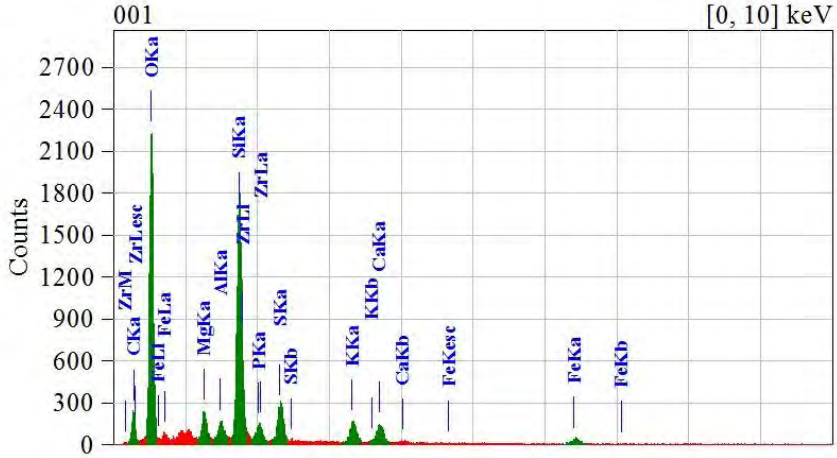

Acquisition Parameter
Instrument : 7600F
Acc. Voltage : 15.0 kV
Probe Current: 1.00000 nA
PHA mode : T3
Real Time : 30.48 sec
Live Time : 30.00 sec
Dead Time : 1 %
Counting Rate: 1814 cps
Energy Range : 0 - 20 keV

ZAF Method Standardless Quantitative Analysis
Fitting Coefficient : 0.0588

Element	(keV)	Mass%	Sigma	Atom%	Compound	Mass%	Cation	K
O K	0.525	32.10	0.25	35.15				30.4836
Mg K	1.253	2.06	0.07	1.48				2.5725
Al K*	1.486	1.18	0.06	0.76				1.6603
Si K	1.739	17.44	0.20	10.88				28.1432
P K	2.013	1.66	0.08	0.94				2.5016
S K	2.307	4.02	0.09	2.20				6.6694
K K	3.312	3.43	0.11	1.54				6.1716
Ca K*	3.690	3.25	0.12	1.42				6.1105
Fe K*	6.398	2.96	0.18	0.93				4.7185
Zr L	2.042	1.43	0.16	0.27				1.8055
Total		100.00		100.00				

Figure 4.1: Elemental composition of bagasse ash [001]

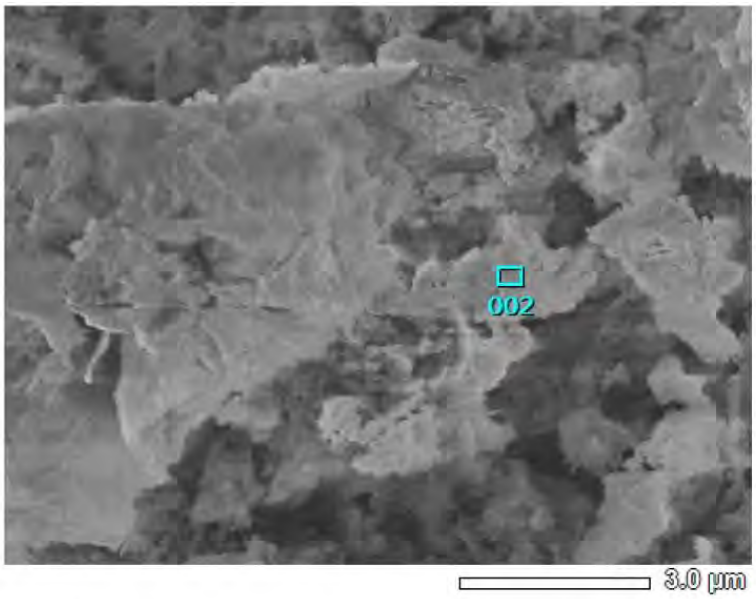


```
Title        : IMG1
-------------------------
Instrument   : 7600F
Volt         : 15.00 kV
Mag.         : x 10,000
Date         : 2017/07/18
Pixel        : 512 x 384
```

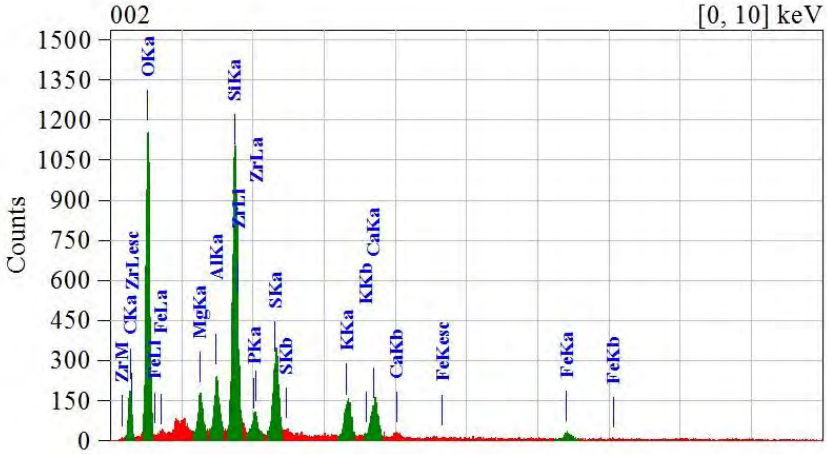


```
Acquisition Parameter
Instrument    : 7600F
Acc. Voltage  : 15.0 kV
Probe Current: 1.00000 nA
PHA mode      : T3
Real Time     : 30.37 sec
Live Time     : 30.00 sec
Dead Time     : 1 %
Counting Rate: 1348 cps
Energy Range :  0 - 20 keV
```

ZAF Method Standardless Quantitative Analysis
Fitting Coefficient : 0.0699

Element	(keV)	Mass%	Sigma	Atom%	Compound	Mass%	Cation	K
O K	0.525	25.37	0.10	27.96				21.6900
Mg K	1.253	2.11	0.05	1.53				2.7798
Al K*	1.486	2.59	0.06	1.69				3.8247
Si K	1.739	14.93	0.13	9.37				24.7697
P K	2.013	1.20	0.06	0.68				1.9092
S K	2.307	5.90	0.07	3.25				10.2617
K K	3.312	4.20	0.08	1.89				7.8203
Ca K*	3.690	4.95	0.10	2.18				9.5815
Fe K*	6.398	2.72	0.10	0.86				4.4687
Zr L	2.042	1.82	0.17	0.35				2.4179
Total		100.00		100.00				

Figure 4.2: Elemental composition of bagasse ash [002]

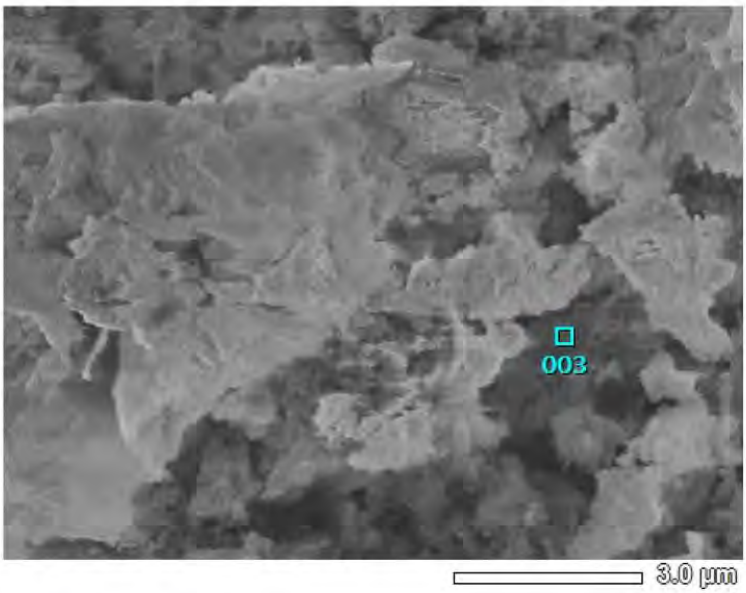


```
Title        : IMG1
-------------------------
Instrument   : 7600F
Volt         : 15.00 kV
Mag.         : x 10,000
Date         : 2017/07/18
Pixel        : 512 x 384
```

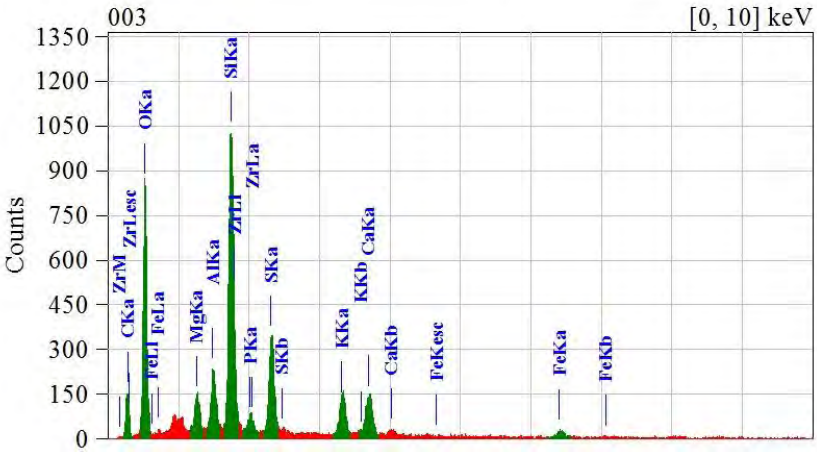


```
Acquisition Parameter
Instrument    : 7600F
Acc. Voltage  : 15.0 kV
Probe Current: 1.00000 nA
PHA mode      : T3
Real Time     : 30.33 sec
Live Time     : 30.00 sec
Dead Time     : 1 %
Counting Rate: 1216 cps
Energy Range  :  0 - 20 keV
```

ZAF Method Standardless Quantitative Analysis
Fitting Coefficient : 0.0753

Element	(keV)	Mass%	Sigma	Atom%	Compound	Mass%	Cation	K
O K	0.525	21.89	0.27	24.42				17.5969
Mg K	1.253	1.99	0.09	1.46				2.6104
Al K*	1.486	2.92	0.11	1.93				4.2682
Si K	1.739	16.37	0.24	10.40				26.7358
P K	2.013	1.43	0.09	0.82				2.2105
S K	2.307	7.12	0.15	3.96				12.1884
K K	3.312	4.86	0.16	2.22				8.8529
Ca K*	3.690	5.60	0.19	2.49				10.5988
Fe K*	6.398	3.01	0.22	0.96				4.8483
Zr L	2.042	0.31	0.18	0.06				0.3975
Total		100.00		100.00				

Figure 4.3: Elemental composition of bagasse ash [003]

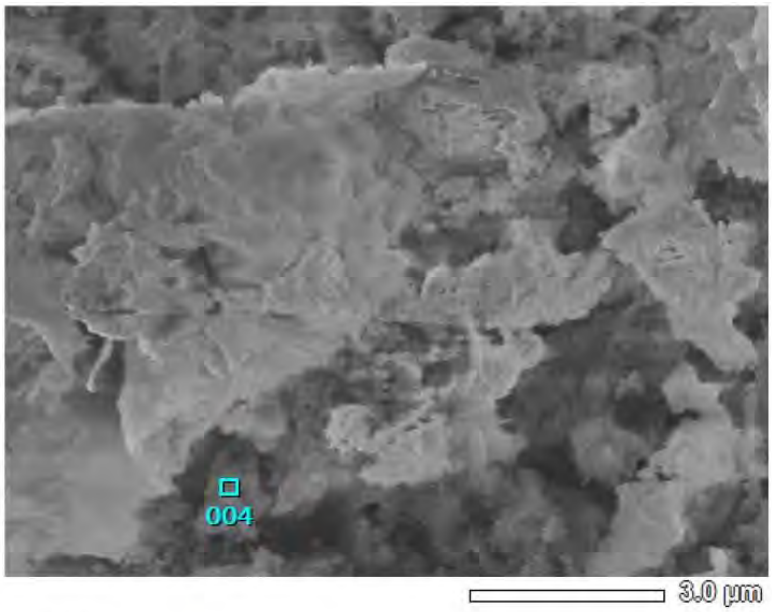


```
Title        : IMG1
-------------------------
Instrument   : 7600F
Volt         : 15.00 kV
Mag.         : x 10,000
Date         : 2017/07/18
Pixel        : 512 x 384
```

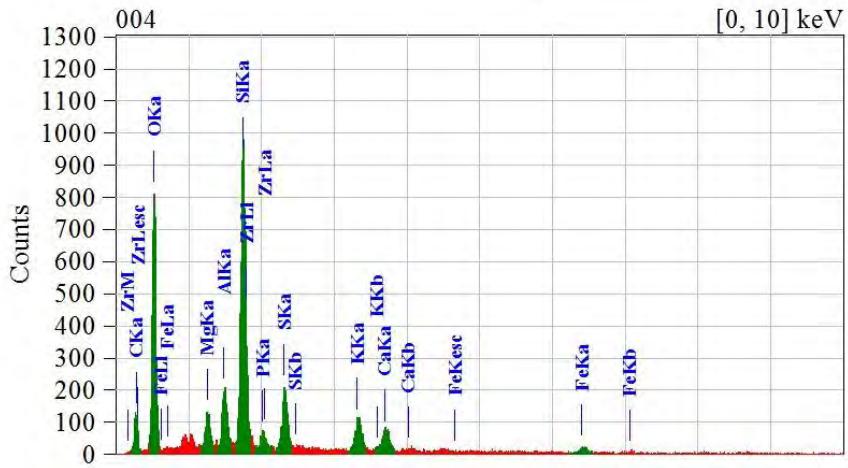


```
Acquisition Parameter
Instrument    : 7600F
Acc. Voltage  : 15.0 kV
Probe Current: 1.00000 nA
PHA mode      : T3
Real Time     : 30.26 sec
Live Time     : 30.00 sec
Dead Time     : 0 %
Counting Rate: 1033 cps
Energy Range :  0 - 20 keV
```

ZAF Method Standardless Quantitative Analysis
Fitting Coefficient : 0.0883

Element	(keV)	Mass%	Sigma	Atom%	Compound	Mass%	Cation	K
O K	0.525	24.32	0.31	26.55				21.5656
Mg K	1.253	2.05	0.10	1.47				2.7741
Al K*	1.486	3.32	0.12	2.15				5.0032
Si K	1.739	18.30	0.28	11.38				30.5370
P K	2.013	1.37	0.10	0.77				2.1246
S K	2.307	4.99	0.14	2.72				8.5807
K K	3.312	4.11	0.17	1.84				7.6459
Ca K*	3.690	3.26	0.17	1.42				6.3188
Fe K*	6.398	2.58	0.23	0.81				4.2637
Zr L	2.042	0.79	0.22	0.15				1.0235
Total		100.00		100.00				

Figure 4.4: Elemental composition of bagasse ash [004]

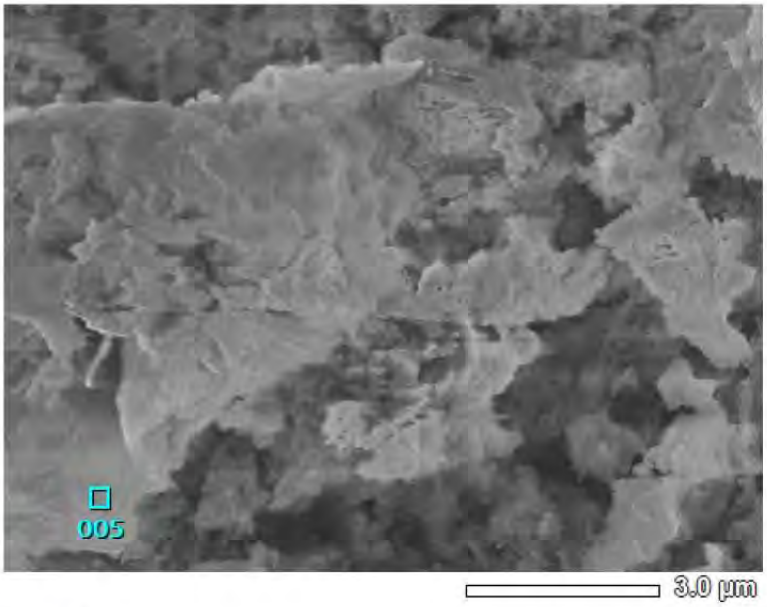


```
Title          : IMG1
--------------------------
Instrument     : 7600F
Volt           : 15.00 kV
Mag.           : x 10,000
Date           : 2017/07/18
Pixel          : 512 x 384
```

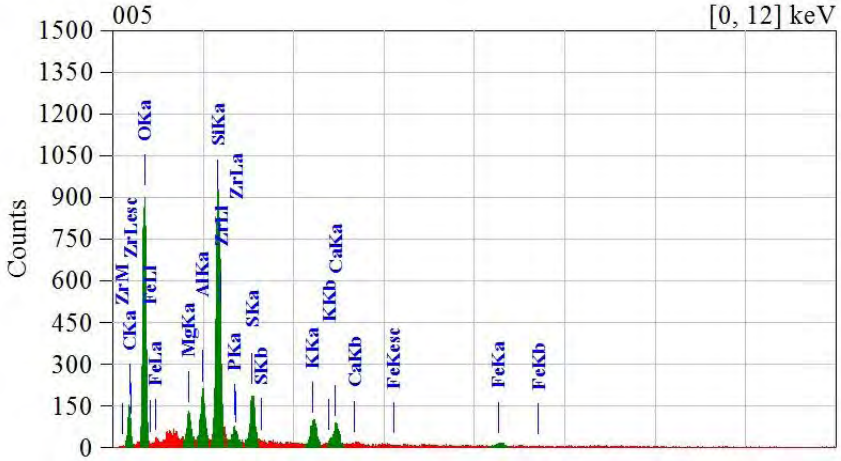


```
Acquisition Parameter
Instrument    : 7600F
Acc. Voltage  : 15.0 kV
Probe Current: 1.00000 nA
PHA mode      : T3
Real Time     : 30.27 sec
Live Time     : 30.00 sec
Dead Time     : 0 %
Counting Rate: 1040 cps
Energy Range :  0 - 20 keV
```

ZAF Method Standardless Quantitative Analysis
Fitting Coefficient : 0.0707

Element	(keV)	Mass%	Sigma	Atom%	Compound	Mass%	Cation	K
O K	0.525	26.52	0.32	28.42				24.2000
Mg K	1.253	1.93	0.10	1.36				2.6566
Al K*	1.486	3.03	0.12	1.92				4.6466
Si K	1.739	17.57	0.27	10.72				29.9540
P K	2.013	1.43	0.10	0.79				2.2743
S K	2.307	4.56	0.14	2.44				8.0037
K K	3.312	3.67	0.16	1.61				6.9483
Ca K*	3.690	3.23	0.16	1.38				6.3943
Fe K*	6.398	1.59	0.19	0.49				2.6606
Zr L	2.042	0.95	0.21	0.18				1.2685
Total		100.00		100.00				

Figure 4.5: Elemental composition of bagasse ash [005]

It is well known that the morphology of ashes mostly depends directly on burning temperature. During burning of bagasse, silica reacts to temperature and changes its properties. A morphological study of the selected ashes was carried out by FESEM. FESEM is the abbreviation of Field Emission Scanning Electron Microscope. The Field Emission Scanning Electron Microscope (FESEM) is an instrument which, just like the SEM, provides a wide variety of information from the sample surface, but with higher resolution and a much greater energy range. It works with electrons (particles with a negative charge) instead of light. These electrons are liberated by a field emission source.

No experiment was performed to determine the particle size distribution of calcined bagasse ash. But particle size can be predicated from SEM photograph of the sample with proper resolution and scale as shown in Figure 4.6-4.11. In Figure 4.6 (at magnification level x500), the particles are observed in dispersed condition but the shape and size cannot be approximated at this magnification level. At higher magnification level in Figure 4.7, the particles observed are of various shapes and sizes .The particle size of the sugarcane bagasse ash approximated in this figure varies from 10–100 μm which is consistent with the results of particle size distribution mentioned by several researchers in their study (typically falls in the 1 - 100 μm range, an average particle size between 20 μm and 70 μm).Their studies have already been mentioned in literature review chapter. For determining the average particle size, ImageJ software was used. This software allows to determine particle size visible in the image and having proper mentioning of scale. Figure 4.7 was analyzed to determine the particle size and average particle size was found to be 10.27 μm as shown in Figure 4.10 and corresponding results have been shown in Table 4.11. Spherical shaped particles were not found, suggesting that the combustion temperature reached in the burning process did not produce the melting of inorganic matter [99]. Further magnification reveals spongy appearance of the particles as shown in Figures 4.8-4.11. Cordeiro et al. [1] showed that burning ashes between the temperatures 400 ^{o} C and 600 ^{o} C produces an increase in the pozzolanic activity index with increasing firing temperatures due to the loss of carbon during the calcination process. According to them, the formation of crystalline silica compounds is observed at a firing temperature around 800 ^{o} C which causes a drop in the pozzolanic activity index at that temperature. These authors suggested that the optimal temperature for the production of pozzolanic SCBA is 600 ^{o} C because at this temperature it is possible to generate predominantly amorphous silica with a pozzolanic activity index of 77%.

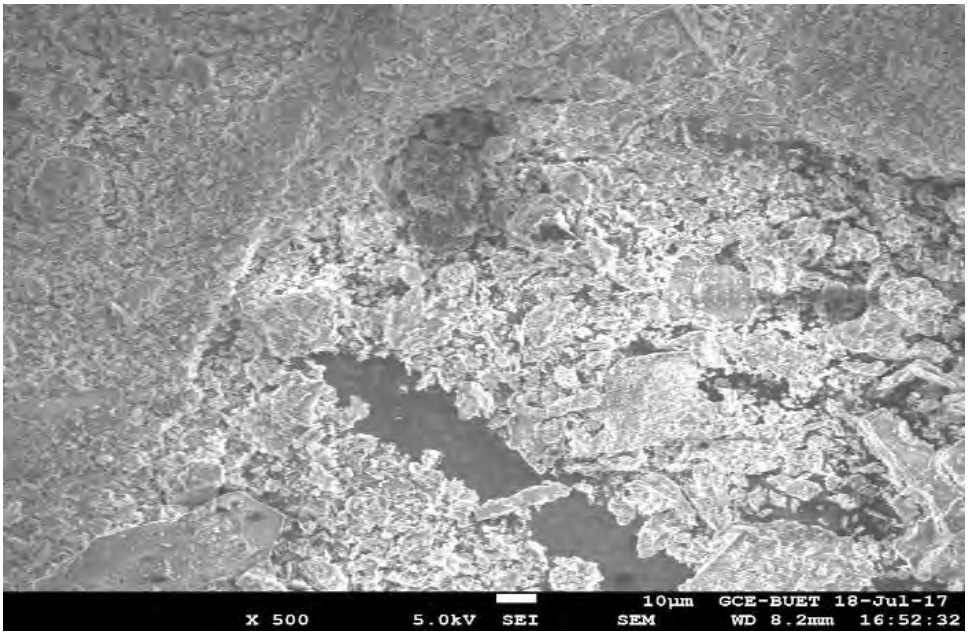

Figure 4.6: The structure of the bagasse ash as revealed by FESEM (X 500)

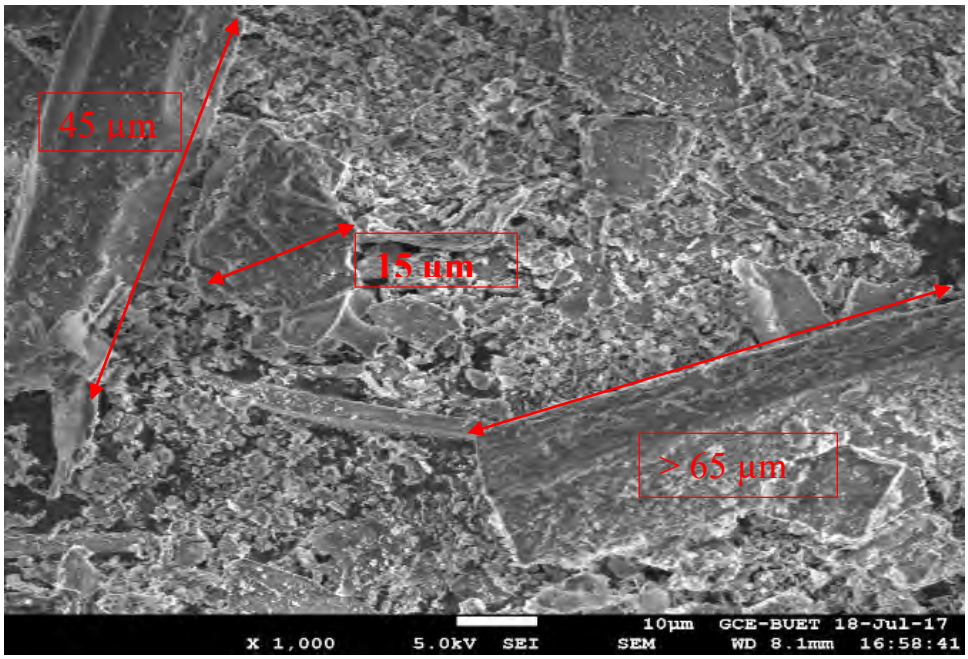

Figure 4.7: The structure of the bagasse ash as revealed by FESEM (X 1000)

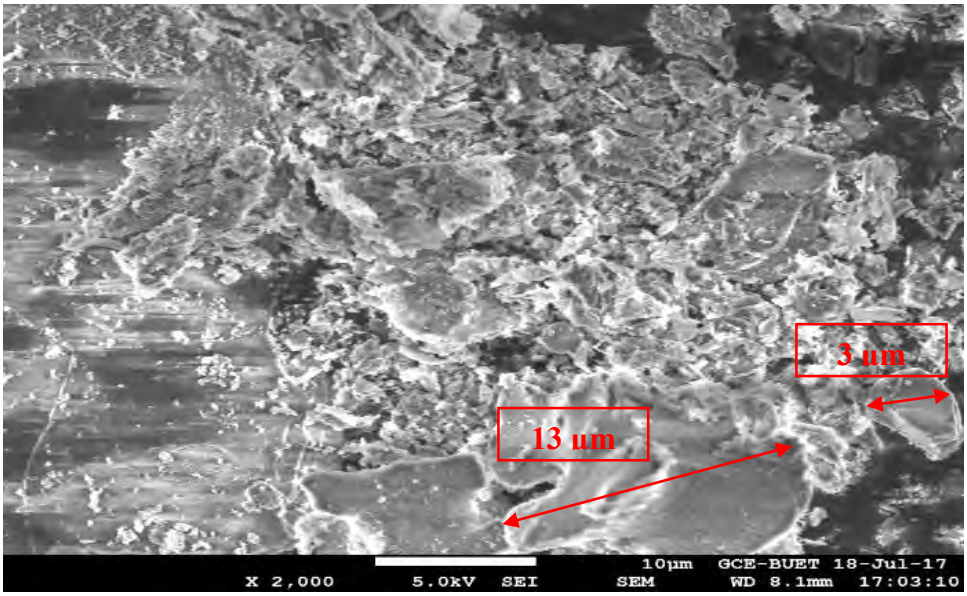

Figure 4.8: The structure of the bagasse ash as revealed by FESEM (X 2000)

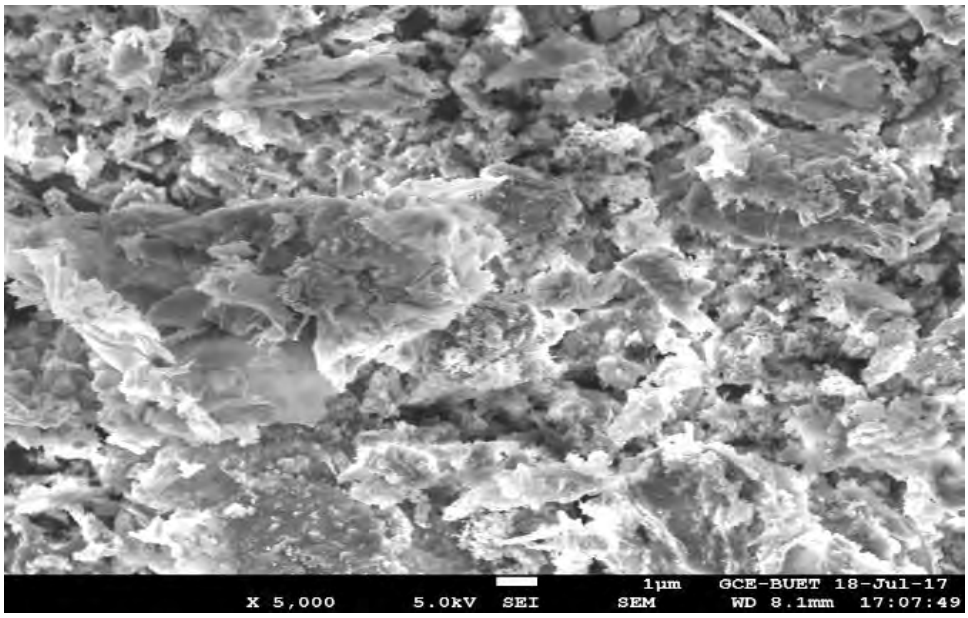

Figure 4.9: The structure of the bagasse ash as revealed by FESEM (X 5000)

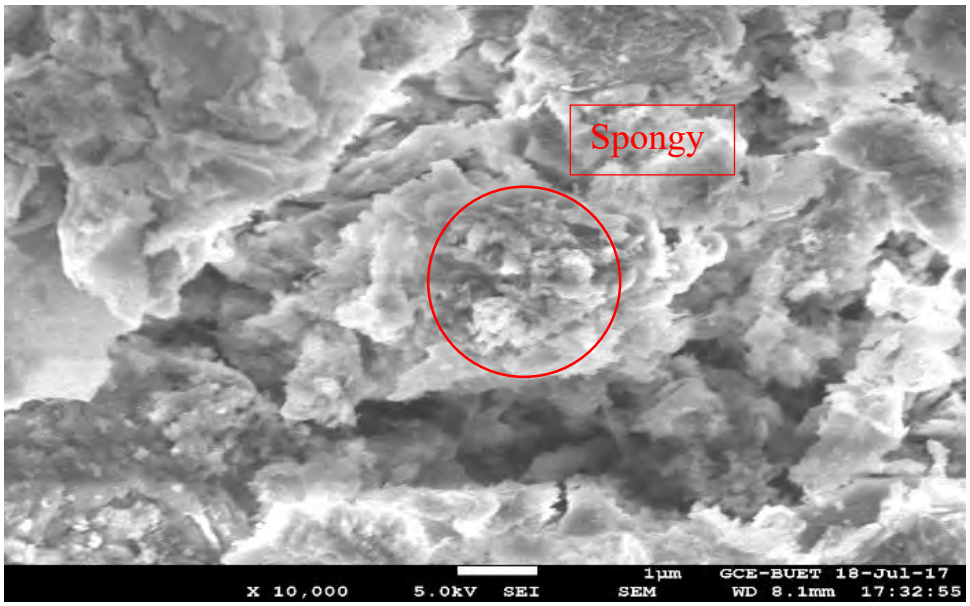

Figure 4.10: The structure of the bagasse ash as revealed by FESEM (X 10000)

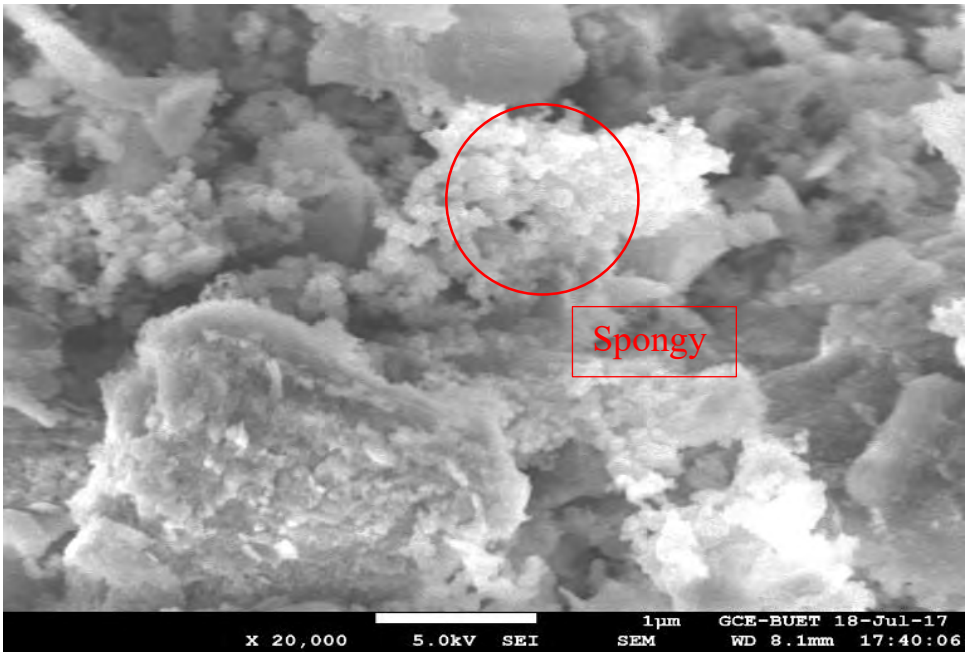

Figure 4.11: The structure of the bagasse ash as revealed by FESEM (X 20000)

Figure 4.12: Particle size determination using ImageJ software

Table 4.10: Particle size of bagasse ash using ImageJ software

	Area	Angle	Particle Size (μm)
Mean	0.972	0.495	10.287
SD	1.234	42.948	13.18
Min	0.044	-110.556	0.406
Max	5.256	72.897	56.052

Similar morphologies were observed by Batra et al. [64] in SEM/EDS results of SCBA. According to him, the prismatic particle consists mainly of Si and O. At higher magnification small pores are observed on the surface of the particles.

At 600-650 ^{o}C temperature, the color of the ash sample in our study turned black to greyish. It means significant amount of carbon has been removed. To determine the amount of unburnt carbon, loss on ignition test (LOI) was performed. The sample presented a loss on ignition of

4.099% at 650 ^{o}C. ASTM C618 limits the LOI of pozzolanic material to be less than 6% [100]. Therefore, the LOI of the sample studied here satisfies the Code limit and could be used as pozzalonic material within cement. A high value is indicative of unburnt carbon, a compound that interferes with the hydration reaction and increases the demand for water.

Some researchers [60,28] calcined bagasse at around 1200 ^{o}C but XRD results revealed their crystalline phase. Such silica can be does not have any pozzolanic property. So considering the above circumstances, it can be concluded that the temperature range of 600-650 ^{o}C is best suited to burn bagasse for highest pozzolan activity.

4.4 Consistency Test Results

The standard test method following ASTM C 187 – 98 [18] was used to determine the amount of water required in preparing hydraulic cement pastes and cement-ash replacement with normal consistency. The normal consistency of bagasse ash blended cement paste was found to be higher than that of cement paste as shown in Table 4.11 and graphically presented in Figure 4.13.

Table 4.11: Consistency Test Results of SCBA blended ash

% Replacement	Consistency (%)
0	28
5	31
10	35
15	37
20	41

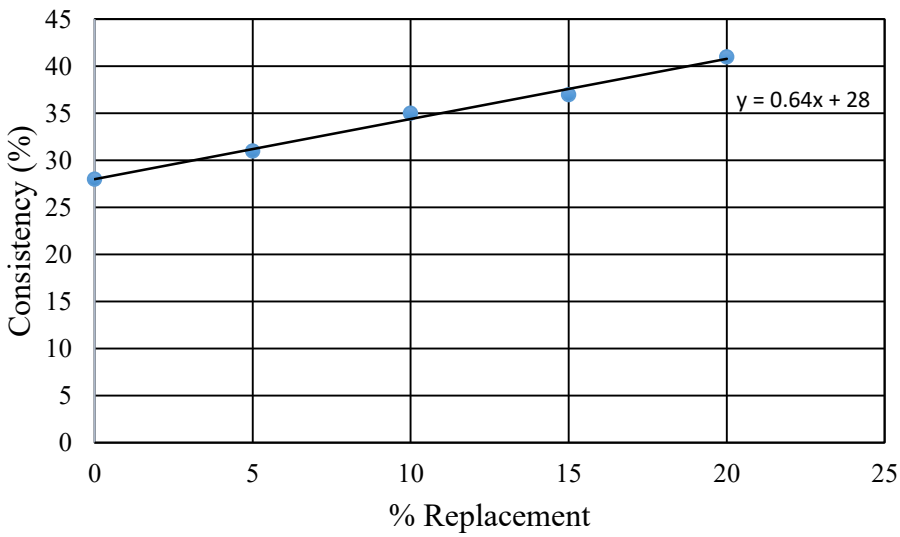

Figure 4.13: Consistency Test Results of SCBA blended ash

Five different percentages of cement replaced by Bagasse Ash of 0%, 5%, 10%, 15%, and 20% were used in this work. The water requirement for consistency increased with an increasing replacing level. For example, the consistency measured for 0% to 20% cement replacement level was found to be 0.28 to 0.41. A previous study reported that SCBA is hygroscopic in nature and it requires more water for proper consistency because of its irregular shape, rough surfaces, and highly porous textures compared with cement. As ashes are hygroscopic in nature and the specific surface area of Bagasse ash is three times higher than cement it needs more water for proper consistency [13].

4.5 Flow Test Results

Table 4.12 shows the flow values of the mixtures containing SCBA, indicating that 0% SCBA replacement has a flow value of 106%. The flow values of the mixtures containing 5%, 10% 15% and 20% SCBA replacement were decreased to 86%, 66%, 55% and 54% respectively as shown in Figure 4.14. The flow value decrease if ash replacement level is increased. However, this flow value was significantly less than that of 0% SCBA replaced cement paste. The highly porous texture of SCBA increases the water demand and consequently decreases the flow value, thus resulting in decreased workability. The small particle size of SCBA increased the specific surface area, and water could not completely flow into each pore, thus decreasing the flow value.

Table 4.12: Consistency Test Results of SCBA blended ash

% Replacement	Flow (%)
0	105.94
5	85.69
10	65.93
15	54.67
20	54.53

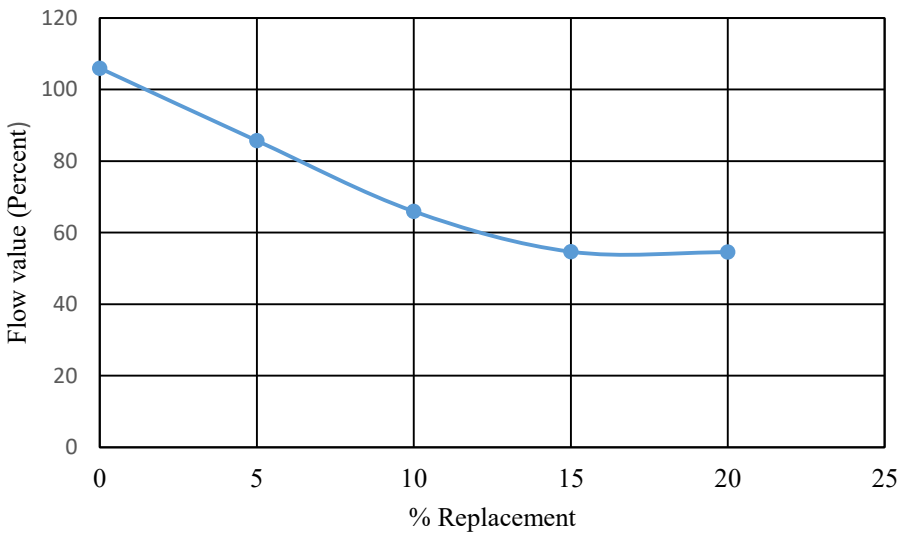

Figure 4.14: Flow test results of SCBA blended ash

Wang et al. [101] reported that during cement mortar mixing, water enters the contact surface spacing between powder particles and forms surface tension and has an adhesive effect, thereby affecting the flowability of powders. Such an effect depends on factors such as particle shape, particle size, and specific surface area. The irregular surface and finer particles of SCBA than those of cement severely influences the SCBA added cement paste flowability.

4.6 Compressive Strength Test Results

The compressive strength results obtained from the experimental investigations are shown in Table 4.13. Compressive strength of SCBA blended mortars at different replacement level is also shown in Figure 4.15. All the values are the average of the three trials in each case in the testing program of this study.

Table 4.13: Compressive strength of SCBA blended mortars

% replacement	3 Days Compressive Strength(MPa)	7 Days Compressive Strength(MPa)	28 Days Compressive Strength(Mpa)	56 Days Compressive Strength(MPa)
0	12.91	20.84	23.23	26.84
5	13.34	22.85	24.85	27.84
10	20.16	25.06	25.68	30.25
15	15.60	17.89	23.36	24.82
20	10.49	14.11	20.35	23.60

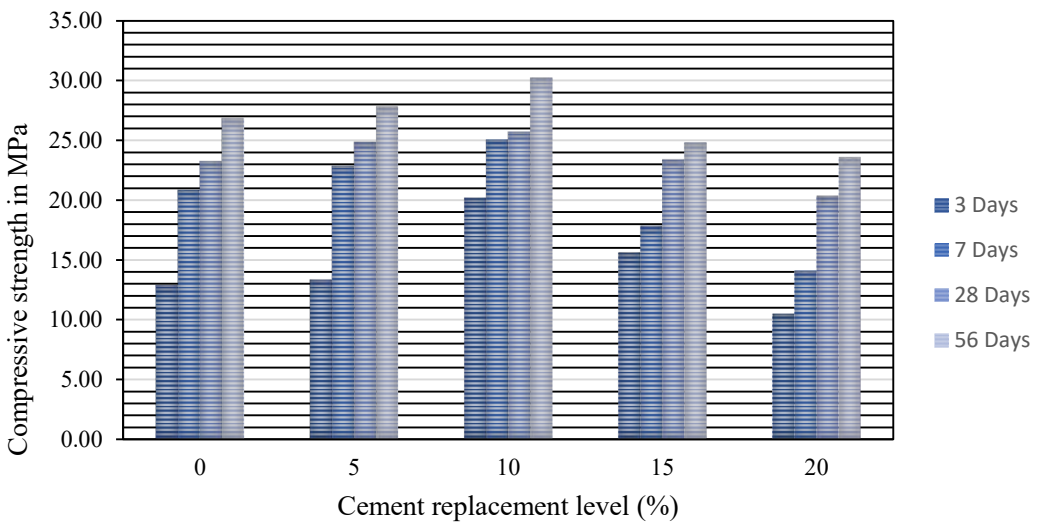

Figure 4.15: Compressive strength of SCBA blended mortars

Compressive strength and percent change in strength at different replacement level of bagasse ash at different days are plotted and shown below in Figures 4.16 to 4.19. Comparison of the data for 3, 7, 28 and 56 days of curing time shows that the compressive strength increases with SCBA up to 10% replacement level and then at 15% SCBA, the compressive strength of mortar attains the equivalent value as observed for OPC. The increase in strength may be due to lime content of SCBA and free lime of OPC that enhance the hydration reaction. Moreover, reaction between calcium hydroxide and reactive silica in SCBA in the alkaline environment could also result in better hydration product as reported by several researchers [41, 46, 102]. The specific surface area of bagasse ash used in this study was measured by using Blains's permeability apparatus. The value of specific surface area was found 9843 cm^2 /gm where the specific surface area of OPC is 3000-5000 cm^2 /gm. So high specific surface area of SCBA leading to number of nucleation sites for additional hydration products [103]. If the cement replacement is above 15%, the strength decreases as observed. As mentioned earlier, free lime in OPC reacts with silica present in bagasse ash. Then formation of silicates produce some additional binding agent and thus strength is increased. If bagasse ash is produced beyond the optimal limit, excess silica remains in the mortar matrix which has no binding property and thus strength is decreased.

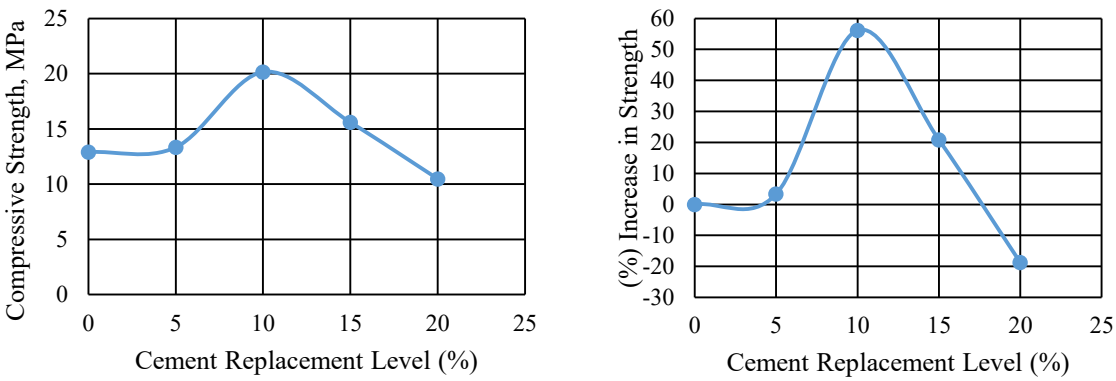

Figure 4.16: Compressive strength of SCBA blended mortars at 3 days curing

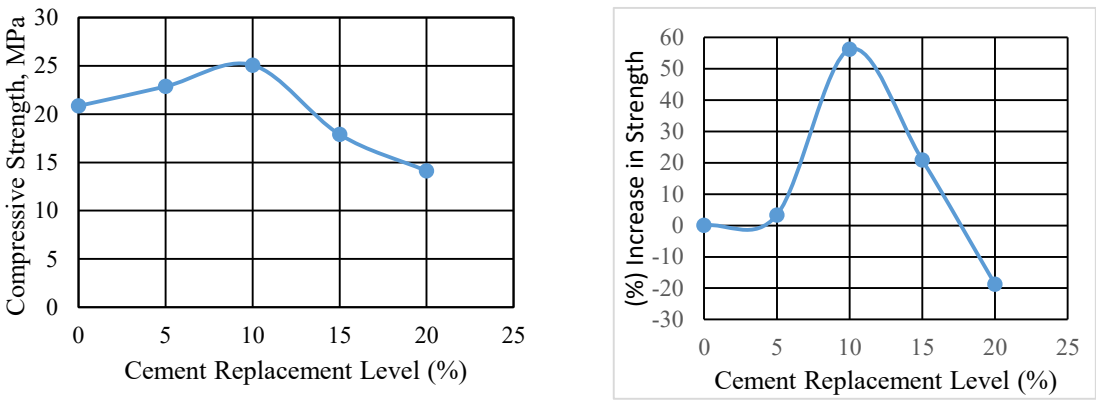

Figure 4.17: Compressive strength of SCBA blended mortars at 7 days curing

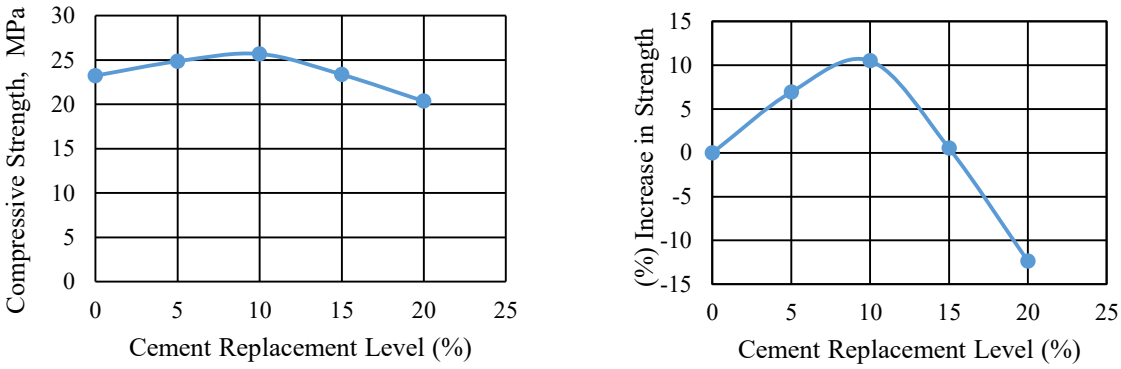

Figure 4.18: Compressive strength of SCBA blended mortars at 28 days curing

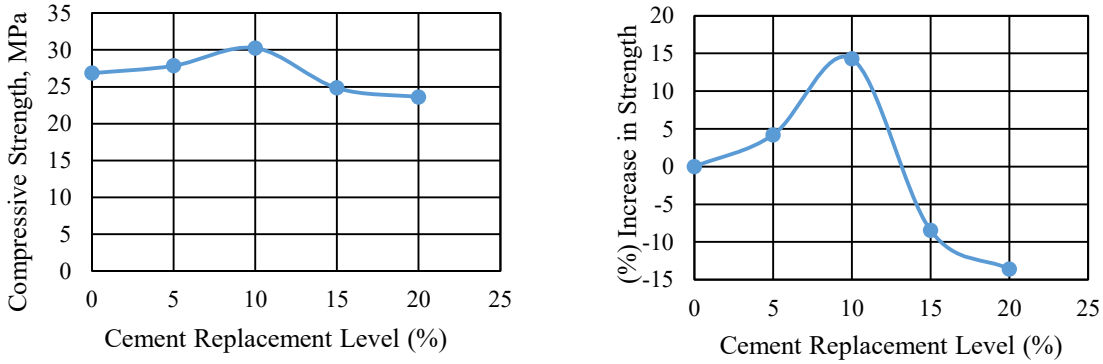

Figure 4.19: Compressive strength of SCBA blended mortars at 56 days curing

Bagasse ash at lower substitution level acts as a nucleating agent for hydration products enhancing the cement hydration while increasing ash content make a dilution effect. This can be a reasonable cause for decrease in strength. Thus 10% replacement of SCBA to OPC is considered as optimal limit.

4.7 Drying Shrinkage Test Results

Drying shrinkage is an important technical parameter influencing structural properties and durability of the material. The drying shrinkage results calculated for the SCBA blended mixes at the ages of 7, 14, 21, and 28 days are presented in Table 4.14 and graphically shown in Figure 4.20.

Table 4.14: Drying shrinkage test results of SCBA blended ash

% Replacement	7 Days	14 Days	21 Days	28 Days
0	0.00042	0.00068	0.00097	0.00101
5	0.0004	0.00065	0.00092	0.00099
10	0.00037	0.00064	0.00088	0.00092
15	0.00036	0.0006	0.00088	0.00092
20	0.00033	0.00059	0.00085	0.00088

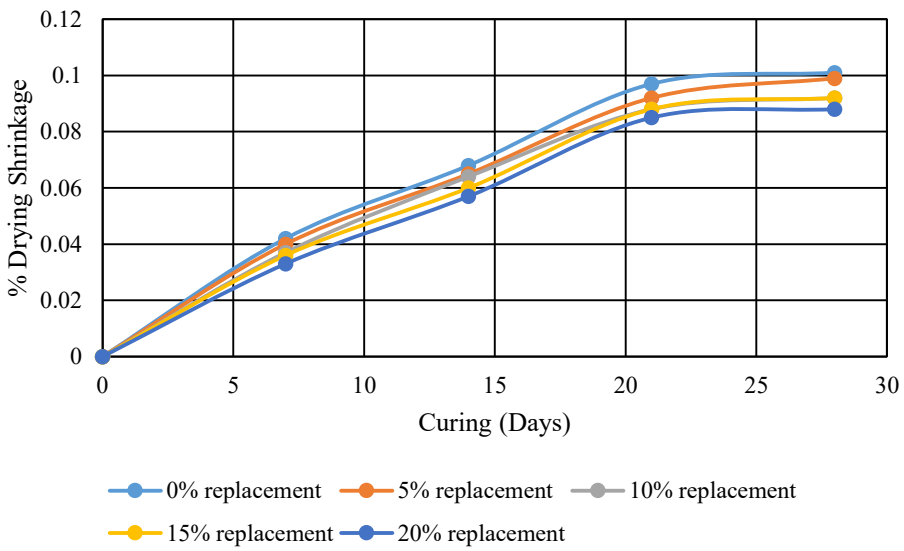

Figure 4.20: Drying shrinkage test results of SCBA blended ash

The drying shrinkage value of the mixes with SCBA is lower than that of the control mix at all ages According to Kaewmanee et al. [104], the presence of SO_3 may causes expansion which compensates shrinkage. OPC itself contained a high value of SO_3 which is in range of 2.19% to 2.95% compared to SCBA [33]. Besides, XRF analysis from Table 4.9 shows the bagasse ash used in this study contains 10.96% of SO_3. The mixture with higher SO_3 content would results in less shrinkage. So in case of mass concreting, blending bagasse ash will add to additional advantage in terms of shrinkage.

Chapter 5

Conclusion

5.1 Conclusions

In this study, importance of bagasse ash as a supplementary cementitious material has been explored. The effect of burning process and temperature for the production of bagasse ash has been discussed. Characterization of bagasse ash was carried out through XRF, SEM and EDS to find the suitability of bagasse ash as a pozzolanic material. Finally, fresh and hardened properties of bagasse ash incorporated cement mortar were investigated. The following major conclusions can be drawn from this study:

I. Bagasse ash derived from leached industrial bagasse can be effectively used within cement as a pozzolanic material. The fresh bagasse without treatment is not suitable for composite cement production if there is high alkali content.

II. The chemical composition of the ash produced from industrial bagasse has nearly similar composition as Class F fly ash when burnt at temperature of 650 ^{o}C for 6 hours.

III. Up to 10% replacement level, the compressive strength of mortar increases and then it shows decreasing trend in strength attainment with higher ash content. At 15% replacement level, the mortar compressive strength is almost equal to the OPC mortar strength. Therefore, 10% of ordinary Portland cement can be optimally replaced with well-burnt bagasse ash without any adverse effect on the strength properties of cement mortar.

IV. It requires 9% more water to maintain same consistency of OPC mortar at 15% replacement level. It is primarily due to irregular shape, rough surfaces, and highly porous texture of bagasse ash.

V. Flowability of the cement mortar was found to decrease with the addition of bagasse ash. For 15% replacement level, flow value was found 55% which is almost 50% lower

than the OPC mortar flow value. This is due to the hygroscopic nature of the ash particles and increase in powder content of the mix.

VI. The drying shrinkage value of the mixes with SCBA is lower than that of the control mix at all ages. For example, the drying shrinkage value decreases 9% at 15% replacement level in comparison to the OPC mortar after 28 curing days.

VII. The most significant advantages of blending bagasse ash with cement is that it is cheaper to produce and needs negligible capital investment to get started. Blending this waste ash in cement will not only have positive impact on environment; but also will reduce the cement production and consequently, reduce the CO_2 emission. Moreover, bagasse ash blended cement showed improved durability cement composites along with comparable strength properties. In addition, it is the most efficient solution to bagasse waste management problem.

5.2 Suggestions for Further Research

Some of the possible future research opportunities in connection to bagasse ash are suggested below:

I. The author recommends that when further study is undertaken on this line of work, more number of specimens should be used to conduct various tests to have statistically significant data.

II. The expansion test is recommended to conduct for longer period of time in future studies.

III. A complete investigation on bagasse ash blended cement concrete is required to evaluate its benefit in terms of durability, absorptivity, heat of hydration, setting time, water permeability and chloride penetration etc.

IV. A detailed analysis regarding reduction in carbon emission and life cycle cost should be carried out to evaluate environmental impact of addition of bagasse ash within cement.

V. XRD analysis is recommended to be performed to determine the phase of silica whether it is in amorphous or crystalline phase.

References

[1] Fairbairn, E. M. R., Paula, T. P. D, Cordeiro, E G. C., Americano, B. B., and Toledo Filho R. D. (2012)."Evaluation of partial clinker replacement by sugar cane bagasse ash: CO_2 emission reductions and potential for carbon credits." Ibracon structures and materials Journal, Volume 5, Number 2, p 229-251.

[2] Wansom, S., Janjaturaphan, S. and Sinthupinyo, S. (2017)." Pozzolanic activity of rice husk ash: comparison of various electrical methods." Journal of Metals, Materials and Minerals, 19(2).

[3] Amin, N. (2011). "Use of bagasse ash in concrete and its impact on the strength and chloride resistivity." Journal of Materials in Civil Engineering (ASCE) 23 (5), 717-720.

[4] Rauf, N., Damayanti, M.C. and Pratama, S.W.I., (2017)." January. The influence of sugarcane bagasse ash as fly ash on cement quality."ProceedingsIn the Conference of AIP (Vol. 1801, No. 1, p. 040009). AIP Publishing.

[5] Embong, R., Shafiq, N., Kusbiantoro, A. and Nuruddin, M.F. (2016)." Effectiveness of low-concentration acid and solar drying as pre-treatment features for producing pozzolanic sugarcane bagasse ash. "Journal of Cleaner Production, 112, pp.953-962.

[6] Ribeiro, D.V., Morelli, M.R., "Effect of calcination temperature on the pozzolanic activity of brasilian sugar cane bagasse ash (SCBA)." Materials Research, v.17, n.10, pp. 974-981, 2014.

[7] Wang, I.F., Lee, C.H.,and Lu, C.K.(2016). "Effect of Bagasse Ash and Pozzolan on the Flowability and Setting Time of Cement Mortar." Proceeding of the International Conference on Power Engineering &Energy, Environment, ISBN: 978-1-60595-376-2.

[8] Hussein, A. A. E., Shafiq, N. & Nuruddin, M. F. (2015). "Compressive strength and interfacial transition zone of sugar cane bagasse ash concrete: a comparison to the

established pozzolans." Proceeding of International Conference on Mathematics, Engineering and Industrial Applications,p. 070002.

[9] Energy Statistics Database: United Nations Statistics Division. (2018). < http://data.un.org>.

[10] BSFIC, MIS Report. Bangladesh Sugar and Food Industries Corporation. Motijheel Commercial Area, Dhaka, Bangladesh, 2008.

[11] BSRI. (2016). http://www.bsri.gov.bd/.

[12] Rainey, T.J.(2009). "A study into the permeability and compressibility properties of Austrealian bagasse pulp." ,Doctor Thesis, School of Engineering Systems Queensland University of Technology – QUT, pp. 221

[13] Ganesan, K., Rajagopal, K., & Thangavel, K. "Evaluation of bagasse ash as supplementary cementitious material". Cement and Concrete Research, 29, 515-524.2007.

[14] Das, B.K., Haque, S.N., Kader, M.A. and Rahman, M.S. (2013). "Prospects of Bagasse Gasification Technology for Electricity Generation in Sugar Industries in Bangladesh." Proceeding of the International Conference on Mechanical, Industrial and Materials Engineering (ICMIME), RUET, Rajshahi, Bangladesh.

[15] ASTM C 109/C 109M, "Standard Test Method for Compressive Strength of Hydraulic Cement Mortars (Using 2-in. or [50-mm] Cube Specimens)."

[16] ASTM C 596-01,"Standard Test Method for Drying Shrinkage of Mortar Containing Hydraulic Cement", ASTM International, West Conshohocken, PA, 2001, www.astm.org.

[17] ASTM C 1437 – 07,"Standard Test Method for Flow of Hydraulic Cement Mortar", ASTM International, West Conshohocken, PA, 2016, www.astm.org.

[18] ASTM C187 – 98," Standard Test Method for Normal Consistency of Hydraulic Cement." ASTM International, West Conshohocken, PA, 1998, www.astm.org.

[19] Kawade, U.R., Rathi, V.R., and Girge, V.D. (2013). "Effect of use of Bagasse Ash on Strength of Concrete." International Journal of Innovative Research in Science, Engineering and Technology 22013; 2997–3000.

[20] Chusilp, N., Jaturapitakkul, C., and Kraiwood.(2009). "Utilization of bagasse ash as a pozzolanic material in concrete" Construction and Building Materials (23)3352–3358.

[21] Sagar, W.,Dhengare, Raut,S.P., Bandwal, and N.V.,Khangan, A."Investigation into Utilization of Sugarcane Bagasse Ash as Supplementary Cementitious Material in Concrete." International Journal of Emerging Engineering Research and Technology, Volume 3, Issue 4, April 2015, PP 109-116.

[22] Srinivasan, R. and Sathiya, K. (2010). "Experimental study on bagasse ash in concrete." International journal for service learning in engineering, 5(2), p.60.

[23] Muangtong, P., Sujjavanich, S., Boonsalee, S., Poomiapiradee, S. and Chaysuwan, D. (2013)." Effects of fine bagasse ash on the workability and compressive strength of mortars." Chiang Mai J. Sci, 40(1), pp.126-134.

[24] Hailu, B. (2011), Addis Ababa Institute of Technology Department Of Civil Engineering (Doctoral dissertation, Addis Ababa University).

[25] Somna, R.,Jaturapitakkul, C., Rattanachu, P., and Chalee, W.(2012). "Effect of ground bagasse ash on mechanical and durability properties of recycled aggregate concrete." Materials and Design (36) 597–603.

[26] Otuoze, H., Amartey, Y., Sada B., Ahmed, H., and Sanni M. (2012). "Characterization of Sugarcane Bagasse Ash and Ordinary Portland Cement Blends in Concrete." Proceeding of the International Conference on Procs 4thWest Africa Built Environment Research (WABER).

[27] Lavanya, M.R., Sugumaran,.B., and Pradeep,T.(2012).“An Experimental study on the compressive strength of concrete by partial replacement of cement with sugarcane bagasse ash.” International Journal of Engineering Inventions, 1, 01-04.

[28] Aigbodion, V. S., Hassan, S. B., Ause, T. and Nyior, G. B. (2010). “Potential utilization of solid waste (bagasse ash).” Journal of Minerals and Materials Characterization and Engineering 9, 67–77

[29] Osinubi, K. J. and Alhassan, M. (2007). “Bagasse ash modification of Shika laterite.” Nigerian Journal of Engineering 14, 96-74104.

[30] Kevorkijan, V. (2003). “Functionally graded aluminum-matrix composites.” American Ceramic Society Bulletin (Ohio: American Ceramic Society) pp 60.

[31] Montakarntiwong, K., Chusilp, N., Tangchirapat, W. and Jaturapitakkul, C. (2013). “Strength and heat evolution of concretes containing bagasse ash from thermal power plants in sugar industry.” Materials & Design, 49, pp.414-420.

[32] Rukzon S, Chindaprasirt P. (2015). “Utilization of bagasse ash in high-strength concrete”. Mater Des 2012; 34:45–50.

[33] Aprianti, E. (2017). “A huge number of artificial waste material can be supplementary cementitious material (SCM) for concrete production–a review part II.” Journal of cleaner production, 142, pp.4178-4194.

[34] Sua-iam, G. and Makul, N. (2013). “Use of increasing amounts of bagasse ash waste to produce self-compacting concrete by adding limestone powder waste.” Journal of Cleaner Production, 57, pp.308-319.

[35] Bahurudeen, A., Kanraj, D., Dev, V.G. and Santhanam, M. (2015). “Performance evaluation of sugarcane bagasse ash blended cement in concrete.” Cement and Concrete Composites, 59, pp.77-88.

[36] Ajay, G., Hattori, K., Ogata, H. and Ashraf, M. (2009). “Processing of sugarcane bagasse ash and reactivity of ash-blended cement mortar.” Transactions of the Japanese Society of Irrigation, Drainage and Rural Engineering, 77(3), pp.243-251.

[37] Castaldelli, V.N., Akasaki, J.L., Melges, J.L., Tashima, M.M., Soriano, L., Borrachero, M.V., Monzó, J. and Payá, J. (2013). “Use of slag/sugar cane bagasse ash (SCBA) blends in the production of alkali-activated materials.” Materials, 6(8), pp.3108-3127.

[38] Frías, M., Villar, E. and Savastano, H. (2011). “Brazilian sugar cane bagasse ashes from the cogeneration industry as active pozzolans for cement manufacture.” Cement and concrete composites, 33(4), pp.490-496.

[39] Moisés, M.P., da Silva, C.T.P., Meneguin, J.G., Girotto, E.M. and Radovanovic, E. (2013). “Synthesis of zeolite NaA from sugarcane bagasse ash.” Materials Letters, 108, pp.243-246.

[40] Sales, A. and Lima, S.A. (2010). “Use of Brazilian sugarcane bagasse ash in concrete as sand replacement.” Waste Management, 30(6), pp.1114-1122.

[41] Hernández, J.M., Middendorf, B., Gehrke, M. and Budelmann, H. (1998). “Use of wastes of the sugar industry as pozzolana in lime-pozzolana binders: study of the reaction.” Cement and Concrete Research, 28(11), pp.1525-1536.

[42] Affandi, S., Setyawan, H., Winardi, S., Purwanto, A. and Balgis, R. (2009).” A facile method for production of high-purity silica xerogels from bagasse ash.” Advanced Powder Technology, 20(5), pp.468-472.

[43] Akram, T., Memon, S.A., Obaid, H. (2009).” Production of low cost self compacting concrete using bagasse ash.” Construction and Building Materials 23 (2), 703e712.

[44] Sirirat Janjaturaphan and Supaporn Wansom, Janjaturaphan, Sirirat & Wansom, Supaporn. (2010). “Pozzolanic activity of industrial sugar cane Bagasse Ash.” Suranaree J. Sci. Technol.. 17.

[45] Lima, S.A., Varum, H., Sales, A. and Neto, V.F. (2012). “Analysis of the mechanical properties of compressed earth block masonry using the sugarcane bagasse ash.” Construction and Building Materials, 35, pp.829-837.

[46] Payá, J., Monzó, J., Borrachero, M.V., Díaz-Pinzón, L. and Ordóñez, L.M. (2002). “Sugar-cane bagasse ash (SCBA): studies on its properties for reusing in concrete production. Journal of Chemical Technology & Biotechnology.” International Research in Process, Environmental & Clean Technology, 77(3), pp.321-325.

[47] Purnomo, C.W., Salim, C. and Hinode, H. (2012).” Synthesis of pure Na–X and Na–A zeolite from bagasse fly ash.” Microporous and Mesoporous Materials, 162, pp.6-13.

[48] Ali, R.F. and El Anany, A.M. (2014). “Recovery of used frying sunflower oil with sugar cane industry waste and hot water.” Journal of food science and technology, 51(11), pp.3002-3013.

[49] Salim, R.W., Ndambuki, J.M. and Adedokun, D.A., (2014) “Improving the bearing strength of sandy loam soil compressed earth block bricks using Sugercane Bagasse Ash.” Sustainability, 6(6), pp.3686-3696.

[50] Singh, N.B., Singh, V.D. and Rai, S. (2000). “Hydration of bagasse ash-blended portland cement.” Cement and Concrete Research, 30(9), pp.1485-1488.

[51] Tantawy, M.A., El-Roudi, A.M. and Salem, A.A. (2014). “ Utilization of bagasse ash as supplementary cementitious material.” International Journal of Engineering Research & Technology, 3(7), pp.1342-1348.

[52] Teixeira, S.R., De Souza, A.E., de Almeida Santos, G.T., Vilche Pena, A.F. and Miguel, A.G. (2008). “Sugarcane bagasse ash as a potential quartz replacement in red ceramic.” Journal of the American Ceramic Society, 91(6), pp.1883-1887.

[53] Tonnayopas, D. (2013). " Green building bricks made with clays and sugar cane bagasse ash."Proceedings of the 11th International Conference on Mining, Materials and Petroleum Engineering (pp. 7-14).

[54] Morais, L.C., Maia, A. A. D., Guandique, M. E. G., and Rosa, A.H.(2017). "Pyrolysis and combustion of sugarcane bagasse." Journal of Thermal Analysis and Calorimetry, Volume 129, Issue 3, pp 1813–1822

[55] Cheng, K.K., Ge, J.P., Zhang, J.A., Ling, H.Z., Zhou, Y.J., Yang, M.D. and Xu, J.M. (2007). "Fermentation of pretreated sugarcane bagasse hemicellulose hydrolysate to ethanol by Pachysolen tannophilus." Biotechnology letters, 29(7), pp.1051-1055.

[56] Li, J., Wei, X., Wang, Q., Chen, J., Chang, G., Kong, L., Su, J. and Liu, Y. (2012). "Homogeneous isolation of nanocellulose from sugarcane bagasse by high pressure homogenization." Carbohydrate polymers, 90(4), pp.1609-1613.

[57] Weng, J.K., Langan, B.W. and Ward, M.A. (1997). "Pozzolanic reaction in Portland cement, silica fume, and fly ash mixtures." Canadian journal of civil engineering, 24(5), pp.754-760.

[58] Pane, I. and Hansen, W. (2005). "Investigation of blended cement hydration by isothermal calorimetry and thermal analysis." Cement and concrete research, 35(6), pp.1155-1164.

[59] Bahurudeen, A. and Santhanam, M. (2015). " Influence of different processing methods on the pozzolanic performance of sugarcane bagasse ash." Cement and Concrete composites, 56, pp.32-45.

[60] Sultana, M.S., and Rahman, M. A. (2013). "Characterization of Calcined Sugarcane Bagasse Ash and Sugarcane Waste Ash for Industrial Use." Proceeding of the International Conference on Mechanical, Industrial and Materials Engineering (ICMIME 2013), RUET, Rajshahi, Bangladesh.

[61] Altwair, N.M., Johari, M.A.M., and Hashim, S.F.S. (2011). “Influence of calcination temperature on characteristics and pozzolanic activity of palm oil waste ash.” Australian journal of Basic and applied sciences 5 (11), 1010-1018.

[62] Ribeiro, D.V., Morelli, M.R., “Effect of calcination temperature on the pozzolanic activity of brasilian sugar cane bagasse ash (SCBA).” Materials Research, v.17, n.10, pp. 974-981, 2014.

[63] Mehta, P.K. (1977) “Properties of blended cements made from rice husk ash.” In Journal Proceedings (Vol. 74, No. 9, pp. 440-442).

[64] Batra, V.S., Urbonaite, S. and Svensson, G. (2008). “Characterization of unburned carbon in bagasse fly ash.” Fuel, 87(13-14), pp.2972-2976.

[65] Ollivier, J.P., Maso, J.C. and Bourdette, B. (1995). “Interfacial transition zone in concrete.” Advanced Cement Based Materials, 2(1), pp.30-38.

[66] Scrivener, K.L. (2004). “Backscattered electron imaging of cementitious microstructures: understanding and quantification.” Cement and Concrete Composites, 26(8), pp.935-945.

[67] Santos, F., Borém, A., Caldas, C., Sugarcane Agricultural Production, Bioenergy and Ethanol, Elsevier,London (2015).

[68] Modesto, M., Nebra, S.A. and Zemp,R.J. (2006) “ Ethanol Production From Sugarcane: Comparison Of Juice Cane Extractions Systems–Mill And Diffuser – Through Exergetic Cost Analysis.” Proceeding of the 19th International Conference on Efficiency, Cost, Optimization, Simulation, and Environmental Impact of Energy Systems, Crete, Greece, July 12 – 14, p. 739-47.

[69] Bender, P. A., J. F. Laukaitis, H. W. Lockman, D. Samela, W. G. Smith, and G. Tsoumpas.(1983)."Operating experience at the Shamokin Culm burning steam

generation plant." Proceeding of the Annular Meeting on Air Pollution Control Association ;(United States) 83, no. CONF-830617.

[70] Paula, M. O. D., Tinôco, I. D. F., Rodrigues, C. D. S., Silva, E. N. D., and Souza, C. D. F. (2009)."Potential of sugarcane bagasse ash as a partial replacement material for Portland cement." Revista Brasileira de Engenharia Agrícola e Ambiental 13, no. 3: 353-357.

[71] Takahashi, G., (2015). "Sample preparation for X-ray fluorescence analysis." Rigaku Journal, 31, pp.26-30.

[72] ASTM C305-14. "Standard Practice for Mechanical Mixing of Hydraulic Cement Pastes and Mortars of Plastic Consistency." ASTM International, West Conshohocken, PA, 2014, www.astm.org

[73] ASTM C 230/C 230M – 08. " Standard Specification for Flow Table for Use in Tests of Hydraulic Cement." ASTM International, West Conshohocken, PA, 2008, www.astm.org.

[74] McKendry, P., (2002). "Energy production from biomass (part 1): overview of biomass. Bioresource technology", 83(1), pp.37-46.

[75] Baxter, L., (2011). "Biomass-coal cofiring: an overview of technical issues."In Solid biofuels for energy (pp. 43-73). Springer, London.

[76] Sami, M., K. Annamalai, and M. Wooldridge. (2001) "Co-firing of coal and biomass fuel blends." Progress in energy and combustion science 27, no. 2: 171-214.

[77] Hjuler, K., (2000). "Prediction of fouling and sintering in thermal conversion of biomass determination of ash fingerprints." Proceeding of the 1st World Conference on Biomass for Energy and Industry, Sevilla, Spain, 5–9 June, Vol. 1, p. 2135, 2001.

[78] Saddawi, A., Jones, J.M., Williams, A. and Coeur, C.L., (2012). "Commodity fuels from biomass through pretreatment and torrefaction: effects of mineral content on torrefied fuel characteristics and quality." Energy & Fuels, 26(11), pp.6466-6474.

[79] Skrifvars, B.J., Öhman, M., Nordin, A. and Hupa, M., (1999). "Predicting bed agglomeration tendencies for biomass fuels fired in FBC boilers: a comparison of three different prediction methods." Energy & fuels, 13(2), pp.359-363.

[80] Gilbe, C., Lindstr.m, E., Backman, R., Samuelsson, R., Burvall, J. and Ohman, M., (2008). "Predicting slagging tendencies for biomass pellets fired in residential appliances: a comparison of different prediction methods." Energy & Fuels, 22(6), pp.3680-3686.

[81] Vassilev, S.V., Baxter, D., Andersen, L.K. and Vassileva, C.G. (2013)." An overview of the composition and application of biomass ash: Part 2. Potential utilisation, technological and ecological advantages and challenges." Fuel, 105, pp.19-39.

[82] ASTM Committee C-09 on Concrete and Concrete Aggregates, (2013). "Standard specification for coal fly ash and raw or calcined natural pozzolan for use in concrete." ASTM International.

[83] ASTM C1567-08, "Standard Test Method for Determining the Potential Alkali-Silica Reactivity of Combinations of Cementitious Materials and Aggregate (Accelerated Mortar-Bar Method)," 2009 ASTM Annual Book of Standards, Volume 04.02, Concrete and Aggregates, ASTM International, West Conshohocken, Pennsylvania, 2009.

[84] Xue, G., Kwapinska, M., Kwapinski, W., Czajka, K.M., Kennedy, J. and Leahy, J.J. (2014). "Impact of torrefaction on properties of Miscanthus× giganteus relevant to gasification."Fuel, 121, pp.189-197.

[85] Deng, J., Wang, G.J., Kuang, J.H., Zhang, Y.L. and Luo, Y.H. (2009). "Pretreatment of agricultural residues for co-gasification via torrefaction," Journal of Analytical & Applied Pyrolysis, vol. 86, no. 2, pp. 331–337, 2009.

[86] Khan, A.A., De Jong, W., Jansens, P.J. and Spliethoff, H. (2009). “Biomass combustion in fluidized bed boilers: Potential problems and remedies.” Fuel processing technology, 90(1), pp.21-50.

[87] Yao, X., Xu, K. and Li, Y. (2016). “Physicochemical properties and possible applications of waste corncob fly ash from biomass gasification industries of China.” BioResources, 11(2), pp.3783-3798.

[88] Jenkins, B., Baxter, L.L., Miles Jr, T.R. and Miles, T.R. (1998). “Combustion properties of biomass.” Fuel processing technology, 54(1-3), pp.17-46.

[89] Wang, L., Hustad, J.E., Skreiberg, Skjevrak, G. and Gronli, M. (2012). “A critical review on additives to reduce ash related operation problems in biomass combustion applications.” Energy Procedia, 20, pp.20-29.

[90] Veijonen K, Vainikka P, Ja¨rvinen T, Alakangas E. “Biomass cofiring—an efficient way to reduce greenhouse gas emissions.” The European Bioenergy Network (EUBIONET), VTT Processes, 2003.

[91] Baxter, L.L., Miles, T.R., Miles Jr, T.R., Jenkins, B.M., Milne, T., Dayton, D., Bryers, R.W. and Oden, L.L. (1998). “The behavior of inorganic material in biomass-fired power boilers: field and laboratory experiences.” Fuel processing technology, 54(1-3), pp.47-78.

[92] http://nutrition.indobase.com/articles/sugarcane-juice-nutrition.php/25-09-2017

[93] Martijn, A. (2012). "Design of a pretreatment installation for the washing of empty fruit bunches at a palm oil mill."

[94] Worathanakul, P., Payubnop, W. and Muangpet, A. (2009).“Characterization for post-treatment effect of bagasse ash for silica extraction.” World academy of science, Engineering and Technology, 56, pp.360-362.

[95] Huggins, F.E., Kosmack, D.A. and Huffman, G.P. (1981). “Correlation between ash-fusion temperatures and ternary equilibrium phase diagrams.” Fuel, 60(7), pp.577-584.

[96] Abbasi, A. and Zargar, A. (2013). “Using bagasse ash in concrete as pozzolan.” Middle-East Journal of Scientific Research, 13(6), pp.716-719.

[97] Amin, Noor, U.(2010) "Chemical activation bagasse ash in cementitious system and its impact on strength development." Journal of the Chemical Society of Pakistan 32, no. 4 : 481-484.

[98] Zerbino, R., Giaccio, G., Batic, O.R. and Isaia, G.C., (2012). “Alkali–silica reaction in mortars and concretes incorporating natural rice husk ash.” Construction and building materials, 36, pp.796-806.

[99] Castaldelli, V.N., Akasaki, J.L., Melges, J.L., Tashima, M.M., Soriano, L., Borrachero, M.V., Monzó, J. and Payá, J. (2013). “Use of slag/sugar cane bagasse ash (SCBA) blends in the production of alkali-activated materials.” Materials, 6(8), pp.3108-3127.

[100] ASTM C618-17a, “Standard Specification for Coal Fly Ash and Raw or Calcined Natural Pozzolan for Use in Concrete.” ASTM International, West Conshohocken, PA, 2017, www.astm.org

[101] Wang, I.F., Lee, C.H.,and Lu, C.K.(2016).“Effect of Bagasse Ash and Pozzolan on the Flowability and Setting Time of Cement Mortar.” Proceeding of theInternational Conference on Power Engineering &Energy, Environment, ISBN: 978-1-60595-376-2

[102] Singh, N.B., Singh, V.D. and Rai, S. (2000). “Hydration of bagasse ash-blended portland cement.” Cement and Concrete Research, 30(9), pp.1485-1488.

[103] Ganesan, K., Rajagopal, K., and Thangavel, K. (2007). “Chloride resisting concrete containing rice husk ash and bagasse ash.” Indian Journal of Engineering & Materials Sciences,Vol.14, pp. 257-265.

[104] Kaewmanee, K., Krammart, P., Sumranwanich, T., Choktaweekarn, P. and Tangtermsirikul, S. (2013). “Effect of free lime content on properties of cement–fly ash mixtures.” Construction and Building Materials, 38, pp.829-836.

APPENDICES

Appendix A

(a)Local juice extraction method

(b) Local fresh bagasse

Figure A1 Locally available bagasse at sugarcane juice seller

Figure A2 Stack bagasse at Faridpur Sugar Mill site.

Figure A3 Grinding of fresh bagasse before burning

Figure A4 Self burning of bagasse before calcination

Figure A5 Muffle Furnace (maximum 1200 ^{0}C range)

Figure A6 Typical temperature profile in Muffle furnace

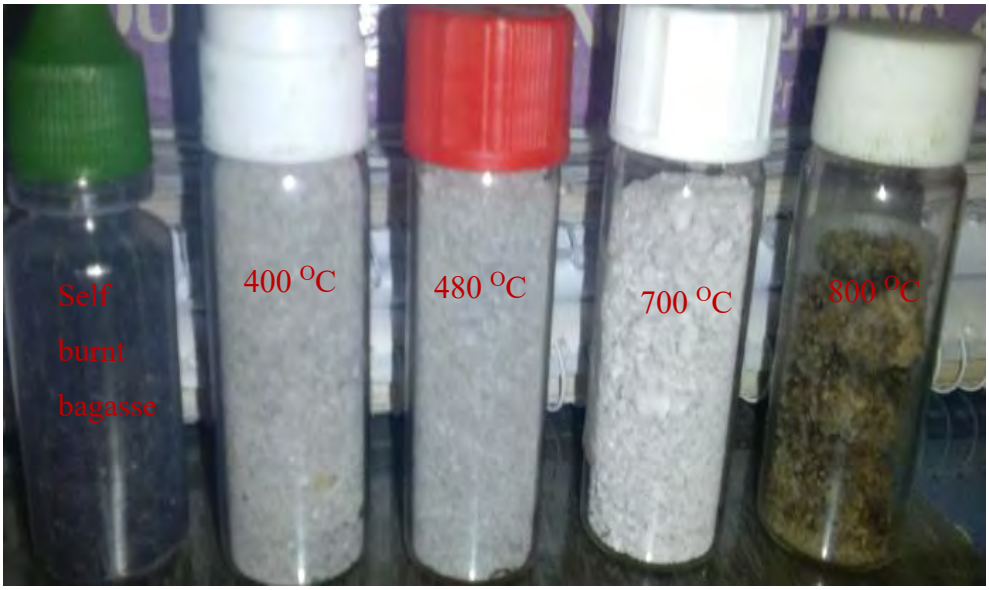

Figure A7 Color comparison of calcined bagasse ash at different temperature

Figure A8 Making of Brick furnace

Figure A9 Top reinforcement to carry suspension bed

Figure A10 Anthracite coal and wood for burning sample

Figure A11 Sample before placing in Brick furnace for calcination

Figure A12 Sample placed in Brick furnace in covered condition

Figure A13 Local fresh bagasse ash after calcination in Brick furnace

Figure A14 Collapsible slab above Brick furnace

Figure A15 Infrared thermometer for temperature measurement

Figure A16 Press machine for XRF sample preparation

Figure A17 Placing of sample in the mold for flow test

Figure A18 Mortar cube compressive strength testing machine

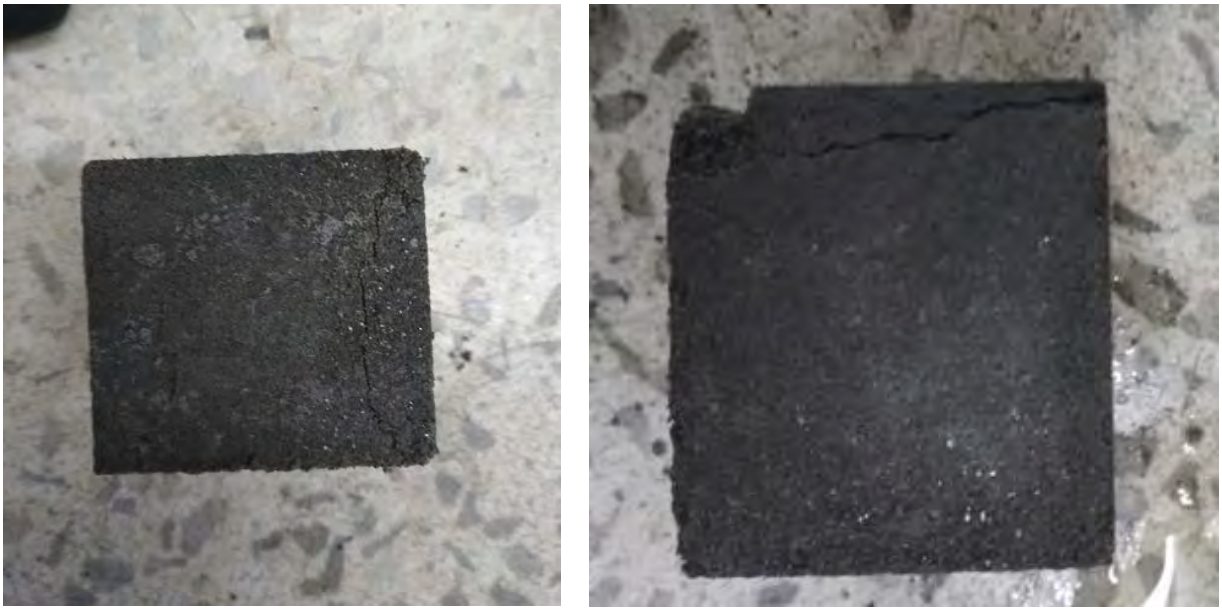

Figure A19 Bagasse ash blended cement mortar cube after failure

Appendix B

Table B1: Chemical composition of local bagasse ash at 280°C

Glass & Ceramic Engineering Department, BUET

Sample : Bagasse_CE_AH_BUET
Operator :GCE,BUET
Comment :20 deg/min, for Oxide
Group :[Qual-Quant,]Std-Oxide for MME
Date : 2017-01-25 16:03

[Quantitative Result]

Analyte	Result	Proc-Calc	Line	Net Int.	BG Int.
K2O	50.7446 %	Quant.-FP	K Ka	236.761	1.777
SiO2	15.5028 %	Quant.-FP	SiKa	22.921	0.107
P2O5	13.0846 %	Quant.-FP	P Ka	35.569	0.472
CaO	5.5224 %	Quant.-FP	CaKa	8.558	0.205
Fe2O3	4.8344 %	Quant.-FP	FeKa	11.016	0.079
MgO	4.3682 %	Quant.-FP	MgKa	2.155	0.110
SO3	4.1460 %	Quant.-FP	S Ka	6.539	0.088
Na2O	0.8194 %	Quant.-FP	NaKa	0.163	0.023
MnO	0.6525 %	Quant.-FP	MnKa	1.300	0.056
Al2O3	0.1995 %	Quant.-FP	AlKa	0.483	0.046
TiO2	0.1257 %	Quant.-FP	TiKa	0.046	0.015

Table B2: Chemical composition of local bagasse ash at 400°C

Glass & Ceramic Engineering Department, BUET

Sample : Bagasse_CE_AH_BUET
Operator : GCE,BUET
Comment : 20 deg/min, for Oxide
Group : [Qual-Quant,]Std-Oxide for MME
Date : 2017-01-25 16:14

[Quantitative Result]

Analyte	Result	Proc-Calc	Line	Net Int.	BG Int.
K2O	39.8204 %	Quant.-FP	K Ka	228.226	1.657
SiO2	28.5549 %	Quant.-FP	SiKa	55.998	0.180
P2O5	13.8707 %	Quant.-FP	P Ka	44.356	0.602
CaO	6.3490 %	Quant.-FP	CaKa	14.275	0.209
MgO	4.6336 %	Quant.-FP	MgKa	3.156	0.042
SO3	3.3799 %	Quant.-FP	S Ka	6.163	0.083
Fe2O3	1.4466 %	Quant.-FP	FeKa	4.808	0.085
Al2O3	1.0751 %	Quant.-FP	NaKa	3.549	0.173
Na2O	0.6533 %	Quant.-FP	NaKa	0.179	0.012
TiO2	0.2164 %	Quant.-FP	TiKa	0.113	0.012

Table B3: Chemical composition of local bagasse ash at 480°C

Glass & Ceramic Engineering Department, BUET

Sample : Bagasse_CE_AH_BUET
Operator :GCE,BUET
Comment :20 deg/min, for Oxide
Group :[Qual-Quant,]Std-Oxide for MME
Date : 2017-01-25 16:48

[Quantitative Result]

Analyte	Result	Proc-Calc	Line	Net Int.	BG Int.
K2O	39.5601 %	Quant.-FP	K Ka	220.482	1.588
SiO2	27.7812 %	Quant.-FP	SiKa	52.650	0.154
P2O5	14.2166 %	Quant.-FP	P Ka	44.321	0.557
CaO	6.7756 %	Quant.-FP	CaKa	14.842	0.216
MgO	4.8612 %	Quant.-FP	MgKa	3.201	0.047
SO3	3.2695 %	Quant.-FP	S Ka	5.791	0.068
Fe2O3	1.3593 %	Quant.-FP	FeKa	4.377	0.079
Al2O3	0.9780 %	Quant.-FP	AlKa	3.112	0.148
Na2O	0.8312 %	Quant.-FP	NaKa	0.221	0.010
TiO2	0.1949 %	Quant.-FP	TiKa	0.099	0.017
MnO	0.1725 %	Quant.-FP	MnKa	0.483	0.049

Table B4: Chemical composition of local bagasse ash at 700°C

Glass & Ceramic Engineering Department, BUET

Sample : Bagasse_CE_AH_BUET
Operator :GCE,BUET
Comment :20 deg/min, for Oxide
Group :[Qual-Quant,]Std-Oxide for MME
Date : 2017-01-25 16:25

[Quantitative Result]

Analyte	Result	Proc-Calc	Line	Net Int.	BG Int.
K2O	34.6481 %	Quant.-FP	K Ka	202.934	1.469
SiO2	32.1219 %	Quant.-FP	SiKa	65.084	0.208
P2O5	14.6765 %	Quant.-FP	P Ka	46.858	0.607
CaO	6.5524 %	Quant.-FP	CaKa	16.345	0.207
MgO	4.8295 %	Quant.-FP	MgKa	3.453	0.052
SO3	3.3822 %	Quant.-FP	S Ka	6.147	0.081
Fe2O3	1.3712 %	Quant.-FP	FeKa	5.864	0.071
Al2O3	1.3712 %	Quant.-FP	AlKa	4.720	0.208
Na2O	0.6034 %	Quant.-FP	NaKa	0.174	0.016
TiO2	0.2132 %	Quant.-FP	TiKa	0.123	0.013

Table B5: Chemical composition of local bagasse ash at 800°C

Glass & Ceramic Engineering Department, BUET

Sample : Bagasse_CE_AH_BUET
Operator :GCE,BUET
Comment :20 deg/min, for Oxide
Group :[Qual-Quant,]Std-Oxide for MME
Date : 2017-01-25 16:48

[Quantitative Result]

Analyte	Result	Proc-Calc	Line	Net Int.	BG Int.
SiO2	36.8618 %	Quant.-FP	SiKa	67.595	0.195
K2O	36.1044 %	Quant.-FP	K Ka	189.736	1.307
P2O5	11.5570 %	Quant.-FP	P Ka	31.874	0.439
CaO	5.6366 %	Quant.-FP	CaKa	12.335	0.181
MgO	3.3005 %	Quant.-FP	MgKa	2.094	0.046
SO3	2.2207 %	Quant.-FP	S Ka	3.604	0.070
Fe2O3	1.5929 %	Quant.-FP	FeKa	5.174	0.065
Al2O3	1.2975 %	Quant.-FP	AlKa	4.054	0.186
Na2O	1.0084 %	Quant.-FP	NaKa	0.260	0.014
TiO2	0.2515 %	Quant.-FP	TiKa	0.129	0.012
MnO	0.1687 %	Quant.-FP	MnKa	0.476	0.051

Table B6: Chemical composition of local bagasse ash at 650°C burnt at Brick furnace for 6 hours

Glass & Ceramic Engineering Department, BUET

Sample : SC_S-01_FlyAsh_DHN
Operator :GCE,BUET
Comment :8 deg/min, for SPC
Group :[Qual-Quant,]Det-Oxide for Soil
Date : 2017-06-06 11.10

[Quantitative Result]

Analyte	Result	Proc-Calc	Line	Net Int.	BG Int.
SiO2	30.6394 %	Quant.-FP	SiKa	64.502	0.207
K2O	28.8038 %	Quant.-FP	K Ka	169.399	1.314
P2O5	10.8690 %	Quant.-FP	S Ka	36.775	0.500
SO3	9.5658 %	Quant.-FP	P Ka	18.858	0.119
CaO	8.0332 %	Quant.-FP	CaKa	22.528	0.207
MgO	4.5651 %	Quant.-FP	MgKa	3.410	0.042
Fe2O3	2.3369 %	Quant.-FP	FeKa	9.338	0.097
Al2O3	1.9466 %	Quant.-FP	AlKa	7.019	0.299
Cl	1.8083 %	Quant.-FP	ClKa	3.739	0.133
Na2O2	0.6381 %	Quant.-FP	NaKa	0.194	0.013
TiO2	0.3134 %	Quant.-FP	ZnKa	0.198	0.019
ZnO	0.2963 %	Quant.-FP	TiKa	2.752	0.146
Rb2O	0.0856 %	Quant.-FP	RbKa	1.965	0.524
Cr2O3	0.0656 %	Quant.-FP	SrKa	0.134	0.035
SrO	0.0254 %	Quant.-FP	ZrKa	0.597	0.585
ZrO2	0.0074 %	Quant.-FP	ZrKa	0.177	0.720

Table B7: Chemical composition of local bagasse ash at 650°C burnt at Brick furnace for 12 hours

Glass & Ceramic Engineering Department, BUET

Sample : SC_S-02_FlyAsh_DHN
Operator :GCE,BUET
Comment :8 deg/min, for SPC
Group :[Qual-Quant,]Det-Oxide for Soil
Date : 2017-06-06 11.25

[Quantitative Result]

Analyte	Result	Proc-Calc	Line	Net Int.	BG Int.
SiO2	32.8895 %	Quant.-FP	SiKa	67.043	0.231
K2O	26.6076 %	Quant.-FP	K Ka	152.191	1.124
SO3	11.1611 %	Quant.-FP	S Ka	21.139	0.109
P2O5	9.9742 %	Quant.-FP	P Ka	32.119	0.427
CaO	6.7185 %	Quant.-FP	CaKa	19.065	0.201
MgO	4.7332 %	Quant.-FP	MgKa	3.470	0.049
Fe2O3	2.5271 %	Quant.-FP	FeKa	10.373	0.088
Al2O3	2.3410 %	Quant.-FP	AlKa	8.247	0.338
Cl	1.4251 %	Quant.-FP	ClKa	2.807	0.157
Na2O2	0.5845 %	Quant.-FP	NaKa	0.176	0.016
ZnO	0.5437 %	Quant.-FP	ZnKa	5.152	0.148
TiO2	0.3815 %	Quant.-FP	TiKa	0.248	0.020
Rb2O	0.0821 %	Quant.-FP	RbKa	1.900	0.516
SrO	0.0241 %	Quant.-FP	SrKa	0.570	0.596
ZrO2	0.0069 %	Quant.-FP	ZrKa	0.165	0.771

Table B8: Chemical composition of industrial bagasse ash at 650°C burnt at Brick furnace for 6 hours

Glass & Ceramic Engineering Department, BUET

Sample : SC_S-03_FlyAsh_DHN
Operator :GCE,BUET
Comment :8 deg/min, for SPC
Group :[Qual-Quant,]Det-Oxide for Soil
Date : 2017-06-06 11.39

[Quantitative Result]

Analyte	Result	Proc-Calc	Line	Net Int.	BG Int.
SiO2	61.6530 %	Quant.-FP	SiKa	111.055	0.311
SO3	10.9614 %	Quant.-FP	S Ka	16.166	0.099
Al2O3	6.9240 %	Quant.-FP	AlKa	23.655	0.944
CaO	5.1400 %	Quant.-FP	CaKa	20.414	0.140
Fe2O3	4.9130 %	Quant.-FP	FeKa	27.078	0.128
K2O	4.1911 %	Quant.-FP	K Ka	21.078	0.224
MgO	2.3954 %	Quant.-FP	MgKa	1.677	0.058
P2O5	1.8630 %	Quant.-FP	P Ka	4.290	0.110
TiO2	0.7953 %	Quant.-FP	TiKa	0.716	0.022
Na2O	0.6622 %	Quant.-FP	NaKa	0.192	0.009
ZnO	0.3697 %	Quant.-FP	ZnKa	4.327	0.194
Cr2O3	0.0553 %	Quant.-FP	CrKa	0.160	0.049
ZrO2	0.0358 %	Quant.-FP	ZrKa	1.068	0.928
SrO	0.0209 %	Quant.-FP	SrKa	0.616	0.661
RbO2	0.0200 %	Quant.-FP	RbKa	0.576	0.558